THE UNIVERSITY OF CALGARY

The Effect of Exercise-Induced Mechanical Stimuli on Cortical Bone

by

Stefan Judex

A DISSERTATION

SUBMITTED TO THE FACULTY OF GRADUATE STUDIES

IN PARTIAL FULFILMENT OF THE REQUIREMENTS FOR THE

DEGREE OF DOCTOR OF PHILOSOPHY

DEPARTMENT OF MECHANICAL ENGINEERING

CALGARY, ALBERTA

March, 1999

© Stefan Judex 1999

National Library of Canada
Acquisitions and Bibliographic Services
395 Wellington Street
Ottawa ON K1A 0N4
Canada

Bibliothèque nationale du Canada
Acquisitions et services bibliographiques
395, rue Wellington
Ottawa ON K1A 0N4
Canada

Your file Votre référence

Our file Notre référence

The author has granted a non-exclusive licence allowing the National Library of Canada to reproduce, loan, distribute or sell copies of this thesis in microform, paper or electronic formats.

The author retains ownership of the copyright in this thesis. Neither the thesis nor substantial extracts from it may be printed or otherwise reproduced without the author's permission.

L'auteur a accordé une licence non exclusive permettant à la Bibliothèque nationale du Canada de reproduire, prêter, distribuer ou vendre des copies de cette thèse sous la forme de microfiche/film, de reproduction sur papier ou sur format électronique.

L'auteur conserve la propriété du droit d'auteur qui protège cette thèse. Ni la thèse ni des extraits substantiels de celle-ci ne doivent être imprimés ou autrement reproduits sans son autorisation.

0-612-38479-9

Canada

ABSTRACT

Physical activity is capable of increasing bone mass. The specific osteogenic component of the mechanical milieu remains, however, unknown. Three experiments were designed to examine the response of the middiaphyseal rooster tarsometatarsus to mechanical stimuli induced by running and high-impact drop-jumping. The mechanical environments produced by walking, running, and drop-jumping were quantified via in vivo strain gages, linear beam theory, and finite element modeling. Distributions of mechanical parameters proposed to drive adaptation, including strain magnitude and distribution, strain rate, and strain gradients, were spatially correlated with exercise-related changes across the middiaphysis.

In the first experiment, young adult (1.5 yr) roosters were subjected to high-speed running for 3 wk (1500 steps per day). Running activated previously quiescent periosteal surfaces in the tarsometatarsal middiaphysis, and the specific sites of activation were highly correlated with circumferential strain gradients (r^2=0.63). In the second experiment, 9 wk old roosters ran (2600 steps per day) for 8 wk. Running modestly altered the mechanical milieu compared to walking, but did not produce significant changes in tarsometatarsal morphology, mechanics, or mineral content. In the third experiment, 200 daily high-impact drop-jumps were applied to 17 wk old roosters for 4 wk. Drop-jumping induced very high strain rates and led to substantially increased bone formation compared to sedentary controls. Strain rates were spatially correlated (r^2=0.44-0.67) with the specific sites of additional bone formation at the endocortical surface. No parameter, however, successfully explained increased periosteal bone formation.

These studies emphasize that the knowledge of the exercise-induced mechanical milieu may help to design exercise protocols that effectively increase bone mass in the growing and young adult skeleton. A previously proposed mechanical parameter (circumferential strain gradients) was confirmed as a good predictor of the specific sites of bone forming surfaces in the young adult skeleton. Comparing the mechanical milieus produced by high-speed running and drop-jumping suggests that the osteotropic efficacy of drop-jumping was accounted for by very high strain rates. The good correlation between the distribution of strain rates and the specific sites of increased lamellar bone formation within the middiaphysis accentuates the sensitivity of growing bone to this mechanical parameter.

ACKNOWLEDGEMENTS

I would like to express my sincere gratitude to my supervisor Dr. Ron Zernicke. His guidance, support, and inspiration enabled me to accomplish this dissertation. His friendship and integrating character made the five years in his laboratory a very memorable experience. The commitment and effort put forth by the members of my supervisory, candidacy, and defense committees – Dr. Bob Bray, Dr. Marcelo Epstein, Dr. Dave Hanley, Dr. Janet Ronsky, and Dr. Christine Snow – is also greatly appreciated.

Special thanks go to my former "PPDF", Dr. Ted Gross, for providing me with invaluable and thoughtful discussions in which he shared some of his insights into the area of bone adaptation with me. I would also like to acknowledge and thank Dr. Adrian Wilson, Friedrich Schaaff, Connor Pardy, Winnie Leng, and Rob Wolff for providing expert technical assistance for different aspects of this dissertation, Dr. John Matyas for contributing his stereo-microscope, and Laural McDonald and Lynn Banach for their invaluable secretarial aid.

All members of the McCaig Centre are gratefully acknowledged for their friendship, help, and support which created a unique atmosphere on our floor. I hope that the friendships with many of the individuals grown over the years will continue into the future. The financial support by the Alberta Heritage Foundation for Medical Research and the Natural Sciences and Engineering Research Council of Canada is recognized.

To my parents Gudrun and Erhard for their infinite support and love throughout my life, and to my wonderful wife Angeline for her unique love and for sharing her life with me.

TABLE OF CONTENTS

Abstract iii
Acknowledgements v
Table of Contents i
List of Tables xi
List of Figures xii
List of Abbreviations xvi

CHAPTER 1 INTRODUCTION AND REVIEW OF THE LITERATURE 1
Anatomy, Physiology, and Function of Bone 2
Exercise Effects on Bone 6
Techniques to Quantify Bone's Response to Loading *6*
Adult Bone *7*
Growing Bone *9*
Exercise and Mechanotransduction in Bone 11
What Component of Exercise is Osteogenic? *11*
What Specific Mechanical Parameter Controls Bone Adaptation? *12*
How do Bone Cells Sense their Mechanical Environment? *17*
Research Question 18
Summary *18*
Objective and Hypothesis *21*
Animal Model and Research Design *21*
Clinical Significance *22*

CHAPTER 2 STRAIN GRADIENTS CORRELATE WITH SITES OF EXERCISE-INDUCED BONE FORMING SURFACES IN THE ADULT SKELETON 24
Abstract 25
Introduction 26
Materials and Methods 28
Experimental Procedures *28*
Strain Gage Procedures *29*

Quantification of Mechanical Parameters 29
Finite Element Modeling (Shear Strain Distributions) 33
Histomorphometry 34
Statistics 35
Results 35
Mechanical Environment 35
Activation of Periosteal Surfaces and Areal Analysis 39
Relation between Mechanical Milieu and Periosteal Activation 40
Discussion 43

CHAPTER 3 DOES THE MECHANICAL MILIEU ASSOCIATED WITH HIGH-SPEED RUNNING LEAD TO ADAPTIVE CHANGES IN THE DIAPHYSEAL TARSOMETATARSUS OF GROWING ROOSTERS? 50
Abstract 51
Introduction 52
Methods 53
Experimental Protocol 53
Determination of the Mechanical Environment 54
TMT Length and Middiaphyseal Areal Properties 55
Histomorphometry 56
Mechanical Testing 57
Ash Content 58
Statistics 58
Results 59
Mechanical Milieu 59
Body Mass, Bone Length, and Areal Properties 62
MAR after 3 wk of Running 62
MAR and Intracortical Remodeling after 8 wk of Running 65
Mechanical and Ash Data 67
Discussion 68

CHAPTER 4 HIGH-IMPACT EXERCISE AND GROWING BONE: THE RELATION BETWEEN HIGH STRAIN RATES AND INCREASED BONE FORMATION IN THE MIDDIAPHYSEAL ROOSTER TARSOMETATARSUS 74
Abstract 75
Introduction 76
Methodology 78
Research Design *78*
Determination of the Mechanical Environment *79*
Histomorphometry *81*
Statistics *84*
Results 84
Body Mass and Tibial Lengths *84*
Mechanical Milieu at the Periosteal Surface *85*
Mechanical Milieu at the Endocortical Surface *89*
Histomorphometry at the Periosteal Surface *90*
Histomorphometry at the Endocortical Surface *92*
Correlations at the Periosteal Surface *94*
Correlations at the Endocortical Surface *96*
Discussion 98

CHAPTER 5 DISCUSSION AND CONCLUSIONS 105
Discussion 106
Summary *106*
Limitations *106*
Correlations of Mechanical Parameters with Sites of Bone Formation *108*
Running versus Drop-Jumping in Growing Roosters *109*
Exercise-Induced Mechanical Milieu in Growing and Adult Roosters *110*
Sensitivity of Growing and Adult Bone to Exercise *111*
Conclusions 111

CHAPTER 6 PUBLICATIONS 114
Refereed Papers (Published or In Press) 115
Refereed Papers (In Review) 115
Conference Proceedings and Abstracts (Peer Reviewed) 116
Book Chapters 117

CHAPTER 7 REFERENCES 118

LIST OF TABLES

Table 3.1 Maximal values for strain magnitude, strain rate, and strain gradients produced in the TMT cortex during walking and running (mean±SE). 61

Table 3.2 Body mass, tarsometatarsal bone length, and middiaphyseal areal properties of control and exercised roosters (mean±SE). Comparisons between controls and runners were non-significant for all parameters. 63

Table 3.3 Endocortical mineral apposition rates (mean±SE) quantified via xylenol orange label 4 wk into the exercise program. 65

Table 3.4 Endocortical mineral apposition rates (mean±SE) quantified via calcein labels 8 wk into the exercise program. The asterisk denotes a significant difference between groups ($p<0.05$). 66

Table 3.5 Middiaphyseal TMT mechanical properties (mean±SE). 67

Table 3.6 Midiaphyseal bone mineral content as determined by percent ash (mean±SE). Different superscripts denote statistically significant differences within groups ($p<0.05$). Values for percent ash of specific regions of the cortex did not differ between groups (control vs runner). 68

Table 4.1 Maximal values for longitudinal normal strain (compressive and tensile), strain rate, and strain gradients produced in the cortex during walking and drop-jumping. 85

Table 4.2 r^2 values produced by correlating the distribution of specific mechanical parameters to mineral apposition rates (MAR) at the periosteal surface. 96

Table 4.3 r^2 values produced by correlating the distribution of specific mechanical parameters to $BFR \cdot BS^{-1}$ at the endocortical surface. 98

LIST OF FIGURES

Figure 1.1 Organization of haversian cortical bone in the middiaphysis of a long bone. Adapted from Nordin and Frankel.[176] 4

Figure 1.2 Micro-photograph of the rod-to-rod lattice arrangement of human trabecular bone in the femoral head. From Gibson.[81] 5

Figure 1.3 Percent changes in BMD following a 10-month aerobic high-impact exercise program in premenarcheal girls. Adapted from Morris et al.[169] 10

Figure 2.1 Example of a microradiograph displaying the three triple-rosette strain gages attached to the TMT middiaphysis. 30

Figure 2.2 Middiaphyseal TMT cross-section subdivided into 12 equal-angle sectors with the centroid as an origin. Mechanical parameters were calculated for the periosteal center of each sector. γ is the angle that was used to express the orientation of the neutral axis. M = medial, A = anterior, L = lateral. 31

Figure 2.3 For each 30°-sector, circumferential strain gradients of longitudinal normal strain were computed as the difference in longitudinal normal strain magnitude ($\Delta\varepsilon$) between the borders of each sector, normalized to the linear distance (d) between these points. 32

Figure 2.4 Sample of longitudinal normal strain magnitude over time recorded from the anterior gage in a rooster running at a speed of 1.66 $m \cdot s^{-1}$. Tensile strains are (by definition) positive and compressive strains are negative. Strain magnitudes produced during swing phase were well below 500 $\mu\varepsilon$ and reached their maximum during mid-stance. 36

Figure 2.5 Distribution of longitudinal normal strain [$\mu\varepsilon$] across the middiaphyseal tarsometatarsal section in a rooster running at a speed of 1.66 $m \cdot s^{-1}$. The distribution in this figure was determined when maximal strains were induced in the cortex (mid-stance). The neutral axis is dashed with strain isopleths plotted parallel to it. Large compressive strains (negative sign) were generated on the

anterior cortex, and large tensile strains were generated on the posterior cortex. (See Fig. 2.2 for orientation). Adapted from Judex et al.[2] 37

Figure 2.6 Distribution of circumferential strain gradients of longitudinal normal corresponding to the strain distribution presented in Fig. 2.5. Circumferential strain gradients generated during stance phase were extremely non-uniform in distribution with the largest strain gradients on the medial and lateral cortices. A = anterior, M = medial. 38

Figure 2.7 Scanned photograph of a middiaphyseal TMT cross-section in which the high-speed running regimen caused activation of medial and antero-lateral periosteal surfaces (bright calcein label). 40

Figure 2.8 Distribution of peak circumferential strain gradients and percentage of labeled surface per sector superimposed on a middiaphyseal TMT cross-section (mean+SE). Sectors with the largest gradients correlated highly (r^2=0.63) with the sectors that exhibited the largest regions of bone forming surfaces..... 41

Figure 2.9 Correlative plot between peak circumferential strain gradients and labeled surface per section. Each data point represents the mean circumferential strain gradient and the mean value of activated periosteal surface per sector. 41

Figure 2.10 Relation between the means of peak longitudinal normal strain and activated periosteal surface per sector. The r^2 value produced by this correlation was 0.06. When absolute strain magnitude was used, the r^2 value increased to 0.24 but the nature of the correlation remained negative. 42

Figure 2.11 Distribution of peak longitudinal periosteal shear strain (mean+SE) contrasted against the distribution of mineralizing surface (mean+SE) demonstrating a lack of correlation (r^2=0.06). A sample finite element mesh of a middiaphyseal section is presented in the inset. 43

Figure 3.1 Example of a middiaphyseal TMT section. Analyses, including the quantification of bone area and surface envelopes, were performed for the entire section as well as site specifically for each sector. A = anterior, M = medial. 57

Figure 3.2 Distribution of longitudinal normal strain superimposed on a middiaphyseal cross-section of a rooster running at a speed of 1.84 $m \cdot s^{-1}$. The distribution in this figure was determined when maximal strains were induced in the cortex (mid-stance). The neutral axis is dashed, and strain isopleths [με] are plotted parallel to the neutral axis. M = medial, A = anterior. 60

Figure 3.3 Distribution of peak circumferential strain gradients (mean+SE) generated at the periosteal surface during walking (0.51 $m \cdot s^{-1}$) and running (1.66 $m \cdot s^{-1}$). Peak values occurring in each sector were averaged across three gait-cycles. Asterisks denote significant differences between running and walking. 61

Figure 3.4 Distribution of cortical bone in runners and controls (mean+SE)..... 64

Figure 3.5 Periosteal mineral apposition rate (MAR) 4 wk into the exercise protocol (mean+SE). Asterisks indicate significant differences between groups ($p<0.05$). . 64

Figure 3.6 Periosteal mineral apposition rate 8 wk into the protocol in controls and runners (mean+SE). The asterisk denotes a significant differences between groups ($p<0.05$). 66

Figure 4.1 Method used to quantify mineral apposition rate (MAR) at the periosteal surface of sector. The original image (a.) was automatically processed to identify the center of the labels with minimal bias. In the processed image (b.) the wide label bands are reduced to thin black lines representing the highest pixels intensities of the labels in the original image. 83

Figure 4.2 Strain recording at the anterior gage during (a.) slow walking (0.51 $m \cdot s^{-1}$) and (b.) drop-jumping. 86

Figure 4.3 Distribution of peak longitudinal normal strain (mean±SE) on the TMT periosteal surface for walking and drop-jumping. Peak values occurring in each sector averaged across three step-cycles (white) and drop-jumps (black). Asterisks denote significant differences between drop-jumping and walking ($p<0.05$). M = medial, A = anterior. 88

Figure 4.4 Distribution of peak strain rate (mean+SE) generated at the periosteal surface during walking and drop-jumping. Asterisks denote significant differences between drop-jumping and walking ($p<0.05$). 88

Figure 4.5 Distribution of peak circumferential strain gradients (mean+SE) generated at the periosteal surface during walking and drop-jumping. Asterisks denote significant differences between drop-jumping and walking ($p<0.05$). 89

Figure 4.6 Distribution of peak strain rates engendered at endocortical and periosteal surfaces during drop-jumping (mean+SE). Asterisks denote significant differences between the two surfaces ($p<0.05$)..... 90

Figure 4.7 Distribution of mineral apposition rate (MAR) in controls and jumpers prior to initiating the study (mean+SE). SEC = value pertaining to the entire section.... 91

Figure 4.8 Distribution of periosteal mineral apposition rate (MAR) in controls and jumpers measured between wk 3 and wk 4 of the experimental protocol (mean+SE). Asteriks denote significant differences between controls and jumpers ($p<0.05$). SEC = value pertaining to the entire section. 91

Figure 4.9 Endocortical bone formation rates (BFR) with bone surface (BS) as referent in control and jump roosters prior to initiation of study (mean+SE). SEC = value pertaining to the entire section. 93

Figure 4.10 Endocortical normalized bone formation rates ($BFR \cdot BS^{-1}$) in controls and jumpers 3 wk into the experimental protocol (mean+SE). Asterisks denote significant differences between jumpers and controls ($p<0.05$). SEC = value pertaining to the entire section. 93

Figure 4.11 Linear regression between strain magnitude and the difference in MAR between jumpers and controls at the periosteal surface. 95

Figure 4.12 Distribution of peak strain rates and increases in $BFR \cdot BS^{-1}$ induced by drop-jumping at the endocortical surface superimposed on a middiaphyseal TMT section (mean+SE). A = anterior, M = medial. 97

LIST OF ABBREVIATIONS

BMC	Bone Mineral Content
BMD	Bone Mineral Density
BS	Bone Surface
BFR	Bone Formation Rate
CT	Computer Tomography
dLS	Double Labeled Surface
DXA	Dual Energy X-Ray Absorptiometry
i.v.	Intravenous
i.m.	Intramuscular
MAR	Mineral Apposition Rate
sLS	Single Labeled Surface
TMT	Tarsometatarsus

Chapter 1

INTRODUCTION AND

REVIEW OF THE LITERATURE

ANATOMY, PHYSIOLOGY, AND FUNCTION OF BONE

Bone is a specialized connective tissue and one of the hardest and strongest tissues in the human body. The function of bone is multifaceted, including serving as levers to facilitate muscle controlled movements, protection of vital organs, storehouse of minerals, and production of hematopoietic cells.[157] These factors are synergistically interrelated and, on a larger scale, may represent mutually antagonistic objectives. For instance, bones have to be strong enough to withstand forces generated during daily activities but, at the same time, should minimize their mass as maintaining bone tissue is metabolically very costly.

Although, macroscopically, bone appears to be inert, it is a very dynamic structure. These dynamics are highlighted by bone's ability to adjust its mass and morphology in response to changes in endogenous (e.g., hormones) or exogenous (e.g., mechanical loading) factors. This ability of bone to adapt functionally to stimuli is vital to meet the changing demands placed on the skeleton throughout life. If triggered, bone's response to stimuli can encompass "remodeling" or "modeling" events. Remodeling is resorption of bone tissue followed by subsequent bone formation. This sequence is often referred to as ARF[157] – activation, resorption, and formation. Upon activation, large multi-nucleated osteoclasts perforate the bone matrix. Osteoblasts (bone forming cells) follow this cutting cone and deposit new bone behind the resorptive front. These groups of cells function as organized units and are called basic multicellular units (BMU).[75] Remodeling may reduce bone mass, but if activation frequency is low (as in healthy young adult bone), reductions in total bone mass are small. Remodeling plays an important role in maintaining stable

serum calcium levels. If serum calcium levels are low, remodeling is initiated, and calcium stored in bone is released into the blood. Another vital function of remodeling is to maintain skeletal mechanical integrity as it may replace bone material that has sustained activity-induced microcracks.[10,168] If microcracks excessively accumulate in bone tissue, stress fractures, a common problem in long distance runners and gymnasts, may occur.[25]

Remodeling is responsible for all events that occur within the cortex (intracortically). Modeling, on the other hand, acts exclusively on endocortical and periosteal surfaces and may, therefore, change the shape of the bone. During modeling, resorption and formation processes do not occur simultaneously on the same surface (i.e., bone resorption is not followed by formation). Modeling comprises activation-formation (AF) and activation-resorption (AR) sequences.[157] Until recently, modeling was only associated with changes during growth, and any changes after skeletal maturation were attributed to remodeling. This view has changed, and it is now generally accepted that osteoinductive signals, including mechanical stimulation and parathyroid hormone, can activate bone formation at previously quiescent surfaces without prior resorption.[26,28,41,42,185]

Grossly, bone tissue can be classified as cortical (also called compact) or trabecular (spongy or cancellous) (Fig. 1.1-1.2). The diaphysis of long bones typically consists of cortical bone whereas the epiphysis and metaphysis comprise trabecular bone covered with a cortical shell. At the tissue level, bone can be divided into woven, primary, and secondary bone. Woven bone can be deposited de novo (without a preexisting bony or

cartilaginous model). It is laid down as a disorganized structure of collagen fibers and osteocytes in situations in which temporary, rapid mechanical support is required, such as after traumatic injuries. Primary bone comprises several types of bone tissue, each with unique morphology and function. For instance, trabecular bone in the epiphyses of long bones consists mostly of primary lamellar bone. Other types of primary bone are plexiform bone, as found in rapidly growing animals, and primary osteons that are formed during growth. Secondary bone is generated when pre-existing primary (or secondary) bone is replaced during remodeling.

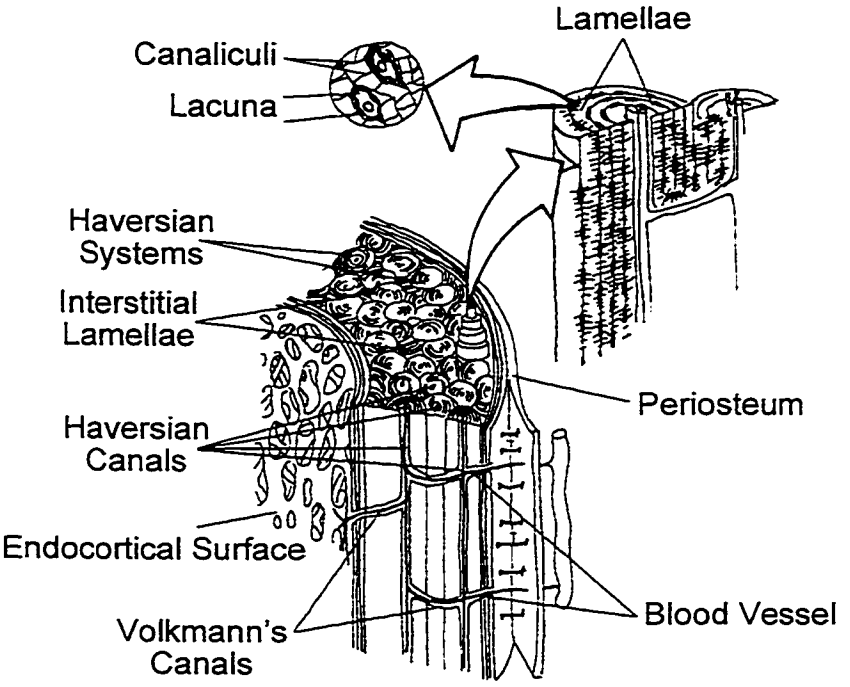

Figure 1.1 Organization of haversian cortical bone in the middiaphysis of a long bone. Adapted from Nordin and Frankel.[176]

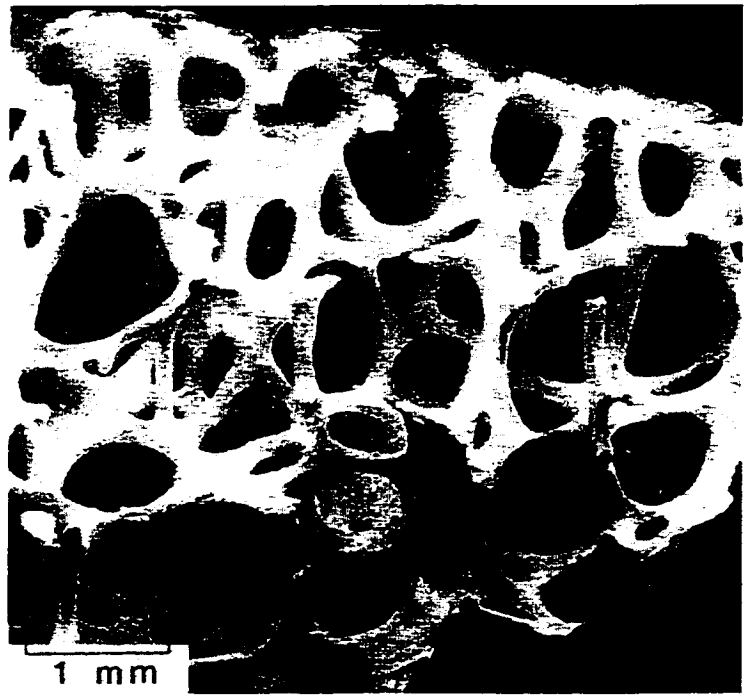

Figure 1.2 Micro-photograph of the rod-to-rod lattice arrangement of human trabecular bone in the femoral head. From Gibson.[81]

Bone is richly innervated and vascularized. An estimated 11% of the cardiac output is sent to the skeleton.[85] Within cortical bone, primary arteries and veins travel within the Haversian canals that are aligned with bone's longitudinal axis (Fig. 1.1). Volkman canals interconnect Haversian canals and are oriented transversely to them. Trabecular bone is void of Haversian and Volkman canals, however, individual trabeculae are in intimate contact with rich vascular supply via bone marrow. Bone's vascular supply has been suggested to play an important role in mediating tissue adaptation.[64,86] When stimulated by blood flow, endothelial cells may express peptides that act directly upon bone cell populations and may, thus, influence bone cell activity.[3,117]

Osteocytes are the housekeeping cells in bone and are located in small caves, called lacunae. Small bone canals (cannaliculi) connect the lacunae. A cellular network exists within the lacunae-cannaliculi system, creating the potential for communication between osteocytes and osteoblasts via gap junctions.[56,57,60,271]

The extracellular matrix of bone comprises inorganic, organic, and fluid components. Calcium hydroxyapatite crystals (inorganic) constitute about half of total bone volume and account for 99% of total body calcium. Another 39% of bone volume consists of organic components, primarily type I collagen (95%) and proteoglycans (5%). The remaining volume is taken up by fluid in lacunea and cannaliculi, within the hydroxyapatite matrix, and in vascular channels. Bone's structure and function is covered in more detail elsewhere.[44,157]

EXERCISE EFFECTS ON BONE

Techniques to Quantify Bone's Response to Loading

The close relation between mechanical forces acting upon bone tissue and skeletal morphology was identified long ago.[79,209,281,283] Exercise may change loading patterns of bone and responses to exercise may include alterations in bone geometry, bone quality, and bone quantity. In exercise studies involving humans, the most common method to quantify these alterations is dual energy x-ray absorptiometry (DXA). This technique is easy to use, non-invasive, and quantifies bone mineral content (BMC [g]). Two dimensional bone mineral density (BMD [$g \cdot cm^{-2}$]) is determined by normalizing BMC to the scanned area. BMD, however, represents an incomplete correction for size as it fails

to take into account information on the depth. Consequently, DXA measurements underestimate true bone mineral density in people with small bones and overestimate bone mineral density in people with large bones.[32] It cannot differentiate between changes in bone quality, bone quantity, or bone geometry. Another potential limitation of DXA is that the respective measure is averaged across the measuring field, and significant focal changes in bone morphology may remain undetected. High resolution quantitative computed tomography (QCT) can overcome these difficulties as it can generate highly detailed three-dimensional images. Presently, however, the higher exposure to ionizing radiation through QCT precludes its wide spread use for routine BMD assessment. Other non-invasive methods to assess bone mineral and structure including quantitative ultrasound (QUS), quantitative magnetic resonance (QMR), and magnetic resonance microscopy (μMR) have been reviewed recently.[80] In animal models, various invasive techniques (e.g., histomorphometrical[183,194] or biomechanical[160,261]) can be used to detect the response of bone to increased mechanical loading in more detail.

Adult Bone

Cross-sectional studies consistently reveal that bone morphology can change markedly in response to long-term exercise. In male tennis players, the cortical wall thickness of humeri in the playing extremity can be up to 45% larger compared to humeri in the non-playing extremity.[92] Similar bone hypertrophy has been reported in feet of classical ballet dancers.[131] Other cross-sectional studies have related a variety of different kind of physical activities to increased bone mass including soccer,[280] weightlifting,[9,72,82,94,150,189]

speed skating,[100] squash,[100] dancing/gymnastics,[100] and a generally higher level of physical activity.[240,247,270] However, self selection bias cannot be discounted in cross-sectional comparative studies and results from longitudinal prospective studies may provide more reliable information on how bone responds to exercise.

Unfortunately, results from prospective studies are more equivocal. Intense exercise in young army recruits stimulated large increases in BMD[145] whereas many other studies found more modest[59,173,238,279] or even negligible[20,39,50,82,101,102,190,272] increases in bone mass. The question as to which exercise mode is the osteogenically most effective has been very inconclusive. The notion prevails that high-load, high-impact exercises using few repetitions are superior to those exercises using low loads and high repetitions.[58,63,94,103,109,206,254] Swimming is an example for a low-load high-repetition exercise and has often failed to produce significant changes in cross-sectional as well as longitudinal studies.[63,254] On the other hand, some reports suggest that aerobic exercise (including swimming) is highly capable of eliciting an adaptive response in bone,[90,101,179,238,250] while some strength exercise regimens did not increase BMD.[39,207,272] Comparative studies often find only modest differences among different modes of exercise, and the largest differences are frequently observed between exercisers and controls and not between athletes subjected to differing exercise programs.[9,12,90,175,238]

After about age 40, significant bone loss occurs at most skeletal sites. Studies involving older subjects indicate that the primary effect of exercise in the adult skeleton is conservation of bone mass and not acquisition of new bone. Nevertheless, some anatomical sites may even gain new bone in response to exercise.[37,59,120,128,133,173,235] The

combination of diminished bone loss and slightly increased bone formation can have substantial effects on the skeleton as demonstrated in a cross-sectional study of competitive runners in their sixth decade.[135] Runners with a running history of 10 years had approximately 40% larger vertebral BMD than non-exercising age matched controls.

Growing Bone

Actively forming and resorbing surfaces in immature bone differ drastically from the predominantly quiescent surfaces in the adult skeleton, and exercise studies involving growing bone have generated even more disparate results than studies involving adult bone. In cross-sectional studies, athletes from a variety of backgrounds exhibit larger BMD than more sedentary controls including tennis and squash players,[92,93] badminton players,[177] ice-hockey players,[177] gymnasts,[35,45] and figure skaters.[232] That exercise can produce significant bone apposition additional to growth effects is supported by several longitudinal studies reporting positive skeletal consequences for numerous activities including high-impact exercise,[169] soccer,[61] swimming,[226] jumping,[269] and running.[174,195,224,246,282] For instance in premenarcheal girls, a 10-month high-impact aerobic exercise regimen significantly increased BMD at all measured regions including the lumbar spine, leg, arm, pelvis, proximal femur, and femoral neck.[169] Depending on the anatomical site, increases in BMD between the start and end of the exercise protocol were 2-7 times larger in the exercise group than in the control group (Fig. 1.3).

Although exercise can produce substantial changes in the immature skeleton several studies have reported only very modest or negligible exercise effects.[14,102,132,177,204,278]

Similarly to mature bone, it appears that weight bearing, higher impact exercises are more osteogenically effective than low-impact exercises.[19,35,45,83] Additionally to positive or negligible responses of bone to exercise, enhanced mechanical loading can cause substantial negative effects in growing animals.[18,68,106,119,121,147,160,171,278] In particular, exercise protocols that are very high in intensity and long in duration have been shown to suppress normal growth and maturation. For example, running 3 wk old roosters for 5 wk at 75% of their maximal aerobic capacity retarded growth of periosteal circumference (28%), medullary area (49%), cortical bone area (21%), moments of inertia (30-46%), and bending stiffness (40%) of the middiaphyseal tarsometatarsus compared to age matched sedentary controls.[160] It is unclear what specific exercise component leads to

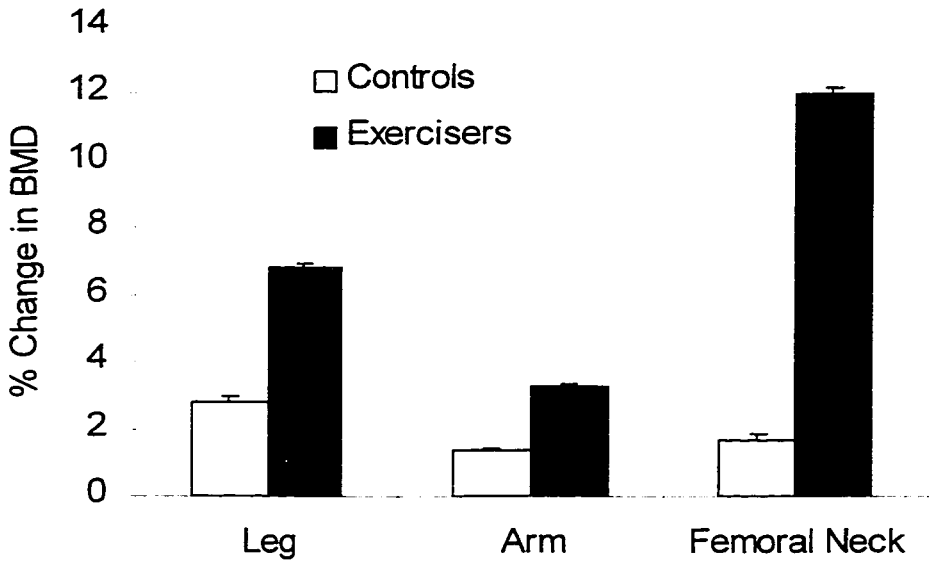

Figure 1.3 Percent changes in BMD following a 10-month aerobic high-impact exercise program in premenarcheal girls. Adapted from Morris et al.[169]

these detrimental effects but there is increasing evidence that they are caused directly by a specific aspect of the mechanical environment (associated with exercise mode, intensity, duration, and frequency) rather than by the indirect influence of a systemic, hormonal response.[68,106,147,171] Certainly, differences in exercise model, exercise history and frequency, physiological status and age of subjects, or measuring technique may also play a role in these discrepant findings among exercise studies involving immature bone. The response of growing and adult bone to physical exercise is covered in more detail by excellent reviews.[5,66,91,233,234,239,241]

EXERCISE AND MECHANOTRANSDUCTION IN BONE

What Component of Exercise is Osteogenic?

Exercise is typically characterized by exercise mode (e.g., running, swimming, weightlifting), intensity (e.g., percent of maximal heart rate), duration, and frequency. These terms, however, are non-specific to bone adaptation and none of these parameters can be directly related to exercise-induced changes in bone. Nevertheless, they define the exercise-generated mechanical environment of bone, and changes between the activity-related and the habitual mechanical environment are primarily responsible for inducing morphological changes. Among the mechanical measures used to quantify bone's mechanical milieu are forces, stresses (forces normalized to unit area), strains (normalized deformations), strain frequency (number of strain cycles per unit time), strain rate (change in strain per unit time), and spatial strain gradients (change in strain per unit length) in various directions within the bone. While it is generally accepted that

the exercise imposed mechanical environment may directly or indirectly affect bone cell populations, it is unknown which particular parameter(s) is most potent for producing new bone or preventing bone loss. This information is critical, however, to design an osteogenically optimal exercise program. For instance, if strain magnitude was the single most important parameter, then large loads should be imposed. If, on the other hand, strain rate was more important, then loads should be applied rapidly.

Because most exercise regimes only locally alter the skeleton's mechanical milieu, it is not surprising that exercise does not produce general, systemic skeletal benefits.[120,256] For instance, running does not generate adaptive changes in the humerus because running does not substantially alter the mechanical environment of this bone. In contrast, running transmits large forces to the tibia that, in turn, can produce adaptive changes. This principle of site-specificity has been overlooked in some studies and may explain some of the discrepant findings related to exercise effects on bone. Conceivably, many other discrepancies are accounted for by the differing exercise-generated mechanical environments, but this has not been tested as the specific mechanical environments were not quantified in almost all exercise studies.

What Specific Mechanical Parameter Controls Bone Adaptation?

The generated mechanical environment must be known to better understand bone's adaptive response. This can be achieved by using exogenous loading models including the turkey ulna loaded through transcortical pins,[217] the rat tibia placed in a four-point bending apparatus,[2,65,259] and the axially loaded rat ulna[258] and rat tail vertebra.[36] The

advantage of these models is that distinct, highly controllable mechanical environments can be generated. Since Wolff's treatise (Wolff's Law),[281] which stated that physical laws govern the modeling and remodeling processes in bone, researchers' attention has focused primarily on strain magnitude. Other parameters have received only limited attention.[230] One of the problems encountered in isolating the effect of a single mechanical parameter is the interrelation of many of the parameters. Changing strain magnitude while maintaining a constant loading frequency, for example, results in a concomitant change in strain rate when sine-like loading patterns are used. Controlled experimental studies that relate the mechanical environment to induced morphological changes indicate that:

(1) Bone is sensitive to applied strain rate, with higher strain rates being more osteogenic.[170,178,266] Static loading (strain rate=0) produces a state similar to disuse resulting in bone resorption.[105,142]

(2) When holding strain frequency and number of loading cycles constant, strain magnitude is highly related to the osteogenic response.[51,70,171,218,231,258] In other words, the larger the generated deformation in the bone matrix, the larger the overall response of the bone. However, the distribution of strain magnitude can be poorly related to the specific sites of bone formation for a given bone section.[87] Thus, bone is possibly not sensitive to strain magnitude per se but rather to a parameter that is related to strain magnitude (e.g., strain gradients or strain rate).

(3) A threshold behavior exists for the number of loading cycles. The full response can be triggered after only a limited number of loading cycles.[22,217,243] In the functionally

isolated ulna preparation, 100 cycles per day of a 1 Hz load regimen with strains approaching 1000 με were necessary to maintain bone mass and new bone formation was stimulated when this level was exceeded.[218] When induced at 0.5 Hz, a loading regime inducing peak strains of approximately 2000 με maintained bone mass by only four cycles a day. Thirty six cycles of the same loading regime saturated the osteogenic response with 1800 cycles being not more effective than 36 cycles.[217] The notion that a finite number of loading cycles employing large loads may increase BMD or inhibit bone loss is supported by exercise studies involving weight lifters.[94,173]

(4) Bone is sensitive to the applied strain distribution. Simply imposing a strain distribution that produces similar peak strain magnitudes in a bone section – but at different locations within the section (i.e., rotating the strain distribution) – may initiate new bone formation.[140,219] Thus, unusual strain events (strain errors) have been suggested to drive bone adaptation.[139,219] Running, for instance, may not be the osteogenically optimal exercise partly because it may generate strain distributions that are very similar to strain distributions induced by normal walking.[112] Additionally, compared to walking, running may not sufficiently elevate peak bone strain magnitudes. It has been suggested that bone not only tries to restore strain distributions but also tries to maintain a certain optimal strain level.[220] This concept is supported by strain gage experiments in a variety of animals in which vigorous physical activity induced similar peak functional strains in the 2000-3000 με range.[16,215,216]

(5) Induced strains do not have to be large to maintain bone homeostasis or to produce an osteogenic response. For instance in the functionally isolated turkey ulna

preparation, a non-linear interdependence between cycle number and induced peak strain magnitude has been observed.[193] When loaded at 1 Hz, peak strains larger than 700 με are necessary to maintain bone mass at 600 cycles a day. This loading threshold can be reduced to 400 με at 36000 loading cycles (30 Hz) and to 70 με at 100000 cycles (30 Hz).[161,193] Whether the high frequency of loading or whether the shear increase in loading cycles accommodated bone homeostasis at these extremely small magnitude strains is unclear. These high frequency, low magnitude loading regimens can be applied non-invasively via vibrating platforms[73] and hold great potential as a mechanical prophylaxis for osteopenia. Preliminary results from sheep[212,213] and humans[198,211] subjected to platform induced low-magnitude high-frequency strains have demonstrated increases in tibial and calcaneal bone mineral density. Other studies have demonstrated an increasing osteogenic response with increasing loading frequency[264] (for a given peak strain magnitude) supporting the conjecture that loading frequency plays an important role in mechanotransduction in bone. It is to note, though, that the concomitant increase in strain rate may have influenced the results in these investigations.

(6) Bone may be capable of distinguishing between different types of strains. Bone strains can be classified as normal strains and shear strains. Normal strains deform the bone matrix in the direction of bone's longitudinal axis or transverse to it and are generated primarily by axial loads and bending moments. Shear strains, that can be generated by shearing loads and torsional moments, cause angular deformations of the bone matrix. Several studies suggest that shear strains have less osteogenic potential than

normal strains,[99,184,210] but shear strains may be important to minimize (intracortical) bone turnover.[210]

(7) Circumferential strain gradients of longitudinal normal strain are highly correlated with periosteal sites of bone forming surfaces in adult bone.[87] Because exercise-related new bone accretion is linked to specific sites within a bone, the structural enhancement of bone can be maximized if the new tissue is added to sites that are at greatest risk to fracture. Thus, it is critical to have a means of controlling the specific sites of new bone deposition. Generally, circumferential strain gradients are largest where strains (deformations) are the smallest. While it is counterintuitive from a structural (engineering) perspective that new bone formation is activated at sites subjected to low strains rather than large strains, physiologically, it is intriguing as strain gradients are proportional to fluid flow in bone.[192] Enhanced fluid flow may affect bone cell populations as discussed below.

These data demonstrate the complexity of the interactions between the produced mechanical environment and bone's response to loading and, in general, support phenomenological observations from exercise studies. However, the variety in bone adaptation phenomena has not been successfully accounted for by a single mechanical parameter and it is likely that bone is responsive to a combination of them or, perhaps, not directly to any of them. The lack of success in explaining bone adaptation by mechanistic approaches has led to phenomenological approaches which attempt to relate loading characteristics to tissue morphology.[31,165] Many of these models use thermodynamical considerations and attempt to calculate the amount of energy absorbed

by the tissue.[99] However, phenomenological models are often poorly supported by in vivo data.[1,193]

How do Bone Cells Sense their Mechanical Environment?

Perhaps one reason for the elusive relation between the mechanical environment and skeletal adaptation is lack of knowledge of how bone cells, the ultimate mediators of bone adaptation, sense biophysical stimuli. The prevailing view is that, in particular, osteoblasts, lining cells, and osteocytes including their osteocytic network may act as sensors of their biophysical environment. Numerous mechanisms by which these cells sense their mechanical environment have been proposed including fatigue micro-damage[163,188] and direct stimulation of bone cells.[244]

Increasing evidence points towards the involvement of bone fluid flow in transducing mechanical signals in bone.[87,182,192,208,264] Bone cells are surrounded by extracellular fluid and, thus, may be sensitive to the following proposed, fluid-flow dependent, parameters: (1) fluid pressure stimulates cells,[110] (2) bone fluid shear stresses excite osteocytes,[127,199,200,277] (3) fluid flow causes mixing and aids in the transport of nutrients to the osteocytes,[134,255] and (4) electrokinetic effects (*i.e.*, streaming potentials).[47,155,181,186,222,245] The driving force for fluid to flow is a pressure differential between two ends of a bone canal[286] that is influenced by spatial and temporal strain gradients.[242] No definite study has demonstrated that biophysical events produced by fluid flow are involved in mechanotransduction in bone. Fluid flow mediated events, however, could account for some experimental inconsistencies in Wolff's Law[281] stating

that the form of bone is related to mechanical stress. For instance, tail suspension in rats increased bone mass significantly in the mandible and skull without significantly increasing bone deformation,[208] a possible result of interstitial bone fluid shift in the head-down position.

While it is unknown how mechanical stimuli are transduced from the tissue to the cellular level, the molecular mechanisms by which individual cells recognize and respond to these mechanical signals are also not well understood. Several hypotheses have been put forward to identify the cellular mechano-electrochemical sensory system, most of which rely on the displacements of cellular and molecular structures.[6,40,107,164,273,274] Once biophysical stimuli trigger the sensory system, bone cells exhibit a great variety of changes in cellular activity in vivo and in vitro including the expression of cytokines and cellular messengers,[152,158,166] prostaglandins,[123,127,152] nitric oxide,[124,126,187] amino acids,[159] proteins,[125,166,167,182,275] enzymes,[51,55,118] and type I collagen.[248]

RESEARCH QUESTION

Summary

Exercise can be a means for moderately increasing bone mass in the growing and young adult skeleton or for mitigating pathological bone loss in the elderly. There is a plethora of studies that associated a great variety of exercise regimens to skeletal changes (or lack of them), thereby generating a substantial amount of information on how different skeletal sites of selected population subsets respond to a given exercise protocol. However, as these studies only identified exercise mode, intensity, duration, and

frequency and did not assess the site-specific skeletal mechanical environment, they contribute little to a direct understanding of how bone responds to its exercise-induced mechanical milieu. This trial and error approach to finding an osteogenically optimal exercise program is inefficient[241] and more controlled exercise studies relating changes (of lack of them) in bone morphology, densitometry, or mechanics to the generated mechanical environment are necessary.

Results from external loading models have identified several parameters important for mechanotransduction in bone. However, strain patterns induced by these means are non-physiological, possibly explaining the extremely large osteogenic response that has not been observed in longitudinal exercise studies. In contrast to external loading models, physiological strain patterns induced by exercise are not a simple imposition and release of loads at the same rate, reflecting the necessity to investigate more physiological signals.

A step towards identifying bone's mechanical milieu during exercise is to record bone strain from in vivo strain gages. Many investigators have utilized strain gages to quantity activity related bone strains in a great variety of species, including humans[27,141] dogs,[29,251,252,268,285] primates,[54,249] roosters,[13,15,112,151] horses,[17,53,88] sheep,[136,137] and rats.[119,171] Yet, only few studies have attempted to relate exercise-induced bone strains to changes in tissue morphology produced by the specific exercise regimen.[13,15,102,119,151] In these studies, changes were investigated in bone strains pre and post exercise intervention. Their data, however, relied on loading assumptions as only strains at gage sites were considered and strain distributions were not determined.[88] A more complete

description of bone's mechanical environment can be accomplished by combining strain gage data with linear beam theory or finite element models.[23,88,221]

Most of the relations between mechanical parameters and bone formation (as discussed previously) were derived for a given cross-section (i.e., the larger the peak magnitude of the specific mechanical stimulus, the larger the response of the bone). This approach is feasible with external loading models in which specific aspects of the loading environment can be adjusted but is very difficult in exercise studies, in particular with animals due to their limited exercise repertoire.

Increasing the magnitude of a specific mechanical parameter within a series of different loading conditions is, however, not the only method for testing the efficacy of a specific parameter. Most aspects of the mechanical milieu (e.g., strain magnitude, strain gradients) are distributed extremely non-uniformly across a bone section during physical activity.[88,112] For instance, in-vivo strain gage data from various animals indicate that, during locomotion, bending is the dominant form of loading in the middiaphysis of limb bones.[215] This causes the neutral axis (line of zero strain) to run across the marrow cavity, with the largest compressive strains generated on one side of the cortex, and the largest tensile strains generated on the opposite side. Morphological changes related to increased mechanical loading are also non-uniform in nature (i.e., addition of new tissue occurs predominantly in certain regions of periosteal and endocortical surfaces).[87,151,160,282] Consequently, a spatial relation between a non-uniformly distributed mechanical parameter and focal changes in bone morphology may exist and the efficacy of these parameters can be tested by the strength of their correlation with the distribution of bone

formation across a section.[23,87,171,229,258] This approach has not been used in exercise models and was adopted for this dissertation.

Objective and Hypothesis

The overall objective of this dissertation was to identify exercise-induced mechanical parameters that stimulate bone growth. It was hypothesized that mechanical parameters that have been associated with fluid flow in bone have the greatest osteogenic relevance. This hypothesis was tested in the adult and growing skeleton.

Animal Model and Research Design

White Leghorn roosters were chosen as the animal model for three main reasons: (1) Roosters are readily trained and exhibit training effects.[14,151,160] (2) Physes close in birds,[96,143] as in humans and unlike in rodents. (3) Similar to human bone, avian bone undergoes haversian remodeling and modeling, however at a rate that is twice as fast. This was considered as an advantage as morphological changes can be observed more rapidly.

All experiments used well-defined mechanical stimuli (high-speed running and high-impact jumping) that were quantified by in vivo strain gages attached to the middiaphyseal tarsometatarsus (TMT). Distributions of several mechanical parameters previously proposed to drive bone adaptation were computed across a middiaphyseal TMT section via linear beam theory and finite element modeling. Thus, unlike in many previous studies, our observations were not limited to the sites of strain gage attachment.

Morphological and histomorphometric measures were used to site-specifically analyze middiaphyseal sections that were subdivided into 12 equal-angle sectors. Thus, different mechanical parameters could be tested by their correlative strength to a response within the middiaphysis.

Clinical Significance

Skeletal pathologies involving bone loss, such as osteoporosis, are having a catastrophic impact upon the quality of life of our elderly population and upon the cost of North American health care. In the United States alone, it is estimated that by the year 2015 more than 41 million women and men older than fifty years will be inflicted with osteoporosis or will be at high risk of developing it.[172] In 1995, the economic burden of osteoporosis was 13.8 billion US dollars[197] and is projected to reach 240 billion dollars by the year 2040.[48] For the treatment of established osteopenia, a variety of pharmacological strategies have been employed with some success, but certainly not to complete satisfaction. Calcitonin, calcium, and vitamin D have been administered with conflicting results.[97,148,149,201] Hormone replacement therapy is considered an effective prevention and treatment of post-menopausal osteoporosis but suffers from low compliance and may possibly increase the risk for endometrial and breast cancer.[24,225] Fluorides[144] can effectively promote bone formation[122] but, depending on the dosage, may also deteriorate bone architecture, decrease bone strength and increase the risk for hip fractures.[205,265,267] Bisphosphonates are powerful anti-resorptive agents and have been successfully used to decrease fracture rates.[62,116] Concern, however, has been expressed

about the lack of long-term data from clinical trials involving bisphosphonates as they inhibit cell activity. Consequently, they possibly diminish bone's capacity to repair inflicted fatigue damage by dramatically decreasing intracortical remodeling (frozen bone). Common to all pharmaceutical interventions is that they are fraught with side-effects and, perhaps as important, that they act indiscriminately throughout the skeleton. Consequently, they may not represent the best strategy to combat a complex disease like osteoporosis that warrants focal prophylaxis.

Alternatively, exercise-induced mechanical stimuli could be used as an exogenous treatment regimen to site-specifically increase bone mass or to prevent bone loss. Although heredity is the principal determinant of bone mineral density, up to half of the variance in bone mineral density is influenced by other factors,[130] including physical activity.[34] Enhancing peak bone mass during skeletal growth and consolidation may represent the optimal primary prevention for diseases involving pathological bone loss.[7,98] To use exercise regimen as mechanical prophylaxis without undesirable side-effects may appear intriguing but attempts to produce substantial morphological changes with exercise regimen have also had limited success.[104] The inability of some exercise protocols to increase bone mass or inhibit bone loss, however, may not stem from an inability of bone to respond to mechanical stimuli, but, rather from a lack of understanding of what specific mechanical stimuli are responsible for controlling skeletal adaptation.

Chapter 2

*STRAIN GRADIENTS CORRELATE WITH SITES OF EXERCISE-INDUCED BONE FORMING SURFACES IN THE ADULT SKELETON**

---

* Reprinted from Judex et al.[113] with the permission of the American Society for Bone and Mineral Research.

ABSTRACT

Physical activity is capable of increasing adult bone mass. The specific osteogenic component of the mechanical stimulus is, however, unknown. Using an exogenous loading model, it was recently reported that circumferential gradients of longitudinal normal strain are strongly associated with the specific sites of periosteal bone formation. Here, we used high-speed running to test this proposed relation in an exercise model of bone adaptation. The strain environment generated during running in a middiaphyseal tarsometatarsal section was determined from triple-rosette strain gages in six adult roosters (> 1 yr). A second group of roosters was run at a high speed (1500 loading cycles per day) on a treadmill for 3 wk. Periosteal surfaces were activated in five out of eight animals. Mechanical parameters as well as periosteal activation (as measured by incorporated fluorescent labels) were quantified site-specifically in 12 30°-sectors sub-dividing a middiaphyseal section. The amount of periosteal mineralizing surface per sector correlated strongly (r^2=0.63) with the induced peak circumferential strain gradients. Conversely, peak strain magnitude and peak strain rate were only weakly associated with the sites of periosteal activation. The unique feature of this study is that a specific mechanical stimulus (peak circumferential strain gradients) was successfully correlated with specific sites of periosteal bone activation induced in a non-invasive bone adaptation model. The knowledge of this mechanical parameter may lead to the design exercise regimens that are able to deposit bone at sites where increased structural strength is most needed.

INTRODUCTION

The dynamic nature of bone is reflected in its ability to generate morphological changes in response to altered mechanical loading. Physical exercise can elevate strain levels in weight-bearing bones,[27,112,215] and thus, it has been suggested that exercise regimens may serve to mitigate osteoporosis by enhancing bone mass in the mature skeleton. The specific osteogenic effects of different exercise regimes (e.g., running, swimming, weightlifting) on the adult skeleton, however, have been equivocal. While cross-sectional studies suggest that long-term exercise may elevate substantially the mass of weight-bearing bones in humans,[92,111] short-term longitudinal studies demonstrate only negligible or modest increases.[101,102,190,238] This may reflect the limited sensitivity of some measuring techniques to detect focal bone adaptation as well as the lack of knowledge of the specific mechanical parameter(s) responsible to initiate new bone formation.

At the tissue level, several mechanical parameters have been proposed to initiate bone formation including, but not limited to, strain magnitude,[218] strain history related parameters,[31] strain rate,[170,178,266] strain energy density,[33,77] and circumferential strain gradients.[87] Most of the relations between mechanical parameters and bone formation (at least those that were observed experimentally) were derived for a given cross-section (i.e., the larger the specific aspect of the mechanical stimulus, the larger the response of the bone). Although it has been proposed that relations determined for a cross-section may also be valid for any given volume of bone, this has not been confirmed. To test this experimentally, the distribution of the mechanical signal could be associated with the distribution of the response across a bone section. If such a site-specific relation exists

between a particular mechanical parameter and changes in bone morphology, then the knowledge of this specific osteogenic component of the mechanical environment may provide information about a mechanism by which bone cells perceive their mechanical environment. Also, if a mechanical parameter consistently predicts the specific sites of bone formation in different models then prophylactic exercise programs may be designed that deposit bone at sites where additional structural strength is required to reduce the risk of fractures.

Recently, gradients of longitudinal normal strain (in particular, peak circumferential strain gradients) have been found to be correlated highly with specific sites of bone formation induced by controlled exogenous loading.[87] Strain gradients reflect differential deformations across a volume of tissue in a given direction. Physiologically, strain gradients are relevant as they generate pressure differentials within bone and, thereby, may contribute to fluid flow in bone.[192] Here, we examined whether circumferential strain gradients of longitudinal normal strain were associated with the sites of bone formation in an exercise model of bone adaptation. Circumferential strain gradients induced by increased gait-speed provide a focal mechanical stimulus,[112] as their magnitudes are non-uniform in distribution at a given cross-section in the rooster tarsometatarsus (TMT) and increase significantly in a non-uniform fashion with increased locomotor speed. TMT middiaphyseal bone formation in response to increased physical activity is also focal in nature as the deposition of tissue is limited to specific sites within a middiaphyseal section.[151,160] Consequently, we hypothesized that sites of bone forming

surfaces stimulated by high-speed running would be significantly correlated with maximal circumferential strain gradients.

MATERIALS AND METHODS

Experimental Procedures

Twenty-two, skeletally mature, White Leghorn roosters were divided into three groups. The first group of six 1-yr old animals previously acclimatized to treadmill running were strain gaged, and the middiaphyseal distribution of selected mechanical parameters was determined. A second group of eight, 60-80 wk old, animals ran (1.66 $m \cdot s^{-1}$) on the treadmill for 3 wk, 6 $days \cdot week^{-1}$, 9 $min \cdot day^{-1}$ ($\approx$ 1500 $step\text{-}cycles \cdot day^{-1}$). The speed of 1.66 $m \cdot s^{-1}$ reflected a balance between a gait speed that significantly elevated circumferential strain gradient magnitudes[112] and a speed at which roosters were capable of running continuously for 9 min. Prior to starting the exercise regimen, animals were acclimatized to treadmill running for 2 wk. Calcein (Sigma Chemical Co., St. Louis, MO) was administered (20 $mg \cdot kg^{-1}$, i.v.) on days 7 and 21 of the exercise regimen to reveal sites of periosteal activation. Animals were killed two days after the second calcein injection with a 1 ml intravenous injection of Euthanyl (MTC Pharmaceuticals, Cambridge, ON). We then correlated the specific sites of mineralization observed in this group of roosters to the distribution of mechanical parameters determined from the group of strain gaged roosters. The third group of eight, 60-80 wk roosters served as (sedentary) controls and received calcein injections but no treadmill exercise. All roosters were group-housed in pens (3x4 m) and received the same standard diet and water ad libitum.

All procedures were approved by the Animal Care Committee of the University of Calgary.

Strain Gage Procedures

In the first group of 6 roosters, triple rosette strain gages (FRA-1-11-1L, Tokyo Sokki Kenkyujo Co., Japan) were attached to the medial, anterior, and lateral aspects of the left TMT middiaphysis (Fig. 2.1) using cyanoacrylate adhesive (Krazy Glue for semiporous materials, Borden Co., Willowdale, ON, Canada). After a 24-h recovery, each animal ran on a treadmill at 1.66 $m \cdot s^{-1}$ while data were sampled (200 Hz) for 10-s periods and filtered at 1 kHz. Post-mortem, the orientation of the rosette strain gages relative to the longitudinal bone axis was obtained from high resolution contact microradiographs (Cabinet X-Ray System, Faxitron X-Ray Corp., Buffalo Grove, IL). Using a diamond wafer saw, middiaphyseal transverse TMT sections (300 μm) were cut from the left legs, and microradiographs of these sections were scanned on a flatbed scanner. The locations of the strain gages were obtained directly from the cross-sectional microradiographs. Custom software calculated values of longitudinal normal strain and longitudinal shear strain at each gage site for each sampled time point.

Quantification of Mechanical Parameters

The distribution of longitudinal normal strain acting upon a middiaphyseal cross section was quantified using linear beam theory.[221] This method models the TMT middiaphysis as a prismatic beam subjected to axial loading and bending moments; it is assumed that

points in a plane passing through the unloaded bone remain in this plane during loading. The relative accuracy of beam theory to determine bone strain distributions during functional loading has been verified experimentally[221] and by finite element models.[2,23] The orientation of the neutral axis during running was expressed with respect to an axis parallel to the anterior cortex (Fig. 2.2). All calculated angles were averaged across three consecutive gait cycles in each animal.

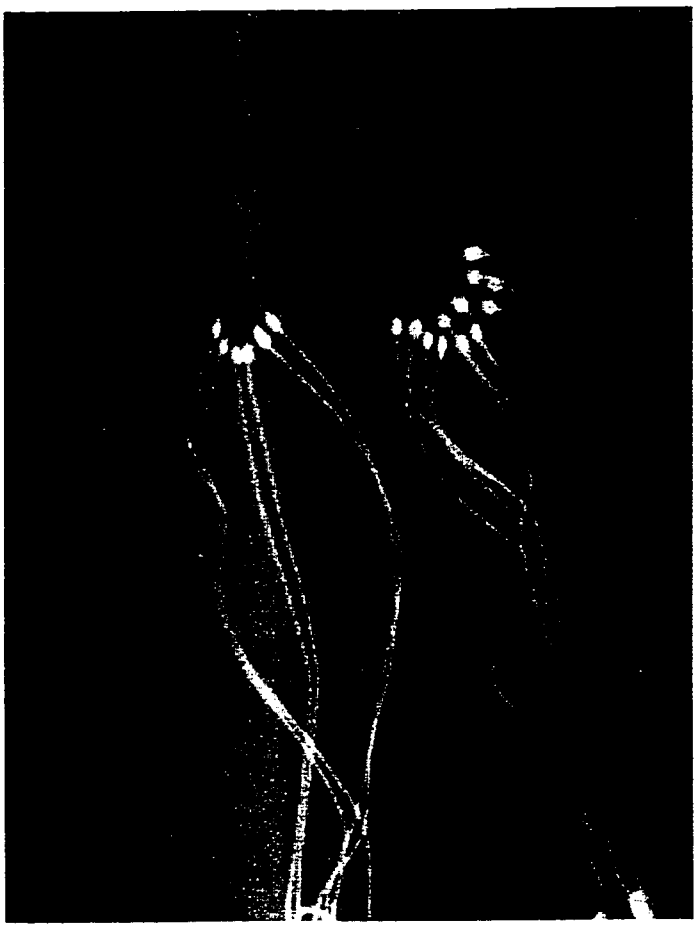

Figure 2.1 Example of a microradiograph displaying the three triple-rosette strain gages attached to the TMT middiaphysis.

Pixel-counting routines (PV-Wave, Visual Numerics, Houston, TX) were used to divide the binary images of the cross-sections into 12 30°-angle sectors with the centroid as an origin (Fig. 2.2). Note that all strain gradients defined in this manuscript are strain gradients of longitudinal normal strain. Circumferential surface strain gradients were calculated in each 30°-sector as the absolute difference between longitudinal normal strain on the periosteum of the borders of each sector normalized to the linear distance between these points (Fig. 2.3). Radial strain gradients were determined, in analogy to circumferential strain gradients, between the midpoints of the periosteal and endocortical surface in each sector.

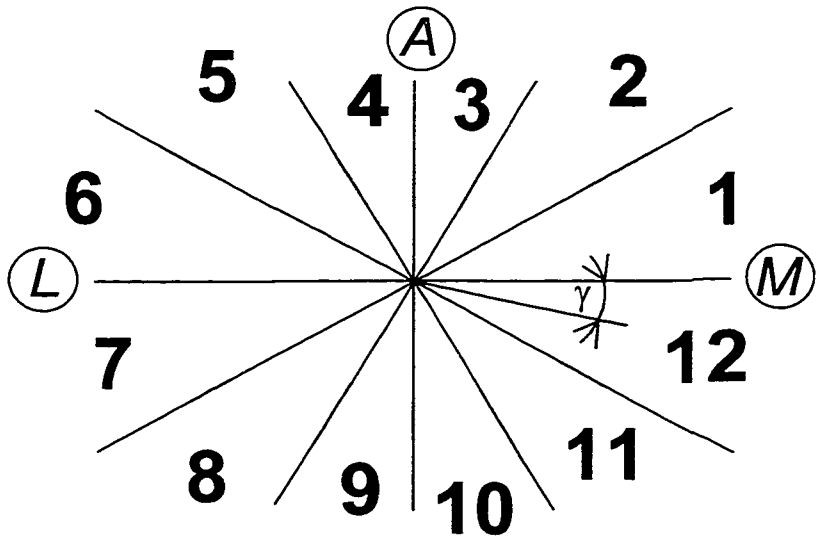

Figure 2.2 Middiaphyseal TMT cross-section subdivided into 12 equal-angle sectors with the centroid as an origin. Mechanical parameters were calculated for the periosteal center of each sector. γ is the angle that was used to express the orientation of the neutral axis. M = medial, A = anterior, L = lateral.

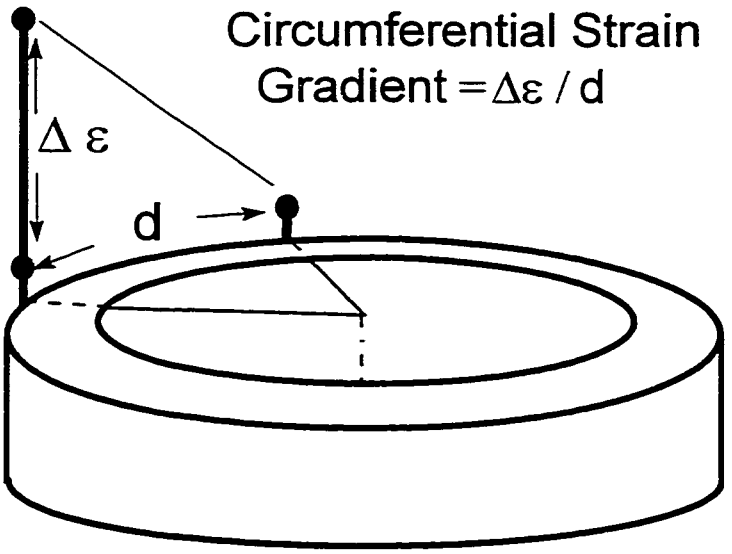

Figure 2.3 For each 30°-sector, circumferential strain gradients of longitudinal normal strain were computed as the difference in longitudinal normal strain magnitude ($\Delta\varepsilon$) between the borders of each sector, normalized to the linear distance (d) between these points.

The distribution of longitudinal strain gradients acting on periosteal surfaces of the middiaphysis was estimated between two transverse sections, 3 mm above and below the gage section. In each sector, the magnitude of the longitudinal surface strain gradient was determined by longitudinal changes in strain magnitude and periosteal surface geometry. Changes in strain magnitude were estimated by extrapolating longitudinal normal strain distributions from the strain gaged section via linear beam theory. Briefly, the forces and moments acting on the gage section were computed and increased (decreased) by 4% for the sections 3 mm above (below) the gage section. The scaled forces and moments were then used to calculate the strain distribution in these sections. Longitudinal changes in middiaphyseal periosteal surface geometry were determined from a different set of six age-matched roosters from the same cohort as the original strain gaged roosters since the

middiaphyses from strain gaged roosters were not intact any more. TMTs from those roosters were embedded in polymethyl-methacrylate (PMMA) and sectioned at the middiaphysis (3 sections per bone at 3 mm intervals). Radiographs of the sections were taken and scanned. Images were then aligned according to groves in the PMMA blocks, and geometrical differences in periosteal midpoints of each sector were calculated between the proximal and distal section.

To contrast strain gradients with other mechanical parameters, we also determined peak longitudinal normal strain and peak strain rate at the periosteal center of each sector. Peak values of all mechanical parameters were averaged across three consecutive step cycles for each animal. We determined the peak magnitude of each mechanical parameter that occurred in each sector during the gait cycle as we assumed that this would be the single most important factor for the potential activation of bone cells.

Finite Element Modeling (Shear Strain Distributions)

The distribution of longitudinal shear strain across a middiaphyseal section was determined by modeling the TMT as a prismatic cantilever subjected to end shearing forces and a torsional moment. Finite element meshes were developed in PATRAN (MacNeal Schwendler Corp., Costa Mesa, CA) for each strain gaged TMT consisting of 2460-2760 isoparametric 20-node brick elements arranged in 20 longitudinal and 3 radial layers (Fig. 2.11). ABAQUS (Hibbit, Karlson & Sorenson Inc., Newark, CA) was used to determine initially the shear strain distribution for an arbitrary torsional moment and end shearing forces. Subsequently, the predicted and the recorded strain values were

compared at all three gage sites and the torsional moment and end shearing forces were scaled.[88] Longitudinal shear strain acting on a middiaphyseal section was expressed as the vector sum of ε_{xz} and ε_{yz} at the periosteal center of each of the 12 30°-sectors (see Fig. 2.11 for orientation of coordinate system).

Histomorphometry

Cross-sections (300 μm) were cut from left and right middiaphyseal TMTs of the exercised group as well as the control group, and consequently, the location of these sections coincided with the location of strain gage attachments in the first group of animals. Sections were hand-ground to 100 μm and microradiographs were taken. Microradiographs were enlarged and scanned on a stereomicroscope (Stemi 2000-C, Carl Zeiss Jena GmbH, Jena, Germany) with a video-camera attached to it. Edge detection programs were used to binarize the image, and pixel counting routines calculated bone cross-sectional area and second moments of inertia about the bending axis imposed during running (as determined from the group of strain gaged animals) as well as about the axis transverse to the bending axis.

Sections were then ground to 60-70 μm and examined under an epifluorescent microscope at magnifications of up to 800 times. Photographs of each quarter of the section were taken, scanned on a flatbed scanner and assembled using image software (Photoshop, Adobe Systems Inc., San Jose, CA). Using the method described above, sections were subdivided into 12 sectors. The beginning and end of each periosteal fluorescent label was determined interactively on the monitor. Custom software (PV-

Wave) quantified the fluorescently labeled periosteal surface relative to the total periosteal surface within each sector. Symmetrical gait of the bipedal birds was assumed, and thus, histomorphometrical data of the left and right TMT were averaged for each animal.

Statistics

Linear regression analysis determined the r^2 values for the correlations between the distribution of each mechanical parameter and the distribution of mean percent labeled bone surface per sector. A non-parametric Mann-Whitney-U test was used to test for significant differences in mineralizing surface between the groups of exercised and sedentary roosters and to test for differences in areal properties between roosters that responded to the exercise regimen and roosters that lacked a response. A significance level of 0.05 was employed for all tests. All values reported in the Results are the means±SE for the respective animal subset.

RESULTS

Mechanical Environment

High-speed running generated an extremely non-uniform strain environment in the middiaphyseal TMT. Peak compressive strains of -1850±80 με were engendered in the anterior cortex. Peak tensile strains of 1220±200 με were located in the posterior cortex. The neutral axis spanned the lateral and postero-medial cortices and varied little during stance phase (Fig. 2.5). During the time period of stance phase at which longitudinal

strains of 1000 με or more were generated, the total range of rotation was only 10±2°. Additionally, the orientation of the neutral axis was similar for each rooster at the point in time at which peak strains were induced in the cortex: 14±5° (see Fig. 2.2 for definition of the angle). This information is important because the distributions of circumferential and radial strain gradients are primarily dependent on the orientation and not on the location of the neutral axis.

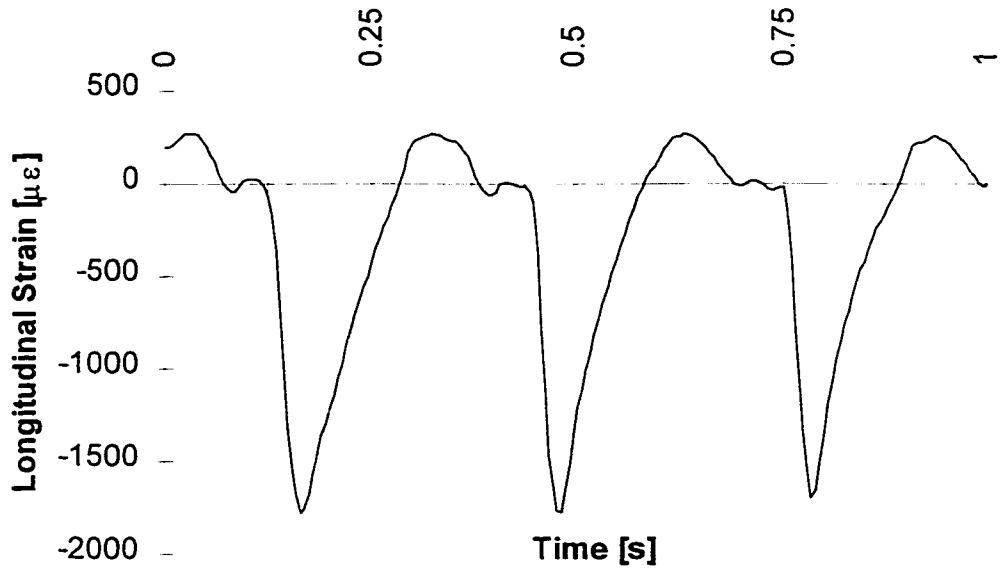

Figure 2.4 Sample of longitudinal normal strain magnitude over time recorded from the anterior gage in a rooster running at a speed of 1.66 $m \cdot s^{-1}$. Tensile strains are (by definition) positive and compressive strains are negative. Strain magnitudes produced during swing phase were well below 500 με and reached their maximum during mid-stance.

The magnitudes of peak circumferential strain gradients were highly non-uniform in distribution, with the smallest circumferential strain gradients located on the anterior and posterior cortices, and with the largest circumferential strain gradients located on the

medial and lateral cortices near the neutral axis (Fig. 2.6) The magnitudes of peak radial strain gradients were in the same range as peak circumferential strain gradients, and sites of maximal radial strain gradients coincided with the sites of minimal circumferential strain gradients and vice versa. Due to the nearly prismatic shape of the TMT middiaphysis, maximal longitudinal strain gradients were an order of a magnitude lower than maximal radial and circumferential strain gradients.

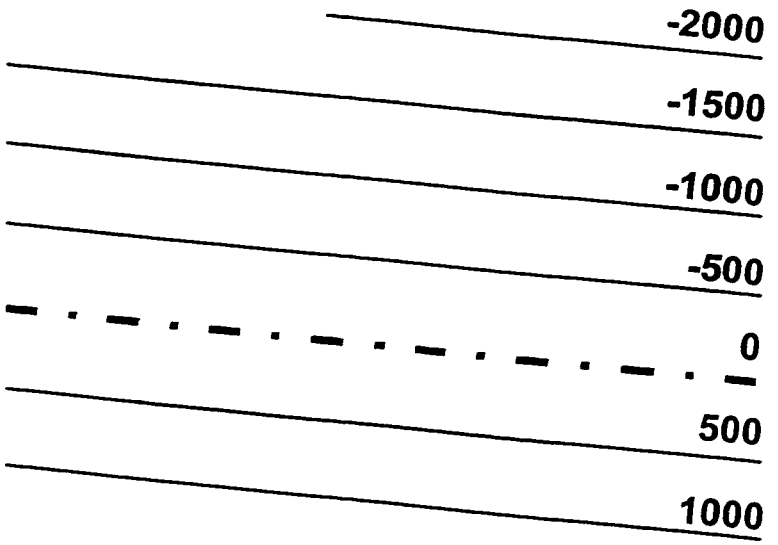

Figure 2.5 Distribution of longitudinal normal strain [με] across the middiaphyseal tarsometatarsal section in a rooster running at a speed of 1.66 $m \cdot s^{-1}$. The distribution in this figure was determined when maximal strains were induced in the cortex (mid-stance). The neutral axis is dashed with strain isopleths plotted parallel to it. Large compressive strains (negative sign) were generated on the anterior cortex, and large tensile strains were generated on the posterior cortex. (See Fig. 2.2 for orientation). Adapted from Judex et al.[2]

Maximal periosteal shear strains generated in the cortex averaged 1580±190 με. The largest shear strain magnitudes were observed at the anterior aspect of the cortex (sectors 3-5) and coincided roughly with the sites of largest compressive strains. Peak

shear strains generated in the remaining sectors were relatively uniform in distribution (Fig. 2.11). Similarly to longitudinal normal strain, shear strains in all sectors reached their peak values during mid-stance. By superposition, peak shear strains at any point of the cortex were the result of a combination of applied shearing forces and a torsional moment. When applied separately, the combined end shearing forces generated shear strain magnitudes that were only between 12% and 29% (depending on the sector) of the shear strain magnitude generated by the torsional moment.

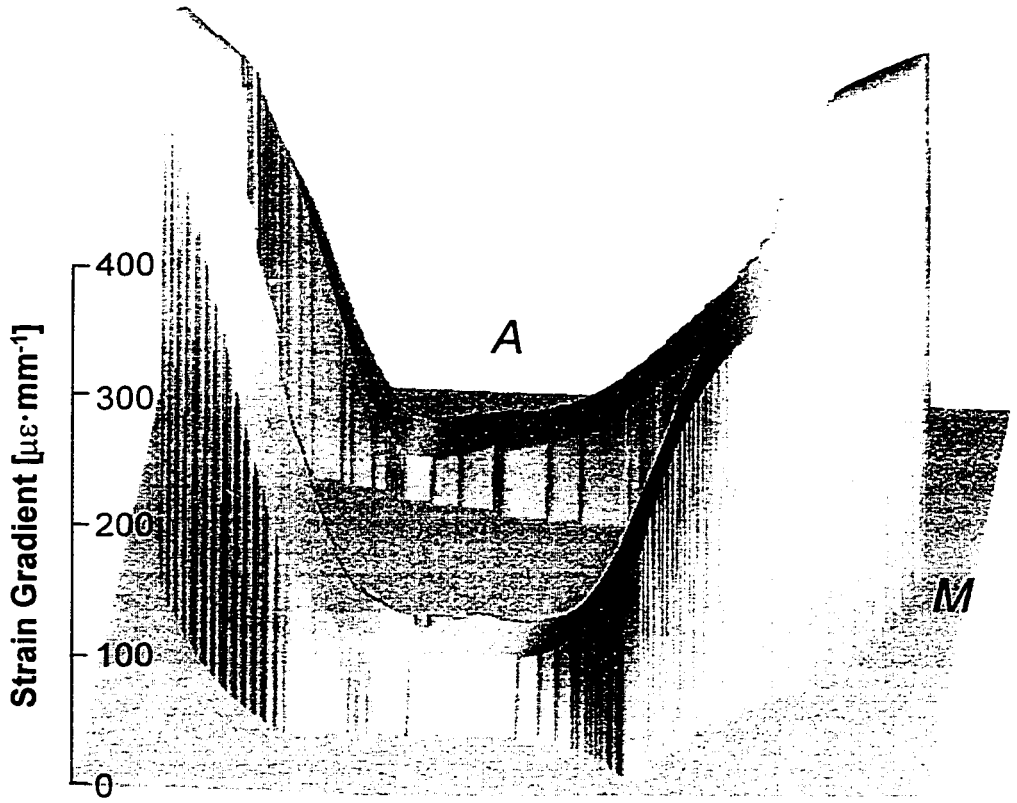

Figure 2.6 Distribution of circumferential strain gradients of longitudinal normal corresponding to the strain distribution presented in Fig. 2.5. Circumferential strain gradients generated during stance phase were extremely non-uniform in distribution with the largest strain gradients on the medial and lateral cortices. A = anterior, M = medial.

Activation of Periosteal Surfaces and Areal Analysis

Focal periosteal activation was observed in five out of eight exercised roosters undergoing the exercise regimen (Fig. 2.7). Partially double-labeled osteonal and endocortical surfaces verified that both calcein injections had worked in all roosters. However, even under high magnifications (800x), a periosteal double label could be detected only in one exercised rooster. In this animal, the double labeled surface accounted for less than 35% of the total labeled periosteal surface. Periosteal surfaces of 7 out of 8 control sedentary roosters were completely quiescent and one rooster demonstrated minimal periosteal mineralization of the anterior cortex (less than 1.5% of the total surface). The ratio of mineralizing surface (MS) to bone surface (BS) was significantly increased in the group of exercised roosters compared to the control group (22.6% vs 0.2%). Consequently, mineralizing periosteal surfaces observed in the exercised roosters could be attributed to the exercise regimen. In contrast, scattered labels were observed on endocortical surfaces in control roosters. As the goal of this study was to relate specific mechanical stimuli to sites where a previously quiescent bone surface was activated, we limited our analysis to periosteal surfaces.

Middiaphyseal cross-sectional area and cross-sectional moment of inertia about the locomotion induced bending axis were not significantly different between the roosters that responded to the exercise regimen and the non-responders (area: 24.1±0.7 mm^2 vs 22.5±1.1 mm^2; $I_{bending}$: 92.1±3.6 mm^4 vs 95.8±17.6 mm^4). Across all 8 roosters, the ratio between the second moment of inertia about the bending axis and the moment about the axis transverse to it was 0.54±0.01.

Figure 2.7 Scanned photograph of a middiaphyseal TMT cross-section in which the high-speed running regimen caused activation of medial and antero-lateral periosteal surfaces (bright calcein label).

Relation between Mechanical Milieu and Periosteal Activation

The distribution of peak circumferential strain gradients correlated significantly with the distribution of mineralizing surfaces across a middiaphyseal section (r^2=0.63, $p<0.002$) (Figs. 2.8-2.9). The correlation between peak circumferential strain gradients and activated surfaces was similar in the left (r^2=0.59) and right (r^2=0.57) TMTs. Due to the inverse relation between radial and circumferential strain gradients, the distribution of peak radial strain gradients produced a significant but negative correlation (r^2=0.72). Peak longitudinal strain gradients were not correlated (r^2=0.02). Combining strain gradients in the three directions via multiple regression analysis generated a R^2 value of 0.72.

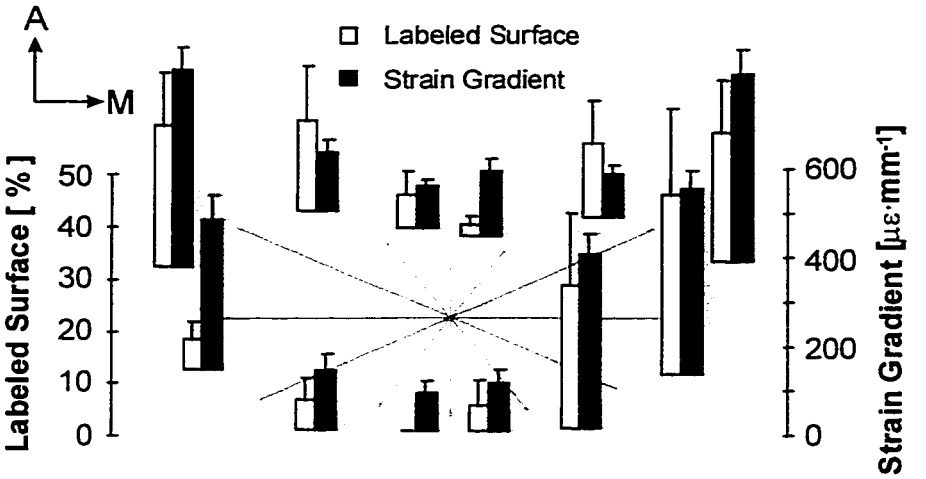

Figure 2.8 Distribution of peak circumferential strain gradients and percentage of labeled surface per sector superimposed on a middiaphyseal TMT cross-section (mean+SE). Sectors with the largest gradients correlated highly (r^2=0.63) with the sectors that exhibited the largest regions of bone forming surfaces.

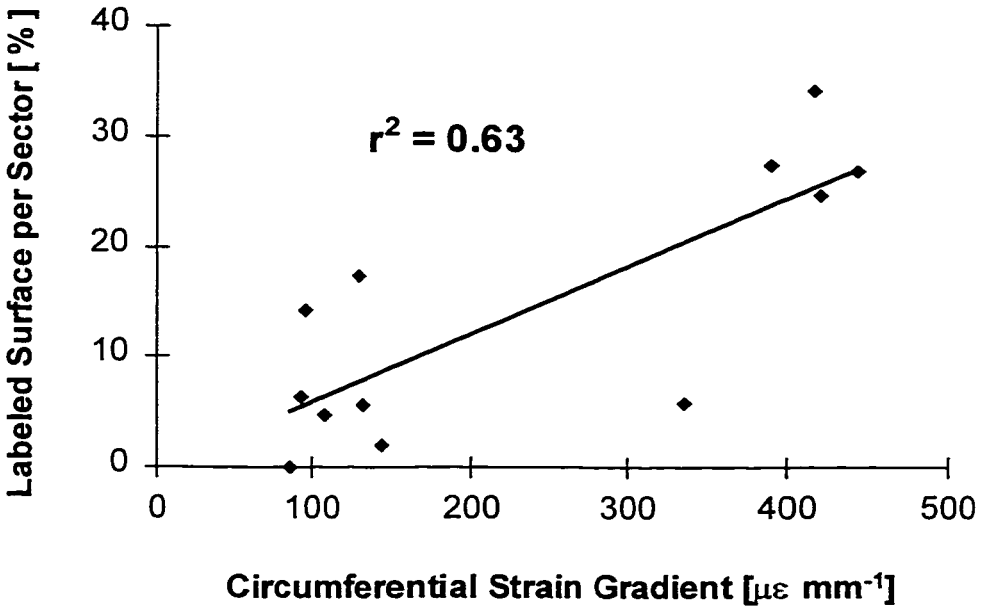

Figure 2.9 Correlative plot between peak circumferential strain gradients and labeled surface per section. Each data point represents the mean circumferential strain gradient and the mean value of activated periosteal surface per sector.

Because new bone formed near locations of least, rather than greatest strains, the specific sites of mineralization were not positively correlated with peak absolute longitudinal normal strain (r^2=0.24, negative correlation). When the sign was incorporated into the correlation between strain magnitude and periosteal bone activation the r^2 value decreased to 0.06 (Fig. 2.10). As the distribution of peak strain rate was highly associated with the distribution of peak strain magnitude, strain rate also failed to produce a significant positive correlation with the osteogenic response (r^2=0.28, negative correlation). Similarly, the distribution of peak longitudinal periosteal shear strain could not account for the distribution of activated surfaces observed (r^2=0.06).

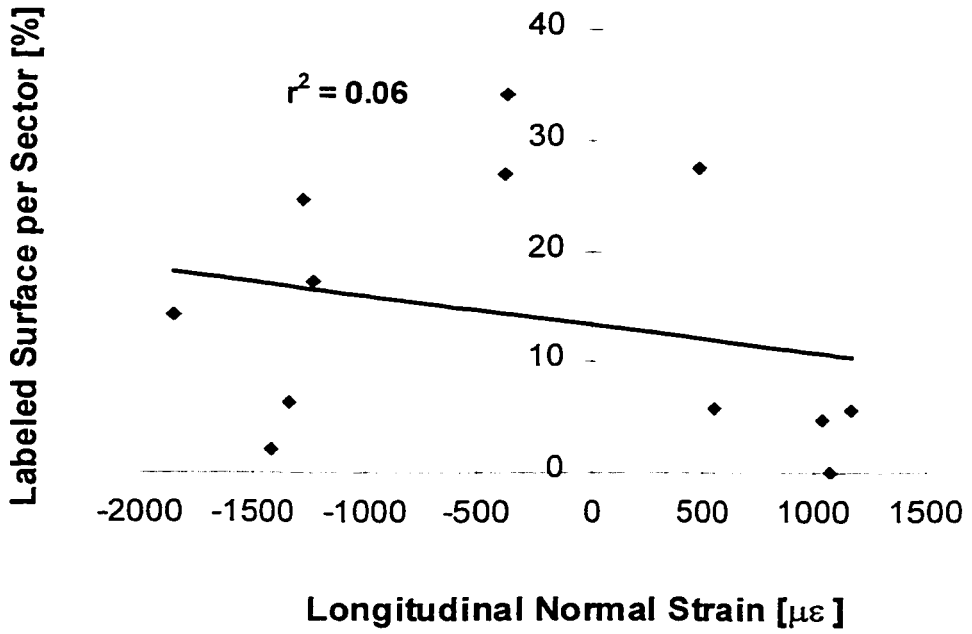

Figure 2.10 Relation between the means of peak longitudinal normal strain and activated periosteal surface per sector. The r^2 value produced by this correlation was 0.06. When absolute strain magnitude was used, the r^2 value increased to 0.24 but the nature of the correlation remained negative.

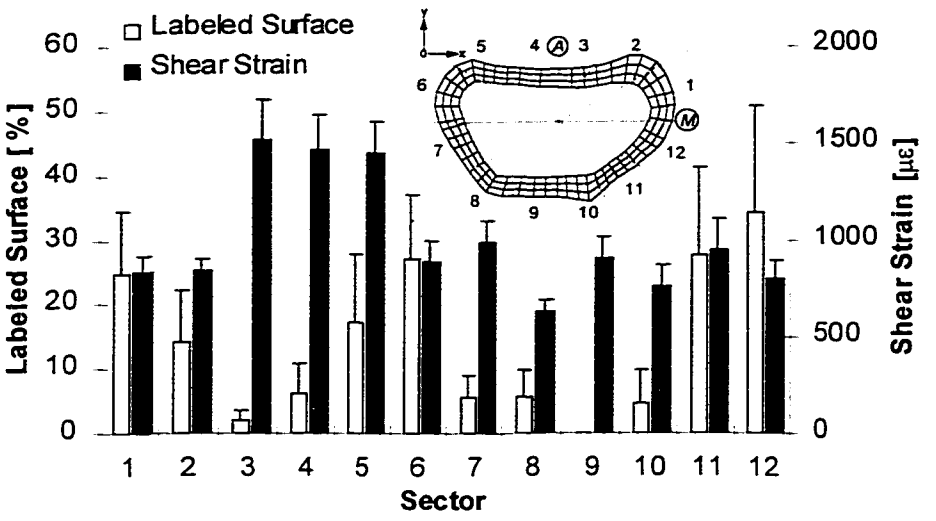

Figure 2.11 Distribution of peak longitudinal periosteal shear strain (mean+SE) contrasted against the distribution of mineralizing surface (mean+SE) demonstrating a lack of correlation (r^2=0.06). A sample finite element mesh of a middiaphyseal section is presented in the inset.

DISCUSSION

The unique feature of this study is that a specific mechanical stimulus was successfully correlated with specific sites of periosteal bone activation induced in a non-invasive bone adaptation model. We determined the distribution of locomotion-induced mechanical parameters acting on the TMT middiaphysis in one group of roosters, and hypothesized that bone would form in another group of exercised roosters at sites subjected to the largest circumferential strain gradients. The brief treadmill running regimen (9 min·day^{-1}) activated previously quiescent periosteal surfaces, and specific sites of mineralization correlated significantly (r^2=0.63) with peak circumferential strain gradients.

Despite this success, the study has several limitations. The design of the study did not allow us to associate the distribution of the mechanical stimulus with the specific sites

of periosteal activation in each individual animal. The long term utility of our observations, however, is with the potential for designing exercise regimens that will optimally enhance bone mass in a group of patients. We found a strong positive linear correlation between circumferential strain gradients and sites of periosteal activation due to the coincidence of bimodal distributions for these two parameters. A non-linear relation between strain gradients and periosteal activation would alter the future determination of what magnitude stimulus is required to initiate bone formation. The mean values for mineralizing surfaces were influenced by the three roosters with absent periosteal labels, however, correlation coefficients were not affected by the non-responders (i.e., correlations performed without these three roosters produced the same r^2 values). The spatial relation between peak circumferential strain gradients and sites of periosteal activation does not necessarily imply causation, and other parameters such as strain magnitude or strain rate may have influenced the magnitude of the observed response. Finally, this was a short-term experiment to investigate the ability of strain gradients to predict sites of exercise-induced periosteal activation. From these data, we can not say whether circumferential strain gradients associated with a longer-term exercise program will produce persisting, structurally relevant, alterations in bone mass and/or morphology. Also, our investigation was limited to cortical bone and we cannot infer to trabecular bone that comprises a large percentage of bone at clinically relevant fracture sites.

In our study, peak normal strain magnitude was poorly linked to specific sites of periosteal activation in the adult rooster skeleton. These results conflict with a recent

report in which peak magnitude strains were related to sites of increased bone formation in the rat ulna.[171] One difference between the studies lies with the active forming and resorbing surfaces present in the young growing rat, as compared to the primarily quiescent adult skeleton present in the roosters in our study. In their study, bone formation was increased most over normal formation in locations of maximal normal strains (approximately 4000 με). It is interesting to note, however, that the areas of greatest bone formation in the control rat ulnas corresponded closely with the location of the neutral axis during normal locomotion (i.e., large circumferential strain gradients, minimal strain magnitude).

Structurally, it seems counterintuitive that increased mechanical loading should produce bone apposition in regions where mechanical integrity is least challenged. Nevertheless, it has been observed that the cross-sectional moment of inertia of long bones in a variety of animals is the least about the bending axis present during locomotion, suggesting that bone sacrifices strength for predictable loading conditions.[11,138] Our data support this observation, as the cross-sectional moment of inertia in the rooster TMT middiaphysis about the bending axis is approximately 50% of the moment about an axis transverse to the bending axis. While the addition of bone mass along the neutral axis does little to reduce peak strains during activity, it would fortify an already stable strain environment (in terms of strain distribution). Alternatively, our results may be approached from a physiological, rather than structural optimization, perspective. Strain gradients (volumetric) are related to fluid flow in bone,[192] and may, therefore, induce a number of osteogenically relevant processes such as fluid shear

stresses[277] or streaming potentials.[84] Here, we assessed gradients of longitudinal normal strain and not volumetric strain gradients, however, their distributions are similar as the magnitude of a volumetric strain gradient in a given direction is dominated by the magnitude of the corresponding gradient of longitudinal normal strain.

Recent experimental and analytical data reveal the sensitivity of bone cell populations to fluid flow induced shear stresses (shear strains).[127,200,208,264] Consistent with previous theoretical[99] and experimental studies,[184,210] we observed a lack of correlation between the distribution of bone matrix shear strain and sites of periosteal activation. This may imply that direct stimulation of bone cells by matrix shear strain is unlikely to be part of the pathway by which bone cells respond to mechanical stimuli. Additionally, matrix shear strains only have a negligible influence on fluid flow in bone[223] while strain gradients are proportional to fluid flow.[192] Thus, the poor correlation between shear strain and sites of periosteal activation provides further evidence that strain gradients stimulate the activation of bone cell populations by influencing fluid flow.

Fluid flow in bone is generated by pressure gradients[286] which are influenced by spatial (e.g., spatial strain gradients) as well as temporal (e.g., strain rate) aspects of the loading environment.[242] The dynamic component is important as a static spatial strain gradient will not cause pressure differentials in bone. For simplicity, we related spatial strain gradients to sites of periosteal activation but the dynamic aspect can be added by calculating strain gradient rates. We found that the distribution of strain gradient rates was closely associated with the distribution of strain gradients, similarly to the relation

between strain magnitude and strain rate. Consequently, using circumferential strain gradient rates rather than circumferential strain gradients produced the same r^2 value.

Unlike studies in which exogenous loads generated strain environments substantially different from the normal strain milieu,[87,105,217] strain distributions engendered in our model were similar to those induced during normal (walking) locomotion.[112] The maximal circumferential strain gradients induced during running were larger than those observed during slow walking, but were located at the same sites.[112] While our study indicates that knowledge of the bone's complete strain history may not be necessary to predict sites of bone formation induced by increased exercise, it is possible that the roosters' daily activity levels affected the responses we observed. Quantification of the 24-hour strain history for group-housed roosters indicates that large strain magnitudes induced during daily activity are rare compared to those induced by treadmill running.[129] However, activity levels among animals may vary and may account for the absence of a periosteal response in 3 of 8 roosters within the exercise group. Even with the null response in 3 roosters, it is significant that every rooster showing periosteal activation had this response at sites of large circumferential strain gradients.

If circumferential strain gradients affect fluid-flow-related cell activation mechanisms, the question arises why maximal radial and longitudinal strain gradients were unrelated to sites of periosteal activation. Longitudinal strain gradients in this study were an order of magnitude smaller than circumferential or radial strain gradients, perhaps mitigating the larger fluid permeability coefficient in this direction.[228] Similarly, dielectric and electrokinetic considerations reflecting bone's microstructure[154,228] suggest

that cortical bone is less permeable radially. Alternatively, fluid flow in a radial direction may have little influence on the activation of periosteal surfaces but may instead influence a different physiological process such as intracortical remodeling. We were unable to test this hypothesis in the present study because of the timing of the fluorescent labels.

Some researchers have reported a minimal or negligible effect of exercise on the adult skeleton.[20,50,82,102] In these studies bone quantity was averaged across a region of bone, as measured, for instance, by dual-energy X-ray absorptiometry (DXA). While these data give important information about how a larger region of bone responds to a prescribed exercise program, significant increases in bone mass within this region may not have been detected. In our study, exercise activated only 23±7% of the total periosteal surface in those roosters that responded to the exercise regimen. This small value emphasizes that it is critical to have a means of controlling the sites of new bone deposition in order to obtain a structural benefit from the exercise regimen.

If bone continues to form and consolidate at the sites of activated periosteal surface, circumferential strain gradients may provide a means of optimizing exercise regimens to reduce fracture risk associated with bone loss pathologies. As we confirmed a previous study[87] that circumferential strain gradients are highly associated with sites of bone forming surfaces induced in adult skeletons, simple exercises with weights could be designed in which the induced neutral axis (large circumferential strain gradients) is aligned with those sites most likely to enhance the strength of the tissue. If, indeed, there is a causal relation between circumferential strain gradients and activation of periosteal

surface, we also hypothesize that exercise should have larger effects on periosteal surface modeling when bones are subjected to bending moments (large strain gradients) than to torsional or axial loading (small strain gradients). To test that hypothesis in a clinical setting, the mechanical environment could be analyzed non-invasively by simple biomechanical models,[102] and site-specific changes in bone morphology could be assessed by techniques such as high resolution quantitative computer tomography.

In summary, this study related specific sites of periosteal activation to an exercise-induced strain parameter. Each of the animals that demonstrated periosteal activation in response to the brief running regimen deposited bone at cortical sites experiencing small strain magnitudes, but large circumferential strain gradients. The strong association between circumferential strain gradients and the specific regions of bone modeling suggests that it may be feasible to design exercise regimens that initiate bone formation at sites most in need of enhanced structural integrity.

Chapter 3

Does the Mechanical Milieu Associated with High-Speed Running Lead to Adaptive Changes in the Diaphyseal Tarsometatarsus of Growing Roosters?

ABSTRACT

Exercise during growth can be important for attaining optimal bone mass, but high-intensity long-duration aerobic exercise can have detrimental effects on immature bone morphology and mechanics. Here, we quantified the mechanical environment of the middiaphyseal roosters tarsometatarsus during high-speed running and examined whether short bouts of this exercise-related mechanical milieu can induce positive changes in cortical bone morphology, mechanics, and mineral density. At 9 wk of age, roosters were assigned to controls (n=9) and runners (n=8). Treadmill running was applied in loading sessions of 5 min, 3x per day (≈ 2600 cycles per day) for 8wk. Both controls and runners received double fluorochrome labels 3 wk and 7 wk into the protocol. Full field distributions of tarsometatarsal longitudinal normal strain, strain rate, and strain gradients engendered by walking and running were determined via in vivo strain gages. Compared to walking, running elevated mean peak strain magnitude by 19%, peak strain rates by 136%, and peak strain gradients by approximately 18%. After 8 wk of running, middiaphyseal areal and mechanical properties, and normalized ash weight were not different between runners and controls. Transient and focal reductions in periosteal mineral apposition rates occurred during the exercise protocol. These data suggested that reducing the number of loading cycles can mitigate the adverse response previously observed in this model. Nevertheless, the mechanical milieu associated with high-speed running failed to elicit positive adaptations in the growing rooster middiaphysis under the given experimental conditions.

INTRODUCTION

As no universal treatment for osteoporosis is currently available, enhancing peak bone mass during skeletal growth and consolidation may represent the optimal primary prevention for these diseases.[7,98] While heredity is the principal determinant of peak bone mineral density, up to half of the variance in bone mineral density can be influenced by other factors[130] including mechanical loading.[5,34]

Bone can respond and adapt to changes in its mechanical loading environment, but longitudinal prospective exercise studies have produced disparate results particularly in growing bone. In these models, bone surfaces are actively forming and resorbing, and exercise may influence the quantity and quality of bone deposited. Running, a commonly used exercise stimulus in animal models, has been reported to enhance[14,174,195,202,224,246] or compromise[68,106,119,121,147,160] bone formation and mechanical properties of growing bones. These discrepant findings may reflect differences in the mechanical environments generated by exercise mode, intensity, duration, and frequency as positive[120,256] as well as negative[18,68,106,147] exercise effects are site-specific in nature. If specific aspects of exercise-related mechanical milieus can be associated with adverse or beneficial effects in growing bone, then exercise regimens could be designed that prevent negative and maximize positive effects. Unfortunately, mechanical milieus produced by exercise have rarely been quantified in bone adaptation studies.

Exercise protocols involving running have previously had negative effects on bone formation in the middiaphyseal rooster tarsometatarsus. Treadmill running at 70-80% of their aerobic capacity decreased periosteal formation, moments of inertia, and mechanical

properties in 3-12 wk old roosters.[160] Reduced bone resorption or enhanced bone deposition was observed at endocortical surfaces. A similar, but less pronounced, response was found in tarsometatarsi of 30 wk old roosters exercising at 70-75% of their aerobic capacity for 9 wk.[151] In both studies, roosters ran continuously for 40-60 min per day. This aspect of the loading environment may have influenced the results as decreasing exercise duration[108] and distributing loading sessions[41,69] have been suggested to positively influence the exercise-related adaptive process.

In the present study we addressed the following questions: (1) Are the negative effects of running on the middiaphyseal rooster tarsometarsus prevented by applying short-duration bouts of high-speed running involving a relatively small number of loading cycles? (2) Does this exercise protocol elicit changes in bone morphology and mechanics, and how are those changes related to the induced mechanical environment?

METHODS

Experimental Protocol

Nine-week-old White Leghorn roosters were divided into runners (n=8) and sedentary age-matched controls (n=9). During the 8-wk duration of the study, each rooster was housed in an individual cage (60 x 65 x 70 cm) and was given free access to a standard diet and tap water. Runners were engaged in a high-speed treadmill running program for 8 wk. Roosters ran 6 day·wk^{-1}, 3 sessions·day^{-1} (morning, noon, evening), 5 min·session^{-1} ($\approx$ 2600 loading cycles·day^{-1}). Roosters were trained at a percentage of their maximum speed to maintain a constant stride frequency and, thus, a uniform mechanical stimulus

during the exercise period.[13,15,215] Thus, exercise speed was adjusted every week: 1.36 $m \cdot s^{-1}$at 9 wk of age, 1.54 $m \cdot s^{-1}$at 12 wk of age, and 1.84 $m \cdot s^{-1}$ for the last two weeks of the exercise regimen. Both groups of roosters received double fluorochrome markers (7 days apart) at weeks 2 and 3 (xylenol orange, 90 $mg \cdot kg^{-1}$, i.m.) and at weeks 7 and 8 of the exercise program (calcein, 10 $mg \cdot kg^{-1}$, i.v.). All roosters were killed 3 days after the last calcein injection (Euthanyl, MTC Pharmaceuticals, Cambridge, ON). Left and right TMTs were harvested, dissected free of soft tissues and frozen (-30°C). Body weights were determined on the first day of exercise protocol and at completion.

The mechanical environment of the middiaphyseal TMT generated by treadmill running and walking was determined in a third group of six 12-16 wk old White Leghorn roosters. Roosters from this group were acclimatized to treadmill running and strain gaged. Subsequently, bone strains were recorded during walking and running. All procedures were approved by the Animal Care Committee of the University of Calgary.

Determination of the Mechanical Environment

Full field solutions of several mechanical parameters previously proposed to drive adaptation, including strain magnitude and distribution,[219] strain rate,[170] and strain gradients[87,113] were determined. The quantification of these parameters via in vivo strain gaging is described in detail in Chapters 2 & 4. Briefly, three triple-rosette strain gages were attached (cyanoacrylate) to the medial, anterior, and lateral aspects of the left middiaphyseal TMT in roosters of the strain gage group. At 24-h post-op, strain data

were recorded (300 Hz) during slow treadmill walking (0.51 $m \cdot s^{-1}$) and during high-speed treadmill running (1.54-1.84 $m \cdot s^{-1}$, depending on age).

Post-mortem, the angular orientation of the strain gages with respect to bone's longitudinal axis as well as strain gage location was determined from microradiographs. Custom software calculated longitudinal normal strain data for each sampled time point. Linear beam theory[221] was used to calculate longitudinal normal strain distributions across a middiaphyseal section. Pixel-counting routines (PV-Wave, Visual Numerics, Houston, TX) divided the binary images of middiaphyseal cross-sections into 12 30° sectors with the centroid as an origin (Fig. 3.1).

Peak longitudinal normal strains, strain rates, and circumferential and radial strain gradients were calculated at the center of each sector for both periosteal and endocortical surfaces and averaged across three gait-cycles. Peak strain rates were defined as the largest increase in strain magnitude over a time interval during which at least one third of the peak strain was produced. Circumferential surface strain gradients of longitudinal normal strain were quantified in each 30°-sector as the absolute difference between normal strains on the periosteal borders of each sector normalized to the linear distance between these points (Fig. 2.3). Radial strain gradients were determined between the midpoints of the periosteal and endocortical surface in each sector.

TMT Length and Middiaphyseal Areal Properties

The length of each left TMT was measured (± 30 μm) with precision calipers (Brown and Sharpe, North Kingstown, RI). A 300 μm thick transverse section was cut (Isomet Low

Speed Saw, Buehler, Lake Bluff, IL) from each left TMT middiaphysis and fixed in 70% ethanol. The section was then handground to 100 μm with 600 grit-paper and radiographed (Cabinet X-Ray System, Faxitron X-Ray Corp., Buffalo Grove, IL) using high-resolution film (Industrex-SR, Kodak, Rochester, NY). Microradiographs were enlarged and scanned on a stereomicroscope (Stemi 2000-C, Carl Zeiss Jena GmbH, Jena, Germany) with an attached video-camera. Edge detection programs were used to create the images, and customized pixel counting routines (PV-Wave) divided the binary images of the cross-sections into 12 30°-sectors with the centroid as an origin (Fig. 3.1). Cortical bone area, area of porosities, periosteal and endocortical envelopes, and cross-sectional moments of inertia about medial-lateral (bending axis) and anterior-posterior axes were calculated for each entire section as well as site-specifically for each sector within the section.

Histomorphometry

Middiaphyseal sections were further ground to 70 μm and mounted under an epifluorescent microscope (x 12.5). A 12 equal-angle sector grid was superimposed upon the bone section and aligned according to the sector subdivision used for the areal analysis (Fig. 3.1). A video camera captured the central portion of each sector (0.28 mm^2) at both periosteal and endocortical surfaces (24 images per section). Fluorescent labels were digitized via digitizing table (VIDAS, Kontron Elektronik, Munich, Germany). Bone apposition in the growing rooster TMT middiaphysis occurs, in particular at the periosteal surface, by primary osteonal bone formation. Hence, mineral apposition rate

(MAR) was calculated by dividing the area between two consecutive labels by the mean length of the label. Endocortical and periosteal MAR were determined for the 2 and 3 wk and for the 7 and 8 wk interval in all sectors in which at least 10% of the total sector surface was double labeled. The number of sites undergoing intracortical remodeling was counted in each sector for the second label period. A remodeling event was defined as any single or double labeled osteon distinctly away from surfaces subjected to primary osteonal modeling.

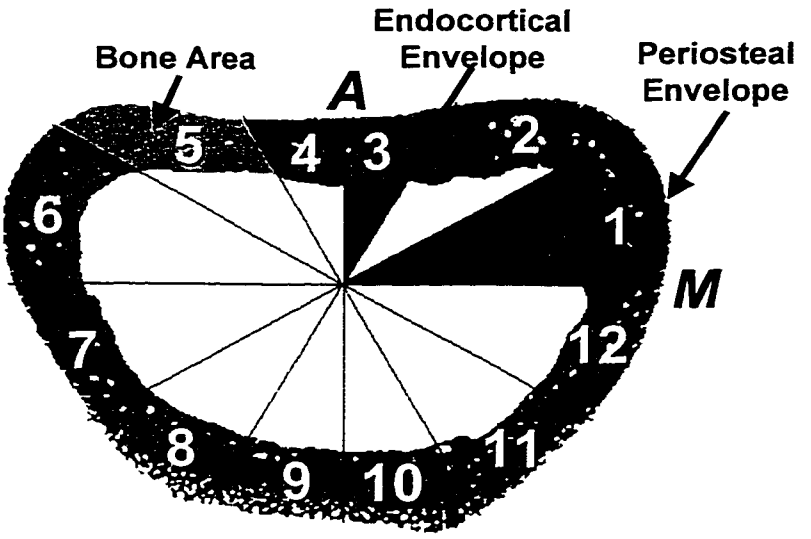

Figure 3.1 Example of a middiaphyseal TMT section. Analyses, including the quantification of bone area and surface envelopes, were performed for the entire section as well as site specifically for each sector. A = anterior, M = medial.

Mechanical Testing

On the day of testing, right TMTs were thawed (22 °C) and subsequently temperature equilibrated (37°C) in physiological buffer solution (PBS, pH 7.4) for at least 1 h prior to

testing. A servo-controlled electromechanical testing system (Model 1122, Instron Corporation, Canton, MA) loaded each bone in three-point bending until failure (loading rate: 42 $mm \cdot s^{-1}$). Bones were loaded in the anterior (compression surface) to posterior (tensile surface) direction. A small pre-load was applied to each bone to ensure the bones rested securely on the support points and did not shift during full load application. Analog load-time data from the Instron were converted to digital data at a sample rate of 2 kHz. A custom-designed program (Run Technologies, Laguna, CA) was used to calculate structural and material properties including load and energy at proportional limit and at maximum, tensile stress at proportional limit, and flexural rigidity.

Ash Content

Left middiaphyseal sections (2 mm) were cut from left TMTs, separated into medial, anterior, lateral, and posterior cortices and subsequently treated in 70% ethanol and 100% acetone for 4 days. Samples were dried in a muffle furnace at 100°C for 24 h, weighed, and ashed at 600°C for 24 h (Model 627000, Barnstead/Thermodyne, Dubuque, IA). Ash content was determined for each cortex by calculating the percentage of the ratio of ash-to-dry mass.

Statistics

Student t-tests were used to detect differences in bone morphology, biomechanics, ash content, and body mass between runners and controls. Mineral apposition rates at the two intervals were assessed via non-parametric Mann-Whitney tests because of the varying

number of observations. The mechanical milieus induced by treadmill walking and running as well as body masses within groups were compared via paired t-tests. Multiple paired t-tests including Bonferroni corrections were employed to test for differences in ash content between different regions within groups. Data analysis was performed using SPSS 8.0 for Windows (SPSS Inc., Chicago, IL). Statistical power was calculated by software developed by the Department of Statistics at the University of California – Los Angeles (Power Calculator for 2 Sample Unequal Variance). A level of 0.05 was considered significant for all tests. Results were expressed as mean±standard error.

RESULTS

Mechanical Milieu

Running generated a highly non-uniform strain environment in the middiaphyseal TMT (Fig. 3.2). Large compressive strains (1870±250 με) were generated on the anterior cortex, and large tensile (960±160 με) strains were generated on the posterior cortex (Table 3.1). Maximal strains associated with running were significantly elevated over walking (19%, $p<0.03$), but the qualitative distributions of peak strains induced by the two speeds were strongly related ($r^2=0.99$). The largest increases in strain magnitude were observed at the anterior cortex (26±2%, sectors 2-5), while increases in the remaining sectors were only 6±4%.

Maximal strain rates generated during running (0.089±0.018 $\varepsilon \cdot s^{-1}$) were 136% larger ($p<0.05$) than those induced by walking (Table 3.1). The distribution of peak strain rates was closely related to the distribution of peak longitudinal strain ($r^2=0.93$) and was

not different between speeds. Maximal circumferential strain gradients increased by 17% ($p<0.04$) and radial strain gradients by 19% ($p<0.03$) with locomotor speed (Table 3.1). The largest circumferential strain gradients as well as the largest speed-related increases were observed at the medial and lateral cortex (Fig. 3.3). The largest radial strain gradients were located at the anterior (sector 2-4) and posterior (sector 8-10) cortices.

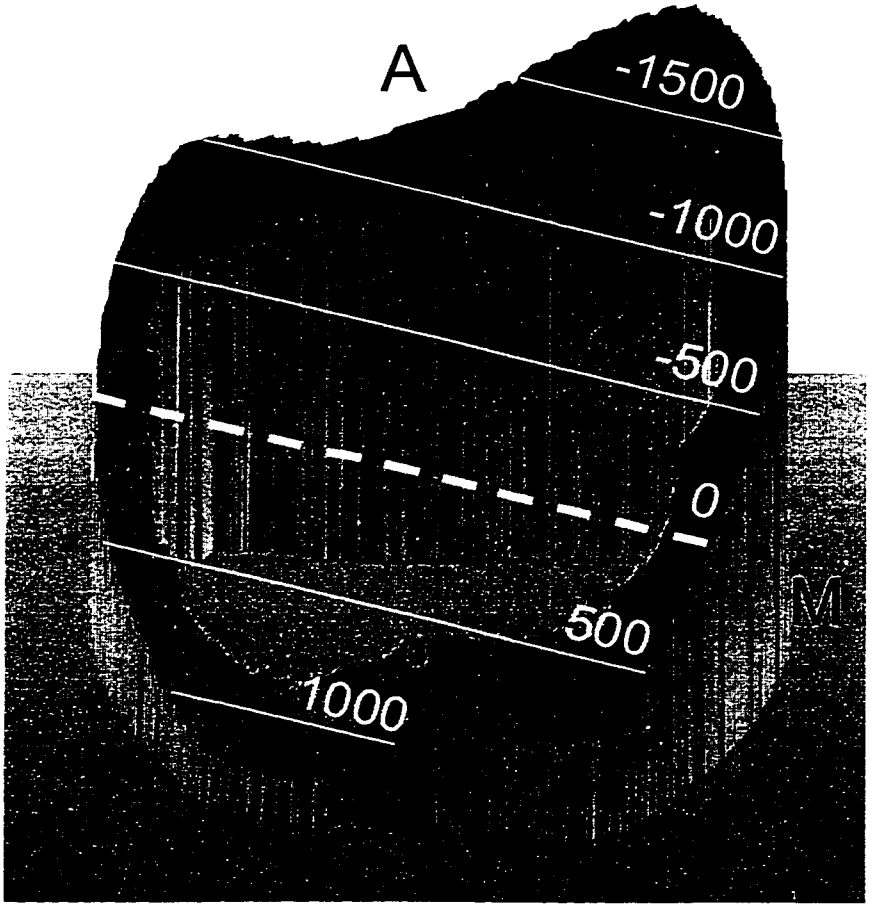

Figure 3.2 Distribution of longitudinal normal strain superimposed on a middiaphyseal cross-section of a rooster running at a speed of 1.84 $m \cdot s^{-1}$. The distribution in this figure was determined when maximal strains were induced in the cortex (mid-stance). The neutral axis is dashed, and strain isopleths [$\mu\varepsilon$] are plotted parallel to the neutral axis. M = medial, A = anterior.

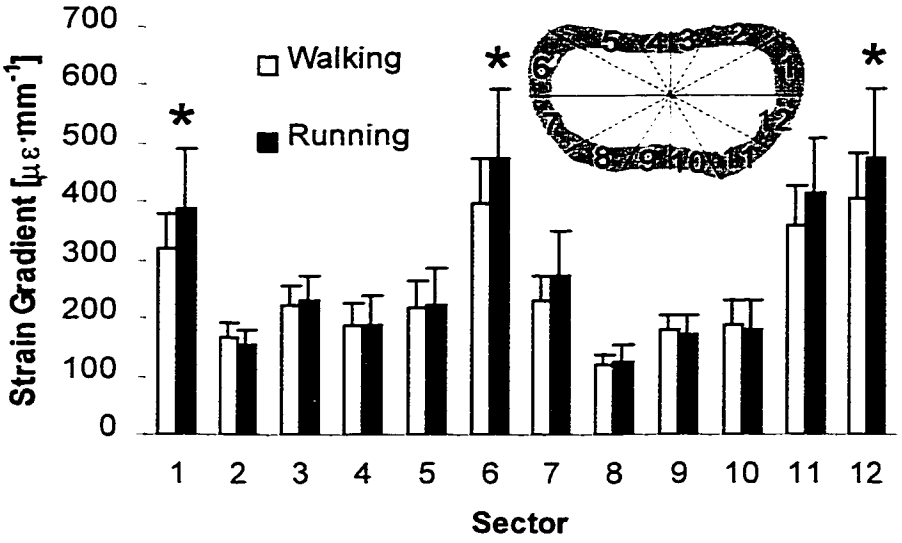

Figure 3.3 Distribution of peak circumferential strain gradients (mean+SE) generated at the periosteal surface during walking (0.51 $m \cdot s^{-1}$) and running (1.66 $m \cdot s^{-1}$). Peak values occurring in each sector were averaged across three gait-cycles. Asterisks denote significant differences between running and walking.

Table 3.1 Maximal values for strain magnitude, strain rate, and strain gradients produced in the TMT cortex during walking and running (mean±SE).

	Walking (0.51 $m \cdot s^{-1}$)	Running (1.54-1.84 $m \cdot s^{-1}$)
Compressive Strain [με]	-1570±220	-1870±250*
Tensile Strain [με]	860±160	960±160
Strain Rate [$\varepsilon \cdot s^{-1}$]	0.038±0.004	0.089±0.018*
Circumferential Strain Gradient [$\mu\varepsilon \cdot mm^{-1}$]	410±70	480±80*
Radial Strain Gradient [$\mu\varepsilon \cdot mm^{-1}$]	400±70	480±70*

Asterisks indicate significant differences between running and walking ($p<0.05$).

Compared to the periosteal surface, maximal events at the endocortical surface were reduced by 23% (compressive strain), 34% (tensile strain), 22% (strain rate), and 2% (circumferential strain gradients) during running. Distributions of all mechanical parameters were qualitatively similar at the periosteal and endocortical surface.

Body Mass, Bone Length, and Areal Properties

Mean body mass of controls and runners more than doubled during the course of the study ($p<0.001$) but was similar between groups at both time points (Table 3.2). Tarsometatarsal length was not affected by exercise. The means of periosteal envelopes, cross-sectional moments of inertia, and porosities were not different between groups – neither for entire sections nor for specific areas within these sections. Endocortical envelopes were indicative of changes in endocortical resorption, and these envelopes were not significantly altered by exercise.

MAR after 3 wk of Running

Although periosteal xylenol-orange double labels were observed in all animals, surfaces were not continuously labeled, and MAR could not be determined in every sector for each rooster. The average number of observations per sector was 7.1±0.6 for the control group and 7.2±0.5 for the run group. Sector 1 ($n=3$ for controls and runners) and sector 7 ($n=5$ for controls and $n=4$ for runners) had the lowest number of observations. Runners had smaller periosteal MAR than controls at the antero-medial and lateral cortex (Fig. 3.5), and these reductions were statistically significant in sector 2 ($p<0.04$) and sector 6

($p<0.02$). Consistent endocortical labels (labels in at least 4 animals per group) at this time point were detectable only in sectors 1 and 2, and MAR was not significantly affected by running (Table 3.3).

Table 3.2 Body mass, tarsometatarsal bone length, and middiaphyseal areal properties of control and exercised roosters (mean±SE). Comparisons between controls and runners were non-significant for all parameters.

	Control	Runner
Body Mass at Start [g]	680±30	670±20
Body Mass at Completion [g]	1750±70	1650±30
Length [mm]	96.1±1.3	93.7±1.0
Bone Area [mm^2]	14.3±0.6	15.0±0.3
Porosities [mm^2]	0.7±0.1	0.7±0.1
Periosteal Envelope [mm^2]	32.5±1.0	32.5±1.4
Endocortical Envelope [mm^2]	16.6±0.8	15.9±1.1
$I_{medial\text{-}lateral}$ [mm^4]	42.2±3.0	44.1±3.2
$I_{anterior\text{-}posterior}$ [mm^4]	77.0±4.4	79.1±5.1

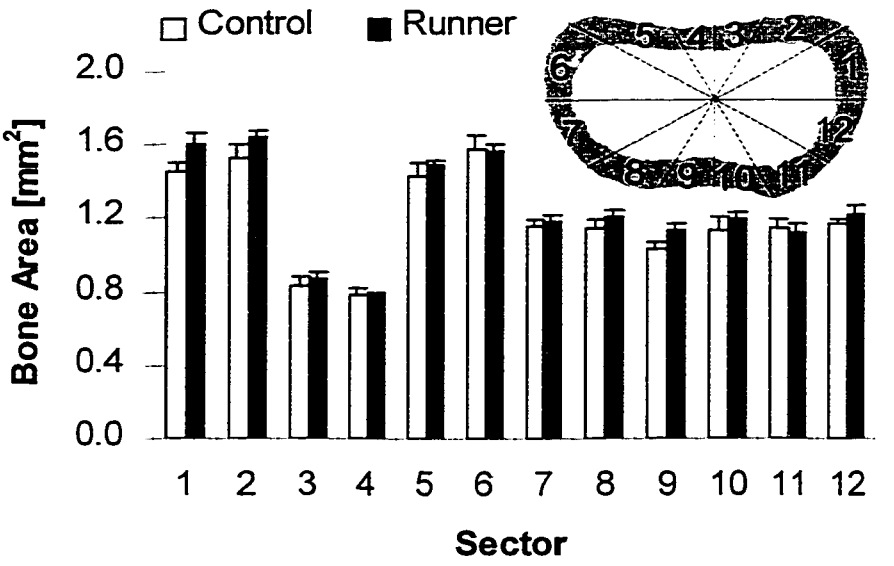

Figure 3.4 Distribution of cortical bone in runners and controls (mean+SE).

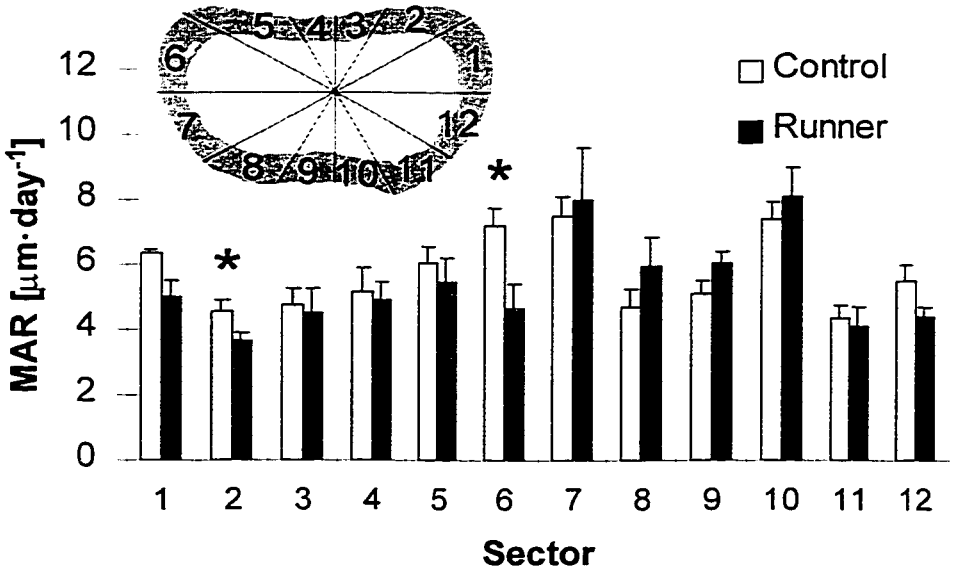

Figure 3.5 Periosteal mineral apposition rate (MAR) 4 wk into the exercise protocol (mean+SE). Asterisks indicate significant differences between groups ($p<0.05$).

Table 3.3 Endocortical mineral apposition rates (mean±SE) quantified via xylenol orange label 4 wk into the exercise program.

MAR [$\mu m \cdot day^{-1}$]	Control	Runner
Sector 1	6.3±0.8 (n=9)	5.0±0.7 (n=7)
Sector 2	4.6±0.5 (n=8)	3.7±0.6 (n=5)

MAR and Intracortical Remodeling after 8 wk of Running

Both calcein labels administered ten and seven days prior to sacrifice were visible over the entire periosteal surface. Average periosteal MAR in runners was significantly reduced only at the lateral aspect (sector 7), and MAR at the antero-medial cortex had returned to normal levels (Fig. 3.6). Consistent endocortical calcein labels were observed only at the antero-medial aspect (sectors 1,2,4). Of these three sectors, endocortical MAR was significantly elevated at the antero-medial cortex (sector 1) (Table 3.4). Remodeling events were similar between controls and runners in any given area of the cortex. The total number of remodeling events in the cortex was 79±10 in controls and 92±8 in runners.

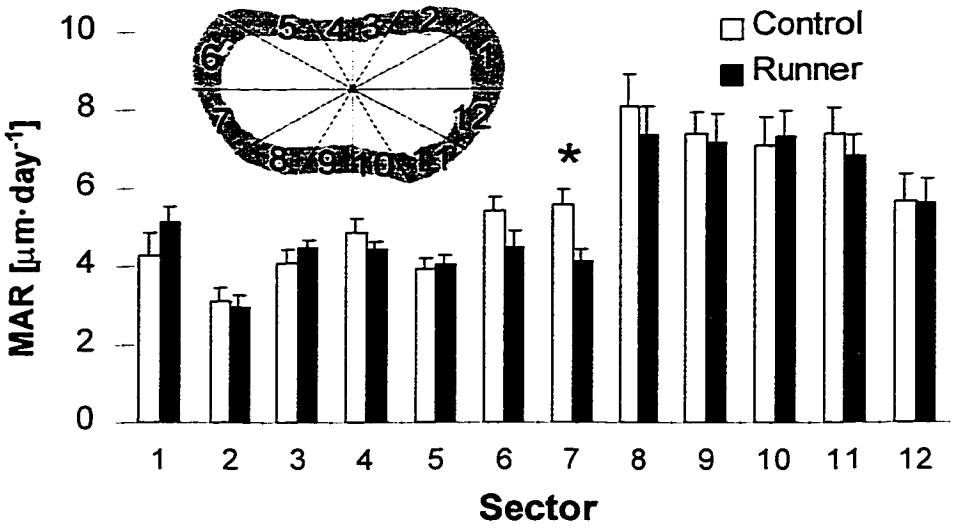

Figure 3.6 Periosteal mineral apposition rate 8 wk into the protocol in controls and runners (mean+SE). The asterisk denotes a significant differences between groups ($p<0.05$).

Table 3.4 Endocortical mineral apposition rates (mean±SE) quantified via calcein labels 8 wk into the exercise program. The asterisk denotes a significant difference between groups ($p<0.05$).

MAR [µm·day^{-1}]	Control	Runner
Sector 1	1.6±0.2 (n=6)	2.3±0.1* (n=6)
Sector 2	1.9±0.1 (n=9)	1.9±0.1 (n=5)
Sector 4	2.3±0.1 (n=5)	2.4±0.3 (n=4)

Mechanical and Ash Data

Structural middiaphyseal TMT properties (loads and absorbed energy at the proportional limit and at maximum, and flexural rigidity) were not significantly different between groups (Table 3.5). Tensile stress at the proportional limit, a measure of bone quality, was also not significantly affected by exercise. Percent ash was largest for the anterior cortex and smallest for posterior cortex in both groups, but these differences were not significant between groups (Table 3.6).

Table 3.5 Middiaphyseal TMT mechanical properties (mean±SE).

Mechanical Properties	Control	Runner
Load at proportional limit [N]	208±7	207±8
Load at maximum [N]	333±12	340±9
Flexural rigidity [$N \cdot m^2$]	0.338±0.013	0.365±0.023
Energy at proportional limit [mJ]	60±3	62±10
Energy at maximum [mJ]	352±28	368±22
Tensile stress at proportional limit [MPa]	128±7	122±4

Table 3.6 Midiaphyseal bone mineral content as determined by percent ash (mean±SE). Different superscripts denote statistically significant differences within groups ($p<0.05$). Values for percent ash of specific regions of the cortex did not differ between groups (control vs runner).

Percent Ash	Control (n=9)	Runner (n=8)
Medial	$62.7\pm0.2^{a,c}$	62.7 ± 0.2^{a}
Anterior	64.1 ± 0.2^{b}	63.8 ± 0.2^{b}
Lateral	63.1 ± 0.3^{c}	$63.1\pm0.5^{a,b}$
Posterior	61.8 ± 0.3^{d}	61.0 ± 0.6^{a}

DISCUSSION

We investigated the response of the rooster TMT middiaphysis to three daily stimuli of approximately 850 loading cycles of high-speed running during a period of rapid growth (physes close at 21 wk of age).[143] Running decreased periosteal MAR shortly after commencing exercise and subsequently increased MAR at the endocortical surface. These differences between groups were modest in magnitude and limited to small regions of the cortex. Changes in MAR did not translate into significant changes in bone gross morphology or bone mechanical properties after 8 wk of exercise.

Our statistical power to detect significant differences was limited by the small sample sizes used. However, most of our analyses had sufficient power to detect a difference of 15-20% in areal or mechanical properties. This value was smaller than relative changes in several variables reported from studies in which running induced

significant changes in cortical bone morphology or mechanics.[160,195,282] For the given variation in our data, the power values to identify 15% differences between runners and controls were, for instance, 0.87 for middiaphyseal cortical bone area, 0.89 for maximum bending load, and 1.00 for middiaphyseal ash content and tarsometatarsal length.

An important feature of this study is that analyses were performed site specifically within a cortical cross section. It is possible that some studies that reported no significant effects of exercise upon bone parameters averaged across a section missed significant changes as exercise effects on bone are non-uniform and targeted to specific regions of the cortex.[14,160,194,282] In the current study, changes in MAR were only detectable within specific sectors but did not yield statistical significance when averaged over all 12 sectors. Nevertheless, even site-specific areal measurements did not reveal any significant differences, indicating that the quantification of mineral apposition rates was more sensitive in detecting short-term exercise-induced changes.

Previously, the response of the TMT rooster middiaphysis to 9-wk exercise programs was examined in 3 wk[160] and 30 wk old roosters.[151] In both studies, high-speed running (70-80% of maximum aerobic capacity) was applied in one daily session for 40-60 min, leading to bones with smaller periosteal and endocortical envelopes. TMT mechanical properties were also compromised. In our current study, MAR showed the same trends towards smaller periosteal and endocortical envelopes as observed in those earlier studies but the adverse effects on gross morphology and mechanics were eliminated. Potentially, the different age of roosters in our study may have contributed to the difference in results, but the age of the roosters in the current study was bracketed by

the age of roosters from the two earlier studies. Thus, it seems likely that an exercise protocol similar to the one used in the earlier studies would have produced similar changes in the current study.

We did not measure oxygen consumption in this study, but extrapolated data on oxygen uptake from immature[160] and mature[21] roosters suggest that exercise intensity with respect to percentage of maximal aerobic capacity was also in the 70% to 80% range. Increased plasma levels of hormones and corticosteroids[71,95,203,236] are linked to exercise intensity and duration. It is questionable, though, whether a systemic factor would solely account for exercise-induced detrimental effects on gross bone morphology as, generally, other bones within the same animal were not affected[18,106,147] or showed increases in bone formation.[68] The focal nature of decreased periosteal MAR and the concomitant focal increase in endocortical MAR in this study also suggests that reduced MAR were not associated with a systemic stress response but rather with the generated non-uniform mechanical environment. However, reductions occurred in regions of large strains, as well as close to the neutral axis and thus could not be accounted for by any of the mechanical parameters examined here.

Full field distributions of shear strains were not determined but have been previously correlated with the inhibition of bony ingrowth into a porous implant.[191] Running induced similar longitudinal shear strains in the rooster TMT at the three different sites (medial, anterior, lateral) measured ($\approx$ -1200 $\mu\varepsilon$). This uniformity in distribution makes shear strains an unlikely factor to be responsible for the focal decrease in periosteal MAR. Despite further evidence that the generated mechanical environment

is involved in negative effects on growing bone, synergistic reactions between mechanical and physiological factors are conceivable. Further research is necessary to clearly differentiate between mechanical and physiological factors and to identify mechanical parameters that are spatially correlated with reductions in bone growth.

Peak strain magnitudes and strain distributions induced by running are maintained during growth.[13,119] In fact, we found a difference of less than 5% in TMT peak strain magnitudes produced by high-speed running between 12-16 wk old and 1 yr old roosters (Chapters 2 & 3). Thus, the similarity in relative running speed (with respect to age) between the previous[151,160] and current TMT exercise studies implies that abnormal strain levels, per se, did not cause the adverse response in the previous studies. Our number of loading cycles was, however, drastically reduced. Given a sufficiently potent mechanical stimulus, relatively few loading cycles (as few as 36 cycles) can stimulate bone formation in adult bone with no further increases beyond that number.[22,70,94,217] Few controlled studies, though, have investigated the influence of extremely large numbers of loading cycles on actively forming and resorbing bone surfaces during growth. It has been suggested that decreasing exercise duration may increase the benefits.[108] Comparing our data to the other two rooster TMT studies[151,160] suggests that a large number of loading cycles can negatively influence normal bone growth.

Increasing the number of loading sessions may increase the osteogenic response.[41,69] Although roosters ran three times per day, our protocol did not significantly enhance middiaphyseal bone morphology and mechanics. One explanation for this result may be that the mechanical parameter(s) responsible for promoting bone apposition were

not sufficiently elevated in any of the loading sessions. Strain magnitude[218] and distribution,[219] strain rate,[170,178,266] and strain gradients[87,113] have all been suggested to influence the mechanically related adaptive process. Interestingly, the only sector in which MAR was elevated was the one that simultaneously experienced large strain magnitudes, strain rates, and large strain gradients.

Strain magnitude has been related to the magnitude of bone's osteogenic response in external loading models.[51,70,76,171,218,231,258] Few studies, however, have related the exercise-related milieu to induced morphological changes or a lack of them. Increasing peak strains by approximately 50% over those experienced by walking, increased bone formation in the diaphyseal tibiotarsus of growing roosters carrying loaded backpacks during treadmill running.[14] The 19% increase in peak strain magnitude compared to habitual loading (walking) in our study is comparable to the estimated 15% increase in a study that used strength training as an exercise stimulus.[102] Similar to our study, their exercise protocol did not reveal an osteogenic effect. We conclude that this moderate increase in strain magnitude in the presence of unchanged strain distributions, and significantly elevated strain rates and strain gradients does not represent a stimulus capable of substantially enhancing bone formation and mechanical properties in the growing rooster TMT. We are now investigating whether high-impact drop-jumps, an activity that produces a mechanical milieu in the rooster TMT distinct from running[114] can increase bone formation in this model.

In summary, our data suggest that reducing the number of loading cycles may mitigate the adverse effects of high-speed running in this model. Compared to walking,

running only moderately altered the mechanical milieu of the tarsometatarsal rooster middiaphysis and did not elicit positive adaptations. Further research is necessary to identify specific aspects of the exercise-induced mechanical milieu that induce adverse or beneficial effects in growing bone. This knowledge will eventually lead to the design of exercise regimens with higher osteotropic efficacy.

Chapter 4

High-Impact Exercise and Growing Bone: The Relation Between High Strain Rates and Increased Bone Formation in The Middiaphyseal Rooster Tarsometatarsus

ABSTRACT

Recent cross-sectional as well as longitudinal studies suggest that growing bone is more sensitive to high-impact exercise than to lower-impact aerobic exercise. Here, we investigated whether a small number of high-impact drop-jumps can increase bone formation in the middiaphyseal tarsometatarsus of growing rooster and whether distributions of mechanical parameters induced by drop-jumping are correlated with the specific sites of additional bone formation across the middiaphysis. Seventeen week old White Leghorn roosters were designated as sedentary controls (n=10) or jumpers (n=10). Upon acclimatization to drop-jumping, jumpers were subjected to 200 drop-jumps per day for 3 wk. In both groups, double fluorochrome labels were administered prior to starting the experimental protocol and prior to completion. The exercise related mechanical environment was quantified via in vivo strain gages and linear beam theory in six age-matched roosters. Histomorphometrical as well as strain data were determined in 12 30°-sectors subdividing the middiaphyseal cortex. Compared to walking, drop-jumping produced very large peak strain rates (+740%) in the presence of moderately increased peak strain magnitudes (+30%) and unaltered strain distributions. Analysis of the fluorochrome labels revealed that 3 wk of jump training significantly increased bone formation rates ($BFR \cdot BS^{-1}$) at periosteal (+40%) and endocortical surfaces (+370%) over formation rates in controls. At periosteal surfaces, none of the mechanical parameters examined could successfully explain the focal increases in bone formation rates. At endocortical surfaces, strain rate was significantly correlated with the specific sites of increased formation rates (r^2=0.44-0.67). These data indicate that large strain rates

induced by high-impact drop-jumps had a powerful osteotropic effect on tarsometatarsal endocortical surfaces in growing roosters.

INTRODUCTION

Exercise during growth may significantly contribute to the enhancement of peak bone mass reached at young adulthood.[5] However, to design an exercise protocol that provides maximal efficacy as a prophylactic tool against bone pathologies later in life, the effects of exercise-related mechanical stimuli on the skeletal system have to be adequately understood. Unfortunately, well controlled longitudinal exercise studies have produced inconsistent results, perhaps reflecting a lack of this understanding. Running, as an example of a common exercise, can have positive,[14,153,174,195,224,279] negligible (Chapter 3), or detrimental effects[68,106,119,121,147,160] on growing bone.

Recent cross-sectional[58,100,177] and longitudinal data[8,45,63,206,253,254,269] from humans and animals suggest that high-impact exercise is osteogenically more effective than lower-impact aerobic exercise. These studies provide encouraging data demonstrating that bone cells are capable of responding to exercise-induced mechanical stimuli with substantial bone formation. From a mechanical point of view, high-impact exercise is ill-defined, and the specific aspect of the exercise-induced mechanical milieu causing bone hypertrophy has not been identified. In external loading models, in which the loading conditions can be controlled and adjusted, strain rate[170,178,266] and strain magnitude[51,70,171,218,231,258] (among others) have been proposed as mechanical parameters that influence the adaptive process in bone. The efficacy of high-impact exercise has

often been attributed to the presumed increase in these two parameters, but this has not been verified. The lack of data describing bone's mechanical milieu during high-impact exercises makes it difficult to extrapolate from these studies to other exercise protocols. For instance, changes in loading directions during landings are also characteristic of many high-impact exercises such as badminton or soccer, possibly altering strain distributions in bone. As changes in strain distribution may cause bone hypertrophy,[139,219] it is unclear whether high-impact exercise is still effective in the absence of changes in loading direction.

Here, we investigated the effects of mechanical stimuli produced by drop-jumping on the middiaphyseal tarsometatarsus (TMT) in growing roosters. In previous studies using this animal model, running for one hour per day exerted highly negative effects on TMT cortical bone morphology and biomechanics[160] while running for 15 min per day produced no adverse effects but failed to enhance bone growth (Chapter 3). In this study, three specific research questions were asked: (1) Does high-impact drop-jumping produce a distinct mechanical milieu in which mechanical parameters previously proposed to drive adaptation such as strain magnitude[218] and distribution,[219] strain rate,[170,178,266] and strain gradients[87,113] are significantly elevated? (2) Can 200 cycles per day of this mechanical milieu significantly enhance bone formation in this model? (3) Does a site-specific spatial relation between a mechanical parameter and enhanced bone formation exist within the middiaphysis?

METHODOLOGY

Research Design

Twenty-six 12 wk old White Leghorn roosters were received from a poultry farm (Starline Poultry, AB) and were randomly assigned to strain gaged (n=6), jumpers (n=10), or controls (n=10). All roosters were housed in pairs (60 x 65 x 70 cm) and were given free access to tap water and feed.

Roosters of the strain gaged group were used to quantify the mechanical environment of the TMT during slow treadmill activity (0.51 $m \cdot s^{-1}$) and drop-jumping. Roosters from this group were strain gaged and recorded between 12 wk and 16 wk of age (four 16 wk old, one 13 wk old, and one 12 wk old). Roosters of the control and jump groups were injected with calcein (15 $mg \cdot kg^{-1}$, i.v.) at 16 wk and 17 wk of age (6 days apart). Jumpers started the exercise training one day after the second calcein injection (day 0). For a jump, a rooster was lifted 50-60 cm off the ground, moderately accelerated and released. A thin piece of carpet served as landing mat to prevent slipping. The loading (jump) frequency was approximately 1 Hz. The same person handled the roosters during the exercise protocol and during strain recordings to minimize variability in jump intensities. The first week of jump-training consisted of acclimatization during which the number of daily drop-jumps was gradually increased from 50 to 200. For the following 3 wk, jump roosters were subjected to 200 high-impact drop-jumps per day following a schedule of three days on, one day off. Control and jump roosters were injected with tetracycline (20 $mg \cdot kg^{-1}$, i.m.) on day 21 and day 28 of exercise intervention. Roosters were killed with an overdose of sodium pentobarbitone (Euthanyl, MTC Pharmaceuticals,

Cambridge, ON) 72 h after the last tetracycline injection. All procedures were approved by the Animal Care Committee of the University of Calgary.

Determination of the Mechanical Environment

Three triple rosette strain gages (FRA-1-11-1L, Tokyo Sokki Kenkyujo Co., Japan) were attached to left middiaphyseal TMTs of roosters in the strain gage group similarly as reported previously.[113] Under general anesthesia, a narrow (10 mm) transverse strip of skin was removed covering the medial, anterior, and lateral aspect of the left middiaphyseal TMT. The periosteum was carefully scraped off and the underlying bone was degreased with chloroform. Cyanoacrylate adhesive (Krazy Glue for semiporous materials, Borden Co., Willowdale, ON) was used to bond the strain gages to the medial, anterior, and lateral aspect. A circular patch of latex, slightly larger than the strain gage, was glued on top of the triple-rosette gage facilitating waterproofing. Lead wires were strain relieved by taping them firmly to the distal part of the TMT. Upon recovery, an analgesic (Turbogesic, Ayerst Laboratories, Montreal, QU) was administered to minimize post operative pain.

At 24-h post-surgery, roosters were recorded during slow treadmill walking (0.51 $m \cdot s^{-1}$) and during drop-jumps. All strain gage output was amplified (Model 2310, Measurements Group, Raleigh, NC) and sampled at 300 Hz for 10 s. Prior to and post recording, gage attachment and functionality was confirmed separately for each gage by subjecting the bone to a wave ramp of bending and torsion. Post recording, strain gaged roosters were killed with an intravenous overdose of sodium pentobarbitone. The angular

orientation of the strain gages with respect to the longitudinal TMT axis was determined from whole bone microradiographs (Fig. 2.1). Subsequently, a hole was drilled through the center of each rosette gage using a fine (0.6 mm) engraving cutter (Dremel, Racine, WI). A transverse section containing the three holes was cut, micro-radiographed (Cabinet X-Ray System, Faxitron X-Ray Corp., Buffalo Grove, IL), scanned, and transferred to a computer where the position of the holes (gages) was determined interactively.

Strain gage recordings from various animals indicate that during late swing phase, the strain pattern at all sites changes slowly, and the limb is under the least load.[13,16,88,112,137,215] Thus, for the zeroing process involving walking, a zero strain range during late swing phase was specified for each channel. Similarly, zero strain was assumed to occur just prior to impact during drop-jumping. These procedures were applied for each recorded trial.

Custom software (PV-Wave, Visual Numerics, Houston, TX) calculated longitudinal normal strain for each sampled time point. Recorded strain gage data are only relevant to the small patch of bone they are attached to,[88] and finite element modeling[23] or linear beam theory[221] can be applied to determine the distribution of longitudinal normal strain acting on the mid-shaft. We used linear beam theory, thereby modeling the TMT middiaphysis as a prismatic beam subjected to axial loading and bending moments. No assumptions about material properties and boundary conditions had to be made; the linear strain distributions across the middiaphyseal section exclusively reflected strain data measured by the three rosette strain gages.

Pixel-counting routines (PV-Wave) were used to divide the binary images of the cross-sections into 12 30°-angle sectors with the centroid as an origin (see inset Fig. 4.3). Maximal longitudinal normal strains, strain rates, and strain gradients occurring over three gait-cycles/drop-jumps were calculated at the center of each sector for both periosteal and endocortical surfaces. Peak strain rates were defined as the largest increase in strain magnitude over a time interval during which at least one third of peak strain was produced. Note that strain gradients defined in this study are strain gradients of longitudinal normal strain. Circumferential surface strain gradients were quantified in each 30°-sector as the absolute difference between longitudinal normal strain on the borders of each sector normalized to the linear distance between these points (Fig. 2.3). Radial strain gradients were determined, in analogy to circumferential strain gradients, between the midpoints of the periosteal and endocortical surface in each sector.

Histomorphometry

Left TMTs were used for histomorphometric analyses. TMT-length was measured from the most distal phalange to the center of the proximal plateau in both control- and jump roosters (± 30 μm). Using a slow speed diamond wafer saw (Isomet Low Speed Saw, Buehler, Lake Bluff, IL), a transverse section (300 μm) was cut at 45% of total TMT length measured from the proximal end. This site coincided with the plane at which the strain gages were attached in roosters of the strain gage group and was considered as the functional middiaphysis. All sections were fixed in 70% ethanol and subsequently hand-ground to 120 μm using a 1500 grit-paper (wet). Sections were mounted on an

epifluorescent microscope (x 12.5). A 30° equal angle star grid was etched into a plastic cover-slip and superimposed such that the center of the star-grid coincided with the centroid of the section. Angular alignment was achieved by positioning the 0°-180° line of the grid parallel to the anterior cortex (see inset Fig. 4.3).

The percentage of single and double labeled surfaces in each sector was determined at both surfaces. For the quantification of dynamic bone indices, a video camera was used to capture the central portion of each sector (0.28 mm^2) at both surfaces (24 images per section). In each sector, the ratio of single labeled (sLS) and double labeled surface (dLS) to bone surface (BS) was determined.

Between wk 17 and wk 21 of age, bone accretion at the periosteal surface of the growing rooster TMT is facilitated by primary osteonal modeling as well as lamellar bone formation (Fig. 4.1). Mineral apposition rate (MAR) at the periosteal surface was, therefore, quantified as the area enclosed by the double label divided by its mean surface length [$\mu m \cdot day^{-1}$]. A program was developed (PV-Wave) using Gaussian operators[146] to identify automatically the line of highest pixel intensities within the fluorochrome labels, thereby minimizing operator based bias (Fig. 4.2). Subsequently, these thin bands were traced and the mean length of the covered surface was measured. Additionally to calculating MAR based on the calcein or tetracycline double label, MAR was also determined for the 4 wk time period between the second calcein label (start of jump protocol) and second tetracycline label (completion of protocol).

a.

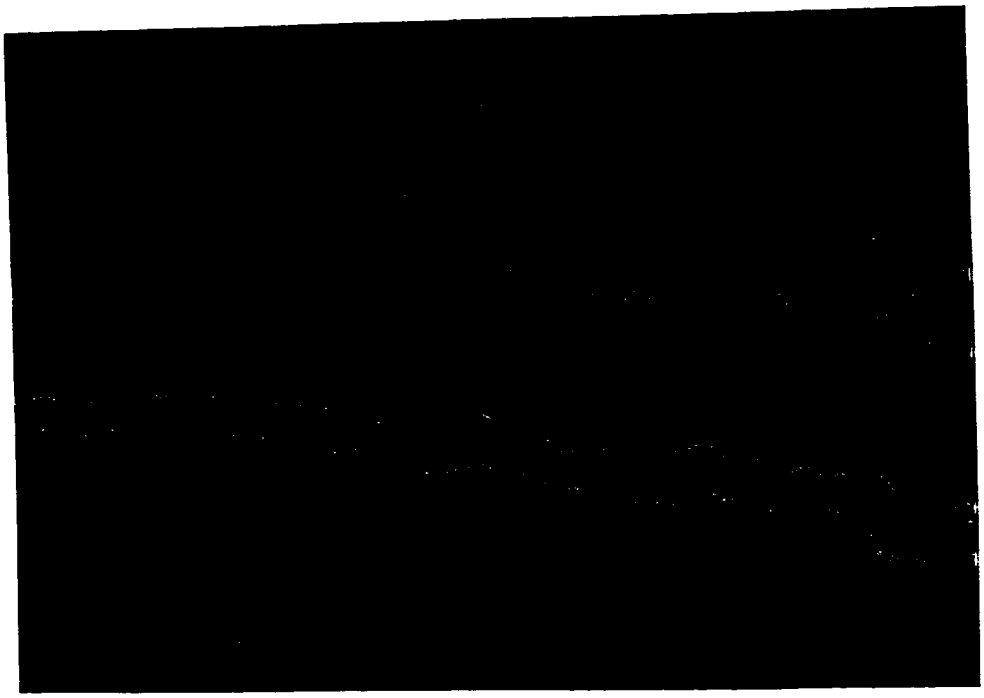

b.

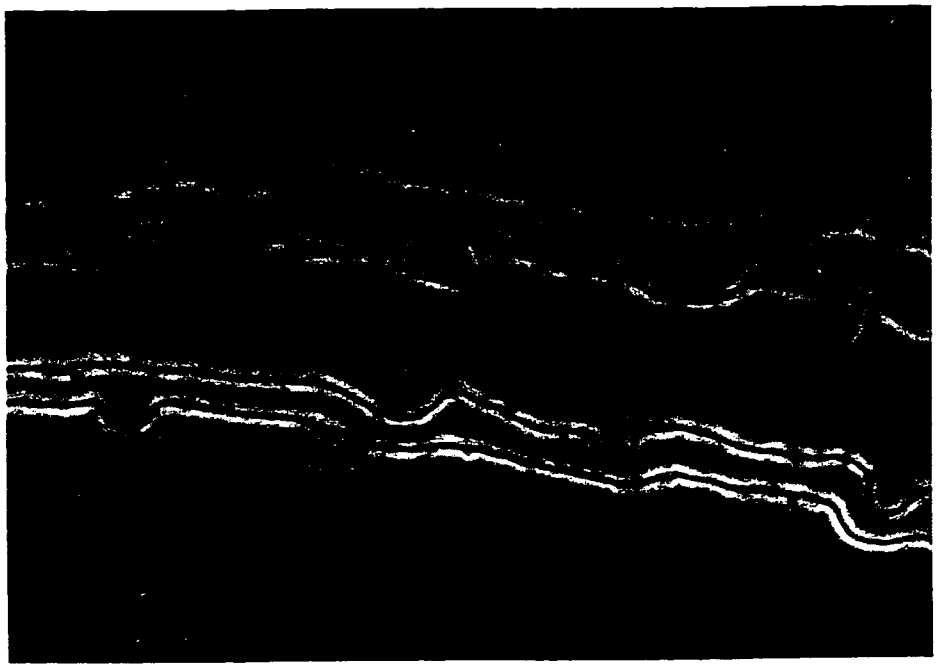

Figure 4.1 Method used to quantify mineral apposition rate (MAR) at the periosteal surface of sector. The original image (a.) was automatically processed to identify the center of the labels with minimal bias. In the processed image (b.) the wide label bands are reduced to thin black lines representing the highest pixels intensities of the labels in the original image.

At endocortical surfaces, bone apposition was lamellar in nature, and MAR was calculated by averaging the directly measured inter-label distances at ten evenly distributed points (VIDAS, Kontron Elektronik, Munich, Germany). Bone formation rate (BFR) with bone surface (BS) as referent ($BFR \cdot BS^{-1}$) was calculated in each sector by multiplying MAR with $dLS \cdot BS^{-1}$.

Statistics

Body mass and histomorphometric measures were compared between the two groups with student t-tests. Paired t-tests were used to detect differences in MAR and $BFR \cdot BS^{-1}$ between label periods, and changes in body mass within groups. Paired t-tests were also employed to contrast the mechanical milieu induced by treadmill walking against the mechanical milieu induced by drop-jumping. Significance for all tests was $p<0.05$. All data were expressed in mean±standard error. The statistical software package SPSS 8.0 for Windows (SPSS Inc., Chicago, IL) was used for data analysis.

RESULTS

Body Mass and Tibial Lengths

Both jumpers and controls gained body mass during the protocol ($p<0.003$). However, body masses were similar between groups, pre (1640±40 g vs 1670±50 g) and post (1830±60 g vs 1800±50 g) exercise intervention. Drop-jumping did not affect TMT longitudinal growth. Post-mortem TMT length in jumpers was 94.8±1.1 mm compared to 94.8±0.9 mm in controls.

Mechanical Milieu at the Periosteal Surface

Drop-jumps induced a highly non-uniform strain environment in the middiaphyseal TMT. Maximal compressive strains (-2070±360 με) were engendered in the antero-medial cortex, and maximal tensile strains (1210±250 με) occurred in the posterior cortex. These values were 30% ($p<0.04$) and 40% ($p<0.03$) greater than maximal strains recorded during slow treadmill walking (Table 4.1). The distributions of longitudinal normal strain across the middiaphysis were similar between drop-jumping and walking; the locations of the largest and smallest magnitudes coincided for both activities ($r^2=0.94$) (Fig. 4.3). When analyzed sector-specifically, changes in absolute strain magnitude ranged from -13% in sector 12 to +74% in sector 10.

Table 4.1 Maximal values for longitudinal normal strain (compressive and tensile), strain rate, and strain gradients produced in the cortex during walking and drop-jumping.

	Walking	Jumping
Compressive Strain [με]	-1570±220	-2070±360*
Tensile Strain [με]	860±160	1210±250*
Strain Rate [$\varepsilon \cdot s^{-1}$]	0.038±0.004	0.316±0.059*
Circumferential Strain Gradient [$\mu\varepsilon \cdot mm^{-1}$]	410±70	590±120*
Radial Strain Gradient [$\mu\varepsilon \cdot mm^{-1}$]	400±70	590±120*

Asterisks indicate significant differences between values induced by walking and drop-jumping ($p<0.05$).

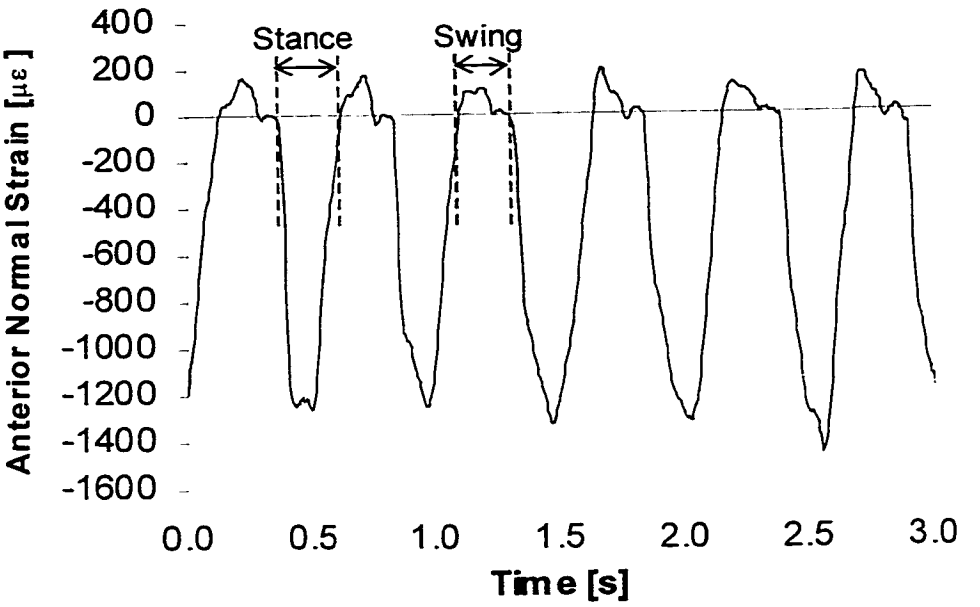

a.

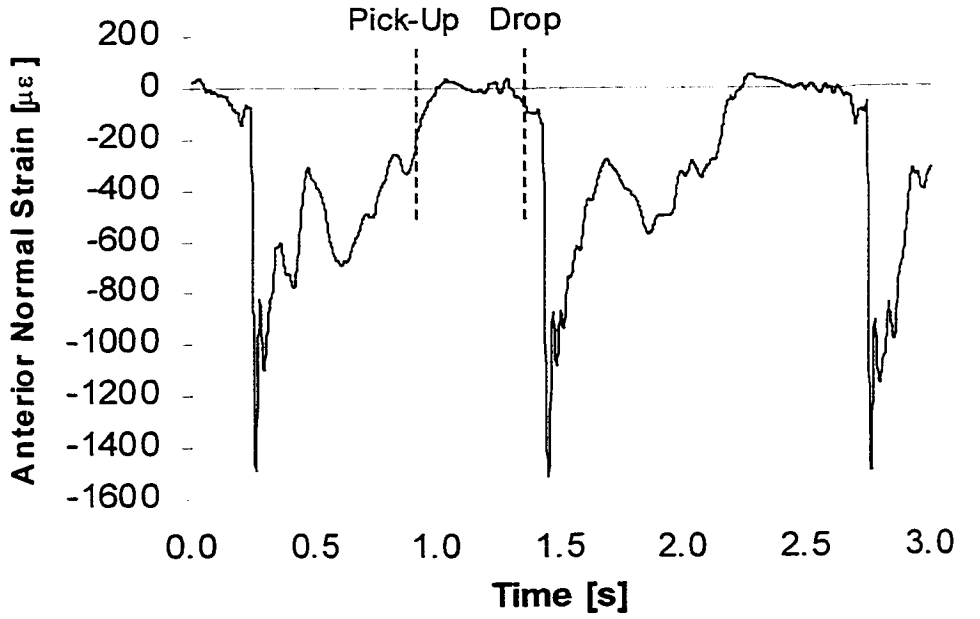

b.

Figure 4.2 Strain recording at the anterior gage during (a.) slow walking (0.51 $m \cdot s^{-1}$) and (b.) drop-jumping.

Maximal strain rates in the cortex produced by drop-jumping were 740% greater ($p<0.006$) than by walking (Table 4.1). At the periosteal surface, the distribution of peak strain rates was highly associated with the distribution of peak strain magnitude ($r^2=0.90$). Peak strain rates during walking were relatively uniformly distributed and increased in a highly non-uniform fashion during drop-jumping (Fig. 4.4). The smallest increases were observed at the lateral cortex (265% in sector 6), while the antero-medial (905% in sector 3) and posterior cortex (1090% in sector 10) experienced the largest increases. Consequently, strain rate distributions engendered by walking and drop-jumping were only moderately correlated ($r^2=0.64$).

Maximal strain gradients induced in the cortex by drop-jumping were approximately 45% greater ($p<0.02$) than during walking (Table 4.1). Both peak circumferential and peak radial strain gradients were non-uniformly distributed during walking. Drop-jumping significantly increased these values only in those sectors exhibiting large gradients (Fig. 4.5). The largest circumferential strain gradients were located at the medial (sectors 11-1) and lateral cortices (sectors 6-7) (Fig. 4.5) while the largest radial gradients occurred at the anterior (sectors 2-4) and posterior cortices (sectors 8-10).

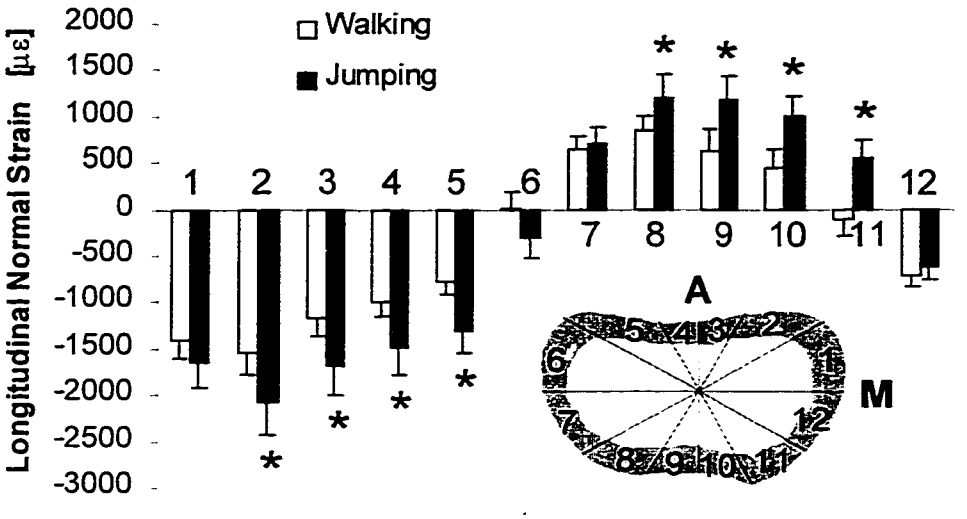

Figure 4.3 Distribution of peak longitudinal normal strain (mean±SE) on the TMT periosteal surface for walking and drop-jumping. Peak values occurring in each sector averaged across three step-cycles (white) and drop-jumps (black). Asterisks denote significant differences between drop-jumping and walking ($p<0.05$). M = medial, A = anterior.

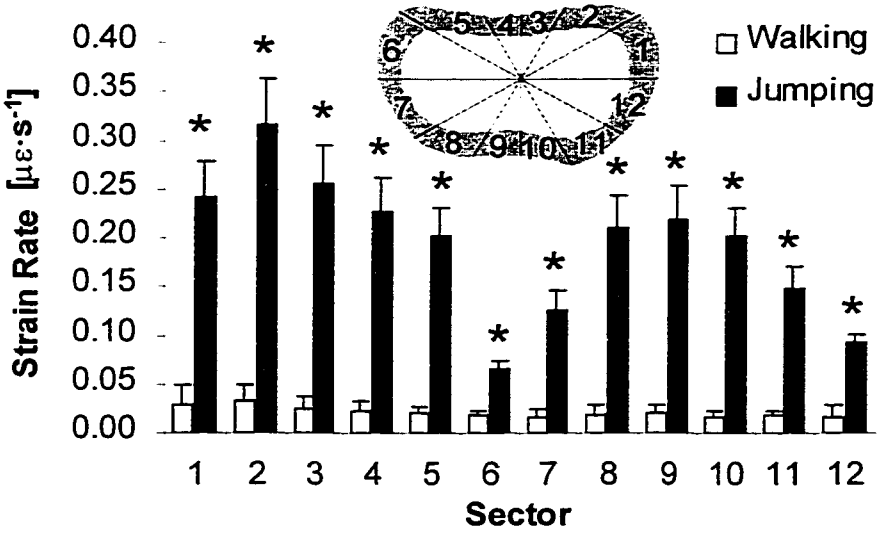

Figure 4.4 Distribution of peak strain rate (mean+SE) generated at the periosteal surface during walking and drop-jumping. Asterisks denote significant differences between drop-jumping and walking ($p<0.05$).

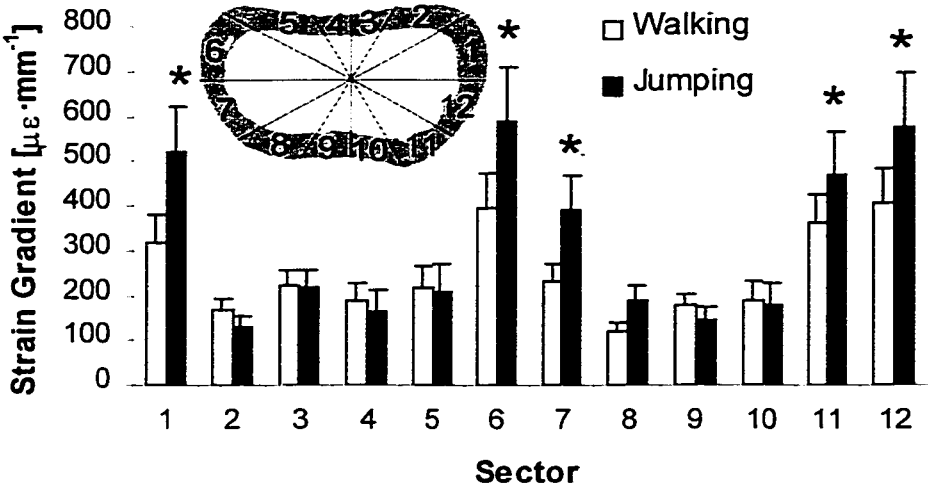

Figure 4.5 Distribution of peak circumferential strain gradients (mean+SE) generated at the periosteal surface during walking and drop-jumping. Asterisks denote significant differences between drop-jumping and walking ($p<0.05$).

Mechanical Milieu at the Endocortical Surface

Maximal strain magnitudes and strain rates produced during drop-jumping and walking were smaller at the endocortical surface than at the periosteal surface, while maximal circumferential strain gradients were similar at both surfaces. Specifically, peak events induced in the cortex by drop-jumping and walking were reduced by 28% (22%) for compressive strains, by 31% (33%) for tensile strains, by 28% (17%) for strain rates, and by 1% (2%) for circumferential strain gradients.

Despite lower peak magnitudes at the endocortical surface, the distributions of all mechanical parameters were strongly correlated between the two surfaces during drop-jumping and walking (Fig. 4.6); r^2 values for middiaphyseal distributions during drop-jumping (walking) were 0.93 (0.94) for peak strain magnitudes, 0.95 (0.77) for strain rates, and 0.95 (0.93) for circumferential strain gradients.

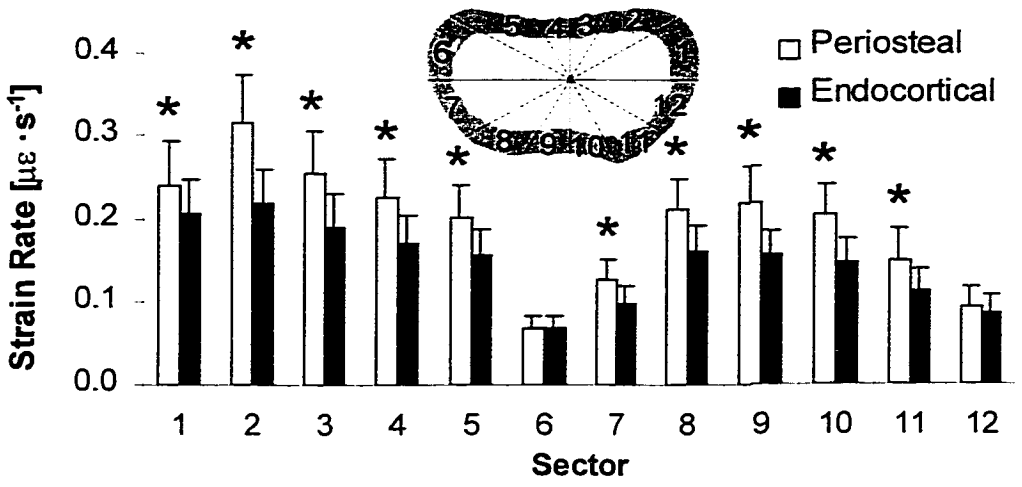

Figure 4.6 Distribution of peak strain rates engendered at endocortical and periosteal surfaces during drop-jumping (mean+SE). Asterisks denote significant differences between the two surfaces ($p<0.05$).

Histomorphometry at the Periosteal Surface

Both double fluorochrome labels covered the entire periosteal surface in controls and jumpers ($dLS \cdot BS^{-1} = 1$). Thus, values for MAR at periosteal surfaces coincided with values for $BFR \cdot BS^{-1}$ and, in the following, only values for MAR are reported. MAR measured in controls and jumpers prior to exercise intervention was not different for the two groups (Fig. 4.7). After 3 wk of jump training, MAR was significantly elevated in jumpers compared to controls (Fig. 4.8). Depending on the sector, increases ranged from 1% to 148% (mean: 38%). The largest increases were observed at the medial and postero-lateral cortices. When MAR was calculated taking the entire span of the 4 week protocol into account rather than just the last week, results were qualitatively similar ($r^2=0.83$). In accord with data obtained from the 3/4 wk label, the largest differences in MAR were detected in sector 1 (+52%), sector 8 (+39%), and sector 12 (+36%).

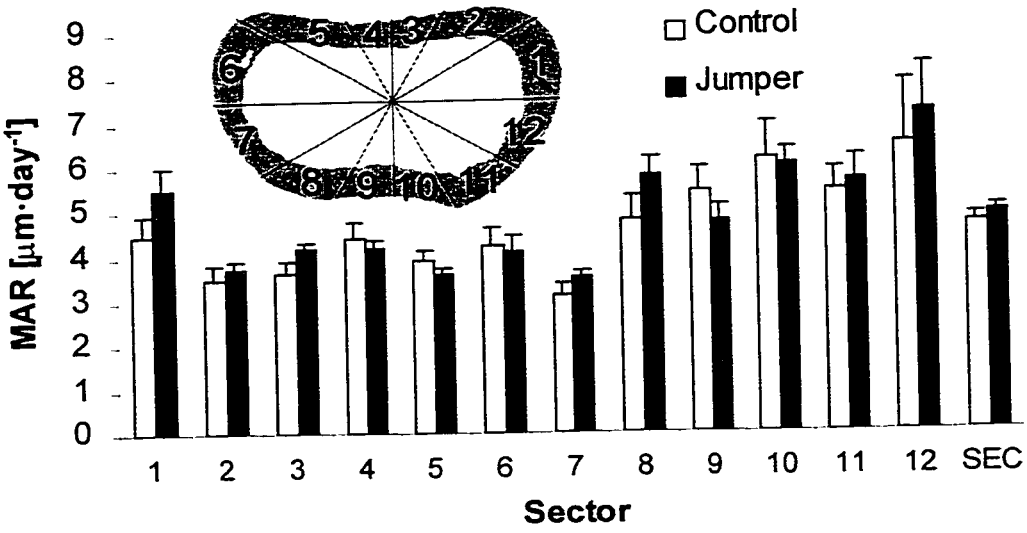

Figure 4.7 Distribution of mineral apposition rate (MAR) in controls and jumpers prior to initiating the study (mean+SE). SEC = value pertaining to the entire section.

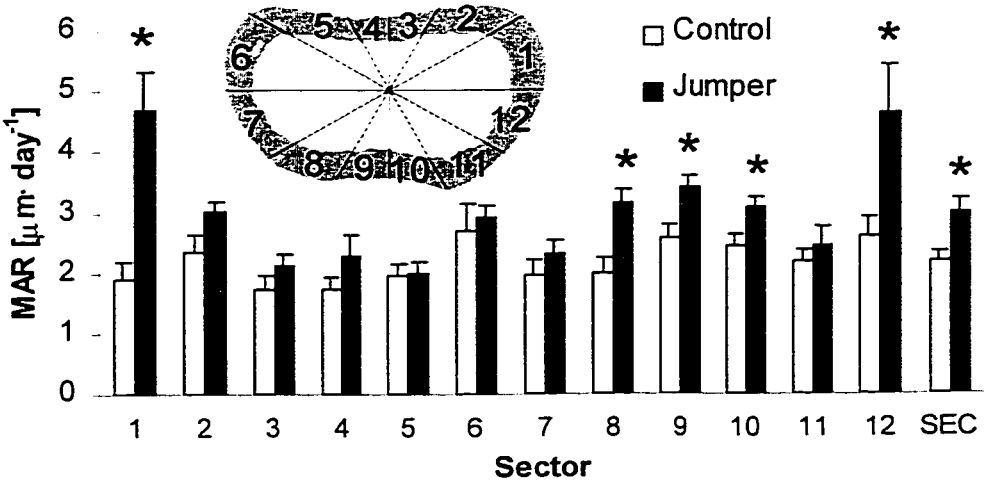

Figure 4.8 Distribution of periosteal mineral apposition rate (MAR) in controls and jumpers measured between wk 3 and wk 4 of the experimental protocol (mean+SE). Asteriks denote significant differences between controls and jumpers ($p<0.05$). SEC = value pertaining to the entire section.

In control roosters, MAR significantly decreased between the first (calcein) and the second (tetracycline) label interval in all sectors. Calculated for the entire section, this genetically related decrease was 53±6%. In drop-jump roosters, high-impact exercise muted this decrease to 38±5% (Figs. 4.7-4.8). Decreases occurred in all sectors, and only decreases in sectors 12 and 1 were statistically not different from zero.

Histomorphometry at the Endocortical Surface

Unlike periosteal surfaces, which comprised continuous double calcein and double tetracycline labels in all animals, endocortical surfaces were only partially active (single or double labeled) at either label interval. During the first label interval, 68±11% of endocortical surfaces were active in controls compared with 63±8% in drop-jumpers. Consistently inactive surfaces were not observed. Across animals, at least 35% of each sector was labeled. There were no significant differences in the quantity of active surface between controls and jumpers in any sector. Similarly, no significant differences in MAR and $BFR \cdot BS^{-1}$ were detected, neither for the entire section nor for any specific sector (Fig. 4.9).

After 3 wk of jump training, $BFR \cdot BS^{-1}$ at the endocortical surface was dramatically increased over control values (Fig. 4.10). Expressed for the entire surface, $BFR \cdot BS^{-1}$ in jumpers was increased five-fold over controls. The largest values for $BFR \cdot BS^{-1}$ were observed at the antero-medial and postero-lateral cortices. Differences in $BFR \cdot BS^{-1}$ was facilitated by greater $dLS \cdot BS^{-1}$ as well as increased MAR.

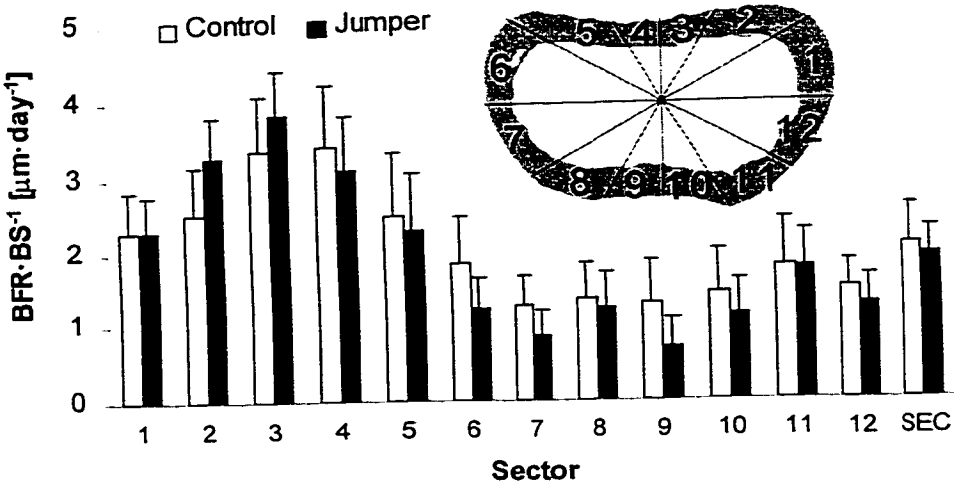

Figure 4.9 Endocortical bone formation rates (BFR) with bone surface (BS) as referent in control and jump roosters prior to initiation of study (mean+SE). SEC = value pertaining to the entire section.

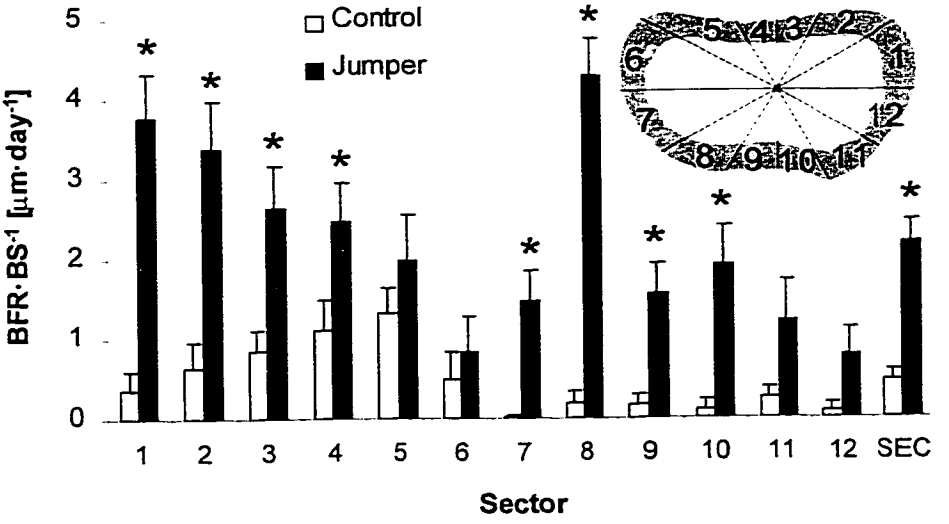

Figure 4.10 Endocortical normalized bone formation rates ($BFR \cdot BS^{-1}$) in controls and jumpers 3 wk into the experimental protocol (mean+SE). Asterisks denote significant differences between jumpers and controls ($p<0.05$). SEC = value pertaining to the entire section.

In control roosters, BFR·BS^{-1} significantly slowed down in all sectors between wk 17 and wk 21 of age in a genetically prescribed manner (mean 77±27%) (Figs. 4.9-4.10). In contrast, jumpers demonstrated significantly increased BFR·BS^{-1} in sectors 1 and 8 after 3 wk of drop-jump training. At the anterior cortex (sector 3), BFR·BS^{-1} significantly decreased while changes in the remaining sectors were statistically not different from zero.

Correlations at the Periosteal Surface

At the periosteal surface, none of the mechanical parameters quantified was significantly correlated with the exercise-induced increases in MAR. Increases in MAR at the medial cortex occurred in regions of large circumferential strain gradients while increased MAR at the posterior cortex was associated with regions of large tensile strains. The r^2 values relating the distribution of a mechanical parameter to the difference in MAR across the middiaphysis were: 0.03 for absolute strain magnitude, 0.01 for strain rate, 0.14 for circumferential strain gradients, and 0.03 (negative correlation) for radial strain gradients (Table 4.2). When tensile strains were treated differently from compressive strains the r^2 value for tensile strain increased to 0.87 ($p<0.05$) while the correlation for compressive strains remained weak ($r^2<0.01$) (Fig. 4.11). Combining circumferential and radial strain gradients via multiple regression analysis also did not lead to significant correlations.

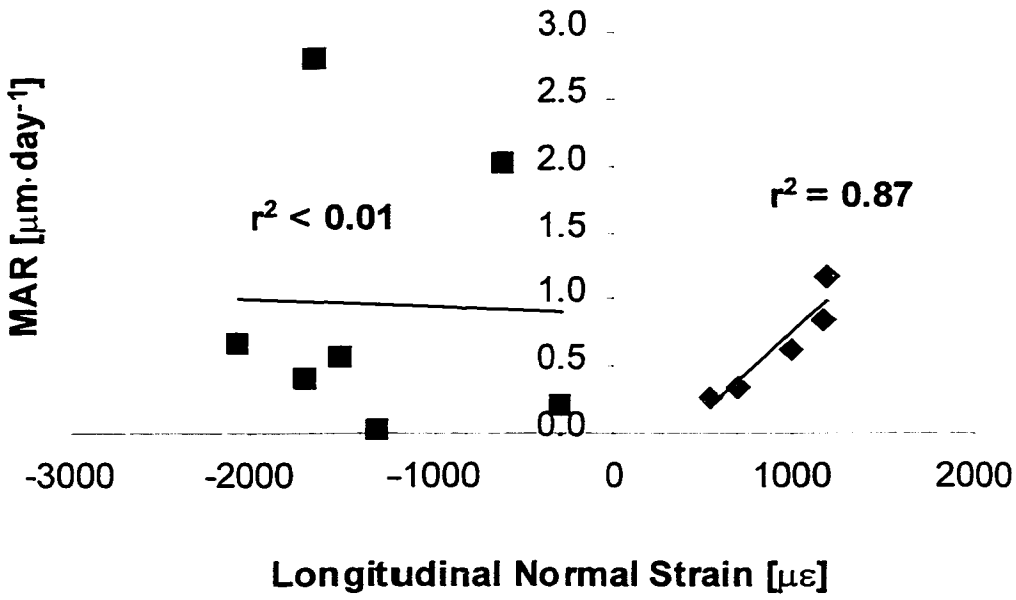

Figure 4.11 Linear regression between strain magnitude and the difference in MAR between jumpers and controls at the periosteal surface.

Using the difference in mechanical parameters produced by drop-jumping and running, rather than the absolute values produced by drop-jumping, did not lead to a significant correlation between a specific parameter and MAR at the periosteal surface. The correlation for strain magnitude and radial strain gradients became negative (r^2=0.15 and r^2=0.14), and less than 1% (22%) of the variation in MAR was accounted for by strain rate (circumferential strain gradients). Similarly, correlating the total values of MAR in jumpers to mechanical parameters induced by drop-jumping or to differences between drop-jumping and walking did not produce significant correlations.

Table 4.2 r^2 values produced by correlating the distribution of specific mechanical parameters to mineral apposition rates (MAR) at the periosteal surface.

	Jumping		**Jumping-Walking**	
	Δ MAR	Total MAR	Δ MAR	Total MAR
Absolute Strain	0.03, n.s.	0.15, n.s.	<0.01, n.s.	0.01, n.s.
Compressive Strain	<0.01, n.s.	0.05, n.s.	n.a.	n.a.
Tensile Strain	0.87, p<0.02	0.86, p<0.03	n.a.	n.a.
Strain Rate	0.01, n.s.	0.01, n.s.	<0.01, n.s.	0.02, n.s.
Circum. Gradients	0.14, n.s.	0.21, n.s.	0.21, n.s.	0.23, n.s.
Rad. Gradients	0.03, n.s.	0.10, n.s.	0.14, n.s.	0.24, n.s.
Comb. Gradients	0.26, n.s.	0.26, n.s.	0.21, n.s.	0.25, n.s.

Jumping = values produced during drop-jumping, Jumping-Walking = values reflecting the difference in the mechanical milieus between drop-jumping and walking, Δ MAR = difference in MAR between jumpers and controls, Total MAR = MAR of jumpers, Circum. = circumferential, Rad. = radial, Comb. = combined, n.s. = not significant, n.a. = not applicable.

Correlations at the Endocortical Surface

At the endocortical surface, strain rates related to drop-jumping were significantly associated with the specific sites of increased $BFR{\cdot}BS^{-1}$ (r^2=0.44, p<0.02). Absolute strain magnitude and strain gradients failed to generate significant correlations (Table 4.3). When absolute strain magnitude was separated into compressive and tensile strains, compressive strains were significantly correlated with elevated $BFR{\cdot}BS^{-1}$ (r^2=0.73, p<0.02) but not tensile strains (r^2=0.56) because of the limited number of data points.

Associating the mechanical milieu induced by drop-jumping to absolute BFR·BS^{-1} in jumpers led to significant correlations for strain magnitude (r^2=0.54, p<0.006), strain rate (r^2=0.67, p<0.001), and compressive strains (r^2=0.94, p<0.001). Correlating the difference in mechanical environments produced by drop-jumping and running to differences in BFR·BS^{-1} (or total BFR·BS^{-1}) associated with drop-jumping produced significant correlations only for strain rate (Table 4.3).

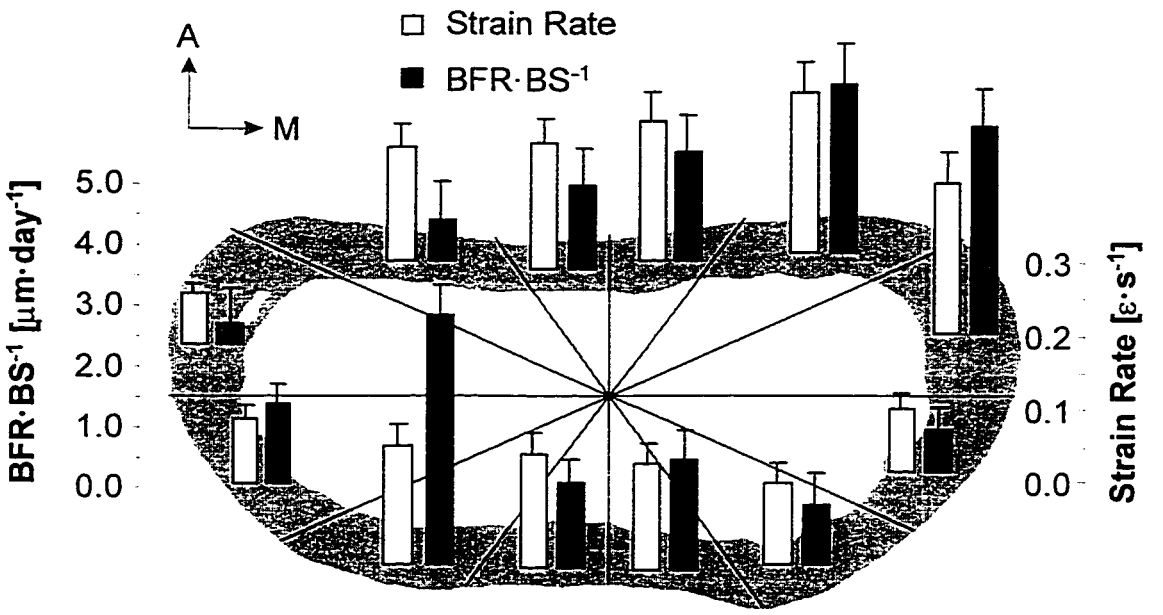

Figure 4.12 Distribution of peak strain rates and increases in BFR·BS^{-1} induced by drop-jumping at the endocortical surface superimposed on a middiaphyseal TMT section (mean+SE). A = anterior, M = medial.

Table 4.3 r^2 values produced by correlating the distribution of specific mechanical parameters to $BFR{\cdot}BS^{-1}$ at the endocortical surface.

	Jumping		**Jumping-Walking**	
	Δ $BFR{\cdot}BS^{-1}$	Total $BFR{\cdot}BS^{-1}$	Δ $BFR{\cdot}BS^{-1}$	Total $BFR{\cdot}BS^{-1}$
Absolute Strain	0.27, n.s.	0.54, $p<0.006$	0.05, n.s.	0.26, n.s.
Compressive Strain	0.73, $p<0.02$	0.94, $p<0.001$	n.a.	n.a.
Tensile Strain	0.56, n.s.	0.54, n.s.	n.a.	n.a.
Strain Rate	0.44, $p<0.02$	0.67, $p<0.001$	0.45, $p<0.02$	0.66, $p<0.001$
Circum. Gradients	0.15, n.s.	0.27, n.s.	0.03, n.s.	0.11, n.s.
Rad. Gradients	0.24, n.s.	0.30, n.s.	0.04, n.s.	0.10, n.s.
Comb. Gradients	0.26, n.s.	0.30, n.s.	0.04, n.s.	0.11, n.s

Jumping = values produced during drop-jumping, Jumping-Walking = values reflecting the difference in the mechanical milieus between drop-jumping and walking, Δ $BFR{\cdot}BS^{-1}$ = difference in $BFR{\cdot}BS^{-1}$ between jumpers and controls, Total $BFR{\cdot}BS^{-1}$ = $BFR{\cdot}BS^{-1}$ of jumpers, Circum. = circumferential, Rad. = radial, Comb. = combined, n.s. = not significant, n.a. = not applicable.

DISCUSSION

Superimposing 200 daily drop-jumps upon normal daily activities led to significantly increased bone formation in the middiaphyseal tarsometatarsus of immature roosters. Despite the short daily exercise duration of approximately two and a half minutes per day, increases were substantial and non-uniform in distribution at both endocortical and periosteal surfaces. The mechanical environment induced by drop-jumping involved very large strain rates and was also highly non-uniformly distributed across the middiaphysis.

At the periosteal surface, only tensile strains were associated with the specific sites of increased bone formation while strain rate was highly correlated with elevated bone formation rates at the endocortical surface.

Limitations should be considered when interpreting results from this study. Firstly, despite the large increases in bone formation rates in jumpers, the structural impact of a long-term exercise program using drop-jumps cannot be inferred from this short-term study. Secondly, we only quantified a few of the many proposed mechanical parameters but strain magnitude and distribution, strain rate, and strain gradients are among the principal parameters that have been derived experimentally.

Peak strain magnitudes and peak strain rates reported here for treadmill walking were similar to those reported from the tarsometatarsus in adult roosters[112] and from the human tibia.[27] Few studies have measured bone strains during jumping. The extremely large strain rates induced by drop-jumps were larger than ulnar bone strains produced by dropping rats from a 30 cm height (0.1 $\varepsilon \cdot s^{-1}$),[171] maybe reflecting the additional acceleration used for our drop jumps.[114]

The middiaphyseal tarsometatarsus of White Leghorn roosters has been previously used to study exercise related bone adaptation. Protocols involving running consistently exerted negative effects on periosteal bone formation in 2-12 wk[160], 9-17 wk (Chapter 3), and 30-39 wk[151] old roosters. Reduced periosteal bone growth may lead to smaller cross-sectional moments of inertia, a risk factor for bone fractures. In contrast, drop-jumping in the current study increased periosteal bone formation, consistent with the phenomenological observation that high-impact exercise regimens have a higher

osteogenic efficacy.[19,35,45,83] Comparing the mechanical milieus induced by drop-jumping and high-speed running revealed that drop-jumping induced much larger maximal strain rates (+256%, $p<0.006$), similar maximal strain magnitudes (+11%, n.s.) and a much smaller number of loading cycles (< -92%). The osteogenic relevance of high strain rates has been suggested previously in invasive or external loading models.[170,178,266] This is the first study, however, that related very high strain rates in the presence of physiological strain magnitudes to a powerful osteogenic response in an exercise model of bone adaptation. Whether the smaller number of loading cycles contributed to the positive effect of drop-jumping is unknown.[108,217] Interestingly, the osteotropic response occurred despite the extremely stable strain environment of the middiaphyseal tarsometatarsus during drop-jumping. Thus, neither changes in loading directions, prevalent in many high-impact activities, nor very large strain magnitudes were necessary to stimulate bone growth. It is possible, though, that changes in these mechanical parameters would have further increased the osteogenic response.

Our observation that the response to exercise was more pronounced at endocortical than at periosteal surfaces is consistent with other studies that examined the morphology of growing bone in response to exercise.[160,282] Mechanical stimuli, however, were smaller in magnitude at the endocortical surface, perhaps supporting evidence that the two surfaces are regulated independently.[262,263] Alternatively, the endocortical surface may have simply comprised the greater potential to increase formation rates (or to attenuate decreases in formations rates) as normal, genetically related, mineral apposition rates and the percentage of actively forming surfaces were lower at this surface.

Peak strain rates were well correlated with the specific sites of bone formation at the endocortical surface where the largest differences between sedentary controls and jumpers were observed. Peak circumferential strain gradients, that were generated close to the neutral axis, could not explain differences in bone formation rates between jumpers and controls at any surface. This is consistent with data from the growing rat ulna model,[171] in which increases in bone formation induced by exogenous loading also occurred in regions of high strain rates away from the neutral axis. In contrast, circumferential strain gradients have been previously successfully correlated with the specific sites of periosteal activation (bone formation) in the young adult avian skeleton.[87,113] The major difference between these models lies in the primarily forming bone surfaces in growing animals versus the primarily quiescent surfaces in young adult animals. Osteocytes, as well as osteoblasts, bone lining cells, and osteoclasts can be responsive to mechanical loading[38,127,182,196,200,284] and, perhaps, the sensitivity of a bone surface to a specific mechanical parameter varies with the presence or absence of specific bone cell populations and their level of activity.

One common aspect of strain gradients and strain rate is that both are strongly related to fluid flow in bone. Fluid flow has been implicated in the process by which bone cell populations sense their mechanical environment.[127,182,192,199,208,264,277] Thus, the strong relation between peak strain rates and the sites of bone formation at the endocortical surface is consistent with the hypothesis that the transduction of mechanical stimuli from the tissue to the cellular level is mediated by fluid flow.

Nevertheless, strain rate was correlated with the sites of additional bone formation rates at the endocortical but not at the periosteal surface, although both surfaces experienced, qualitatively, similar mechanical milieus. Additionally to a different cellular activity level, the periosteal surface was also characterized by a different type of bone. Consistent with bone formation in the rat ulna model,[171] normal, growth related, bone formation at the TMT endocortical surface was lamellar in nature. The periosteal surface of the rooster tarsometatarsus was, however, governed by haversian bone which may give rise to differential bone fluid dynamics.[154] Further research is warranted to find mechanical parameters that are able to consistently predict the specific sites of exercise-induced bone formation.

Most theoretical models of mechanically induced bone adaptation assume that bone perceives biophysical stimuli as the difference between the newly imposed mechanical milieu and the habitual mechanical milieu at equilibrium.[34,46,78,214,260,276] Yet, bone's strain history is complex,[74,162] and the specific component(s) of the habitual mechanical milieu that maintains bone mass in the absence of additional exogenous or endogenous stimuli are unknown. Many studies have assumed that large magnitude mechanical stimuli (as induced during walking) are responsible for bone homeostasis.[23,178] However, more recent data suggest that the mechanical signal preserving bone mass is uniform in distribution[89] and may be related to high-frequency low-magnitude strain stimuli engendered primarily by muscular activity.[162] This would indicate that the distributions of mechanical parameters related to drop-jumping, and not the ones related to the difference

between drop-jumping and walking, should be correlated with site-specific changes in bone cell activity. Interestingly, this approach led to more significant relations.

Similarly, it is conceivable that once mechanical stimuli have triggered a response in bone cells they can override the genetically determined, normal formative processes. If this was true, then the distribution of mechanical parameters should be associated with absolute bone formation rates and not with the difference in bone formation rates between jumpers and controls. This approach also increased, in general, the correlative strength between the distributions of mechanical parameters and bone formation rates.

The response of the periosteal surface to drop-jumping was detectable by comparing MAR between groups based on the 3-4 wk interval or on the 0-4 wk label. Assuming that once bone cells detected the mechanical stimulus produced by drop-jumping, their response was constant (all or nothing) and superimposed on normal MAR for the remaining exercise period, one can determine the initiation of the response at the tissue level (i.e., increase in MAR compared to controls). When data from the three sectors that demonstrated the largest responses were taken, the calculated increase in MAR occurred 8±3 days after the start of the jump protocol. This slightly higher value compared to data from external loading models[36,171,185] may be accounted for by the exercise acclimatization period during which the number of drop-jumps was only gradually increased and by our assumptions mentioned above.

In summary, high impact drop-jumps created very large peak strain rates in the presence of unchanged strain distributions and moderately increased peak strain magnitudes. Our data indicate that the powerful osteotropic effect of high-impact drop-

jumping on tarsometatarsal endocortical and periosteal surfaces was primarily caused by the large increase in strain rate. The good correlation between the distribution of strain rates and the specific sites of increased lamellar bone formation within the middiaphysis emphasizes the sensitivity of growing bone to high strain rates.

Chapter 5

DISCUSSION AND CONCLUSIONS

DISCUSSION

Summary

The experiments designed for this dissertation examined the response of the middiaphyseal rooster tarsometatarsus to exercise protocols involving running and high-impact drop-jumping. A unique feature of these studies was that the mechanical environment induced by these activities was rigorously quantified and linked to exercise-related changes across the middiaphysis. In the first experiment, young adult roosters were subjected to 1500 daily steps of high-speed running for 3 wk. Running activated previously quiescent periosteal surfaces, and the specific sites of activation were highly correlated with circumferential strain gradients. In the second experiment, 9 wk old roosters ran for 8 wk. Running modestly altered the mechanical milieu compared to walking, but the brief loading sessions did not produce significant changes in tarsometatarsal morphology, mechanics, or mineral content. In the third experiment, 200 daily high-impact drop-jumps were applied to 17 wk old roosters for 3 wk. Drop-jumping induced very large strain rates and led to significantly increased bone formation compared to sedentary controls. Strain rates were spatially correlated with the specific sites of additional bone formation at the endocortical surface. No parameter, however, successfully explained increased periosteal bone formation.

Limitations

Some fundamental assumptions and limitations of this dissertation should be considered when interpreting its results. It was assumed that bone adaptation is regulated locally and

site-specifically. This appears to be a reasonable assumption as mechanically modulated bone formation, as well as its corresponding mechanical milieu, are focal in nature. Bone cells, however, have the ability to communicate through gap junctions connecting the three-dimensional osteocytic network.[56,271] If bone cells aggregate and process physical signals from different sites by intercellular communication, then our site-specific approach would be limited in its view of bone adaptation. However, results from several studies argue against the concept of spatial integration as in these studies new bone formation was elicited only by a change in strain distribution while keeping peak strain magnitudes in the physiological range.[87,140,217]

Another assumption used in these studies was that the mechanical stimuli associated with exercise were the principal determinants of adaptive changes. Clearly, exercise not only affects the mechanical environment of a bone but may also change its physiological environment. These changes can include alterations in blood flow,[67,85,227,246,257] calcium metabolism,[4] blood pH,[49] and regulation of hormones and cytokines.[52,71,95,203,237] While this physiological response related to exercise has limited potential to initiate bone (re)modeling on its own,[120,256] it could possibly influence the mechanically related adaptive process of bone. Further research is necessary to investigate synergistic reactions and to clearly differentiate between mechanical and physiological factors.

Exercise was superimposed upon habitual activity in all studies. Bone's strain history related to habitual loading is complex[74,162] and was not quantified in this dissertation. Mechanical parameters related to mechanical loading can only be isolated

when all mechanical stimuli related to background loading are removed between loading sessions. Thus, it is possible that interactions between the mechanical environments induced by exercise and background loading influenced the results. The long term utility of this research, however, lies with the design of exercise regimens that will optimally enhance bone mass in different groups of individuals. As it is currently impossible to assess accurately strain histories in these groups, it appears prudent to search for mechanical parameters that can predict the sites of bone formation induced by *increased* mechanical loading.

Correlations of Mechanical Parameters with Sites of Bone Formation

Results from these studies are consistent with the notion that not a single mechanical parameter can explain all mechanically related adaptive processes.[220] We confirmed a previous report[87] that strain gradients are good predictors of the specific sites of periosteal activation. The utility of this observation, though, may be limited to the adult skeleton subjected to loading regimens that predominantly consist of large bending moments. Our findings that strain rates are well correlated with specific sites of additional lamellar bone formation are consistent with data from the rat ulna model.[171] These disparate results between models involving growing and quiescent bone suggests that the sensitivity of bone to specific mechanical parameters depends on the physiological conditions governing the bone surfaces.

Increasing evidence points towards the involvement of bone fluid in transducing mechanical signals in bone.[127,182,192,199,208,264,277] One common aspect of many of the

proposed mechanical parameters is that they, at some level, influence fluid flow within bones. Increased fluid flow may affect bone cells by altered fluid pressure,[110] fluid shear stresses,[127,199,200,277] enhanced nutrient transport,[134,255] or electrokinetic effects.[47,155,181,186,222,245] Thus, perhaps fluid flow and not mechanical parameters should be related to changes in bone cell metabolism. However, bone fluid flow can currently only be estimated with mathematical models[156,223,242] or measured indirectly via streaming potentials[43,180,192] or molecular tracers.[255] All techniques rely on assumptions about bone's microarchitecture. On the other hand, many mechanical parameters are readily quantifiable and if specific parameters can consistently be linked to adaptive processes in bone, they may clinically be used to optimize exercise regimen.

Running versus Drop-Jumping in Growing Roosters

Reducing the number of loading cycles negated the adverse effects associated with long-duration run protocols in the growing rooster tarsometatarsus.[151,160] Nevertheless, the 8-wk exercise protocol did not positively influence bone morphology or mechanics. High-impact drop-jumping, on the other hand, produced significantly increased bone formation rates at periosteal and endocortical surfaces. The higher osteotropic efficacy of high-impact exercise compared to lower-impact exercise has been proposed previously.[19,35,45,83] These studies, however, did not quantify bone's mechanical environment and the specific aspect of the high-impact exercise induced mechanical milieu that causes hypertrophy in growing bone is unknown. Comparing the mechanical milieus induced by drop-jumping and high-speed running in the current studies revealed

that drop-jumping induced much larger maximal strain rates (+260%), similar maximal strain magnitudes and a much smaller number of loading cycles (-92%). The osteogenic relevance of high strain rates has been suggested previously in invasive or external loading models.[170,178,266] This is the first report, that directly related very high strain rates to a powerful osteotropic response in an exercise model of bone adaptation. It appears that changes in loading directions, prevalent in many high-impact activities, or very large strain magnitudes are not critical for the osteotropic efficacy of high-impact exercise. It is possible, though, that additional changes in other mechanical parameters, including strain magnitude and distribution, may increase the magnitude of the osteogenic response.

Exercise-Induced Mechanical Milieu in Growing and Adult Roosters

It has been suggested that peak strains as well as strain distributions engendered by physical activity do not change with age.[13,119] This, however, has not been rigorously tested as, in these studies, full field strain distributions were not determined, and their observations were limited to the sites of strain gage attachment. Nevertheless, data from this dissertation support the hypothesis of a stable strain environment during growth. Comparing strain data induced by high-speed running between immature and mature roosters revealed that mean maximal strain magnitudes induced in the cortex (including strain distributions) as well as mean maximal strain rates varied by less than 5%. Maximal strain gradients in the TMT were slightly higher (+8%) in the immature roosters due to smaller bone areal properties in the presence of similar strain magnitudes.

It is remarkable that not only strain distributions generated by running were similar in immature and mature roosters, but also that strain distributions remained consistent across activities. Neither a three-fold increase in locomotor speed nor a change in activity (drop-jumping) qualitatively altered strain distributions across the middiaphysis.

Sensitivity of Growing and Adult Bone to Exercise

Some studies have proposed that immature bone is more sensitive to changes in its mechanical environment than mature bone.[30,115] Although normal activity levels at bone surfaces greatly vary with age – from actively forming and resorbing to quiescent – other studies have found little experimental evidence for this hypothesis.[61,195,250] Running produced similar mechanical environment in the tarsometatarsus of mature and immature roosters, yet, different experimental designs precluded direct comparisons between the two exercise studies. It is interesting to note, though, that a small number of loading cycles of the mechanical milieu associated with high-speed running was capable of activating periosteal surfaces in the young adult skeleton but it failed to produce significant changes in the growing skeleton. Results from the three studies are discussed in more detail in the Discussion sections of Chapters 2-4.

CONCLUSIONS

These studies indicate that growing and adult cortical bone is capable of perceiving exercise derived mechanical stimuli as osteogenic. They also emphasize that the quantification of the exercise-induced mechanical environment may help to design

exercise protocols that effectively increase bone mass in the growing and young adult skeleton. A previously proposed mechanical parameter (circumferential strain gradients) was confirmed as a good predictor of the specific sites of bone forming surfaces in the young adult skeleton. This knowledge may enable the design of exercise regimens that initiate bone formation at sites most in need of enhanced structural integrity. Decreasing the number of loading cycles abolished the negative response related to long-duration running protocols in growing roosters but only high-impact drop-jumping increased bone formation. Comparing the mechanical milieus produced by high-speed running and drop-jumping in the growing tarsometatarsal middiaphysis suggests that the osteotropic effect of drop-jumping was caused by very high strain rates. It appears that the efficacy of high-impact exercise does not depend on altered strain and strain gradient magnitudes, or changes in strain distributions. The good correlation between the distribution of strain rates and the specific sites of increased lamellar bone formation produced by drop-jumping emphasizes the sensitivity of growing diaphyseal bone to high strain rates.

In summary, the relation between exercise-induced mechanical parameters and the specific sites of bone formation is not a simple one and no single parameter could successfully explain bone's adaptive response in the three studies. Nevertheless, both parameters that were correlated with skeletal changes (strain gradients and strain rate) are strongly associated with bone fluid flow. Strain magnitude, a parameter that many studies have focused on in the past, was not associated with the specific sites of bone formation. Future efforts should seek to validate and further investigate the skeletal response to exercise-induced mechanical stimuli under alternate loading conditions. Additionally,

molecular techniques such as in situ reverse transcription polymerase chain reaction (RT-PCR) will provide important clues on mechanisms underlying these tissue level observations.

Chapter 6

PUBLICATIONS

The following publications were produced during the course of this dissertation.

REFEREED PAPERS (PUBLISHED OR IN PRESS)

Judex S, Gross TS, Bray RC, and Zernicke RF (1997) Adaptation of bone to physiological stimuli. *Journal of Biomechanics* **30**, 421-429.

Judex S, Gross TS, and Zernicke RF (1997) Strain gradients correlate with sites of exercise-induced bone forming surfaces in the adult skeleton. *Journal of Bone and Mineral Research* **12**, 1737-1745.

Gross TS, Damji AA, **Judex S,** Bray RC, and Zernicke RF (1999) Bone hyperemia precedes disuse induced intracortical bone resorption. *Journal of Applied Physiology* **86,** 230-235.

Judex S, Whiting WC, and Zernicke RF (in press) Exercise induced bone adaptation: Considerations for designing an osteogenically effective exercise program. *International Journal of Industrial Ergonomics.*

Banes AJ, Horesovsky G, Larson C, Tsuzaki M, Noel S, **Judex S,** Archambault J, Zernicke RF, Herzog W, Kelly S, and Miller L (in press) Mechanical load stimulates expression of novel genes in vivo and in vitro in avian flexor tendon cells. *Osteoarthritis and Cartilage.*

REFEREED PAPERS (IN REVIEW)

Judex S, Wohl GR, Wolff RB, Leng W, Gillis AM, and Zernicke RF. Dietary fish oil supplementation adversely affects cortical bone morphology and biomechanics in growing rabbits. *Calcified Tissue International.*

Judex S and Zernicke RF. Does the mechanical milieu associated with high-speed running lead to adaptive changes in the diaphyseal tarsometatarsus of growing roosters? *Bone.*

Judex S and Zernicke RF. High-impact exercise and growing bone: the relation between high strain rates and increased bone formation in the middiaphyseal rooster tarsometatarsus. *Journal of Bone and Mineral Research.*

CONFERENCE PROCEEDINGS AND ABSTRACTS (PEER REVIEWED)

Judex S and Glockner PG (1994) Forces and displacements in rectangular trampoline cable networks. *Proceedings of the Conference 'A World of Shells'*, Banff, Alberta, 255-258.

Judex S, Gross TG, and Zernicke RF (1995) Changes in circumferential strain gradients during Locomotion. *Proceedings of the 19th Annual Meeting of the American Society of Biomechanics*, 53-54.

Zernicke RF, Gross TG, and **Judex S** (1995) Functional adaptation of bone to physiological and mechanical stimuli. *Proceedings of the 15th Congress of the International Society of Biomechanics*, 10-11.

Judex S, Gross TG, and Zernicke RF (1996) In vivo quantification of mechanical parameters potentially affecting fluid flow in bone. *Transactions of the Orthopaedic Research Society* **42**, 597.

Judex S, Gross TG, and Zernicke RF (1996) Locomotion-induced circumferential strain gradients predict periosteal bone formation. *Proceedings of the 9th Biennial Conference and Symposia of the Canadian Society for Biomechanics*, 388-389.

Judex S, Gross TG, and Zernicke RF (1996) Strain gradients predict sites of exercise-stimulated periosteal bone formation in the adult skeleton. *Journal of Bone and Mineral Research* **11**, S269.

Judex S, Gross TG, and Zernicke RF (1997) Strain gradients effects in exercise induced new bone formation. *Transactions of the Orthopaedic Research Society* **43**, 404.

Banes AJ, Horesovsky G, Noel S, **Judex S,** Archambault J, Benjamin M, Ralphs J, McNeilly C, Zernicke R, Herzog W, and Miller L (1997) Mechanical load stimulates expression of novel genes in vivo and in vitro in avian flexor tendon cells. *Transactions of the Orthopaedic Research Society* **43**, 710.

Judex S, Wilson AN, and Zernicke RF (1997) The influence of shear strains on exercise stimulated new bone formation. *Proceedings of the 1997 Bioengineering Conference* (ASME), 169-170.

Judex S, Schaaff FG, and Zernicke RF (1997) Growing bone and exercise: Site specific analysis of middiaphyseal geometry. *Journal of Bone and Mineral Research* **12**, S244.

Judex S and Zernicke RF (1998) The sensitivity of adult cortical bone to calcium deficiency and glucocorticoid excess. *Bone* **23**, S436.

Judex S, and Zernicke, RF (submitted) High-impact exercise and growing bone – changes in bone's mechanical milieu induced by jumping. *Proceedings of the 1999 Bioengineering Conference* (ASME).

BOOK CHAPTERS

Judex S, Whiting WC, and Zernicke RF (in press) Bone biomechanics and fracture. In: *Biomechanics in Ergonomics*. Kumar S (ed). Taylor & Francis, London, U.K.

Zernicke RF and **Judex S** (in press) Effects of age, exercise, and immobility on biological materials. In: *Biomechanics of the Musculo-Skeletal System*. Nigg BM and Herzog W (ed). 2nd edition, John Wiley & Sons Ltd, U.K.

Chapter 7

REFERENCES

1. Adams DJ, Spirt AA, Brown TD, Fritton SP, Rubin CT, and Brand RA (1997) Testing the daily stress stimulus theory of bone adaptation with natural and experimentally controlled strain histories. *J Biomech* **30**, 671-678.
2. Akhter MP, Raab DM, Turner CH, Kimmel DB, and Recker RR (1992) Characterization of in vivo strain in the rat tibia during external application of a four-point bending load. *J Biomech* **25**, 1241-1246.
3. Alam AS, Gallagher A, Shankar V, Ghatei MA, Datta HK, Huang CL, Moonga BS, Chambers TJ, Bloom SR, and Zaidi M (1992) Endothelin inhibits osteoclastic bone resorption by a direct effect on cell motility: implications for the vascular control of bone resorption. *Endocrinology* **130**, 3617-3624.
4. Ashizawa N, Ouchi G, Fujimura R, Yoshida Y, Tokuyama K, and Suzuki M (1998) Effects of a single bout of resistance exercise on calcium and bone metabolism in untrained young males. *Calcif Tissue Int* **62**, 104-108.
5. Bailey DA, Faulkner RA, and McKay HA (1996) Growth, physical activity, and bone mineral acquisition. *Exerc Sport Sci Rev* **24**, 233-266.
6. Banes AJ, Tsuzaki M, Yamamoto J, Fischer T, Brigman B, Brown T, and Miller L (1995) Mechanoreception at the cellular level: the detection, interpretation, and diversity of responses to mechanical signals. *Biochem Cell Biol* **73**, 349-365.
7. Bass S, Pearce G, Bradney M, Hendrich E, Delmas PD, Harding A, and Seeman E (1998) Exercise before puberty may confer residual benefits in bone density in adulthood: studies in active prepubertal and retired female gymnasts. *J Bone Miner Res* **13**, 500-507.
8. Bassey EJ and Ramsdale SJ (1994) Increase in femoral bone density in young women following high-impact exercise. *Osteoporos Int* **4**, 72-75.
9. Bennell KL, Malcolm SA, Khan KM, Thomas SA, Reid SJ, Brukner PD, Ebeling PR, and Wark JD (1997) Bone mass and bone turnover in power athletes, endurance athletes, and controls: a 12-month longitudinal study. *Bone* **20**, 477-484.
10. Bentolila V, Boyce TM, Fyhrie DP, Drumb R, Skerry TM, and Schaffler MB (1998) Intracortical remodeling in adult rat long bones after fatigue loading. *Bone* **23**, 275-281.

11. Bertram JE and Biewener AA (1988) Bone curvature: sacrificing strength for load predictability? *J Theor Biol* **131**, 75-92.
12. Bertram JE and Swartz SM (1991) The 'law of bone transformation': a case of crying Wolff? *Biol Rev Camb Philos Soc* **66**, 245-273.
13. Biewener AA and Bertram JE (1993) Skeletal strain patterns in relation to exercise training during growth. *J Exp Biol* **185**, 51-69.
14. Biewener AA and Bertram JE (1994) Structural response of growing bone to exercise and disuse. *J Appl Physiol* **76**, 946-955.
15. Biewener AA, Swartz SM, and Bertram JE (1986) Bone modeling during growth: dynamic strain equilibrium in the chick tibiotarsus. *Calcif Tissue Int* **39**, 390-395.
16. Biewener AA and Taylor CR (1986) Bone strain: a determinant of gait and speed? *J Exp Biol* **123**, 383-400.
17. Biewener AA, Thomason J, Goodship A, and Lanyon LE (1983) Bone stress in the horse forelimb during locomotion at different gaits: a comparison of two experimental methods. *J Biomech* **16**, 565-576.
18. Bourrin S, Genty C, Palle S, Gharib C, and Alexandre C (1994) Adverse effects of strenuous exercise: a densitometric and histomorphometric study in the rat. *J Appl Physiol* **76**, 1999-2005.
19. Bourrin S, Ghaemmaghami F, Vico L, Chappard D, Gharib C, and Alexandre C (1992) Effect of a five-week swimming program on rat bone: a histomorphometric study. *Calcif Tissue Int* **51**, 137-142.
20. Bourrin S, Zerath E, Vico L, Milhaud C, and Alexandre C (1992) Bone mass and bone cellular variations after five months of physical training in rhesus monkeys: histomorphometric study. *Calcif Tissue Int* **50**, 404-410.
21. Brackenbury JH and Avery P (1980) Energy consumption and ventilaratory mechanisms in the exercising fowl. *Comp Biochem Physiol* **66A**, 439-445.
22. Brand RA and Stanford CM (1994) How connective tissues temporally process mechanical stimuli. *Med Hypotheses* **42**, 99-104.

23. Brown TD, Pedersen DR, Gray ML, Brand RA, and Rubin CT (1990) Toward an identification of mechanical parameters initiating periosteal remodeling: a combined experimental and analytic approach. *J Biomech* **23**, 893-905.
24. Brunelli MP and Einhorn TA (1998) Medical management of osteoporosis. Fracture prevention. *Clin Orthop* 15-21.
25. Burr DB (1997) Bone, exercise, and stress fractures. *Exerc Sport Sci Rev* **25**, 171-194.
26. Burr DB and Martin RB (1989) Errors in bone remodeling: toward a unified theory of metabolic bone disease. *Am J Anat* **186**, 186-216.
27. Burr DB, Milgrom C, Fyhrie D, Forwood M, Nyska M, Finestone A, Hoshaw S, Saiag E, and Simkin A (1996) In vivo measurement of human tibial strains during vigorous activity. *Bone* **18**, 405-410.
28. Burr DB, Schaffler MB, Yang KH, Lukoschek M, Sivaneri N, Blaha JD, and Radin EL (1989) Skeletal change in response to altered strain environments: is woven bone a response to elevated strain? *Bone* **10**, 223-233.
29. Burr DB, Schaffler MB, Yang KH, Wu DD, Lukoschek M, Kandzari D, Sivaneri N, Blaha JD, and Radin EL (1989) The effects of altered strain environments on bone tissue kinetics. *Bone* **10**, 215-221.
30. Carter DR (1984) Mechanical loading histories and cortical bone remodeling. *Calcif Tissue Int* **36**, S19-S24
31. Carter DR (1987) Mechanical loading history and skeletal biology. *J Biomech* **20**, 1095-1109.
32. Carter DR, Bouxsein ML, and Marcus R (1992) New approaches for interpreting projected bone densitometry data. *J Bone Miner Res* **7**, 137-145.
33. Carter DR, Fyhrie DP, and Whalen RT (1987) Trabecular bone density and loading history: regulation of connective tissue biology by mechanical energy. *J Biomech* **20**, 785-794.
34. Carter DR, van der Meulen MC, and Beaupre GS (1996) Mechanical factors in bone growth and development. *Bone* **18**, 5S-10S.

35. Cassell C, Benedict M, and Specker B (1996) Bone mineral density in elite 7- to 9-yr-old female gymnasts and swimmers. *Med Sci Sports Exerc* **28**, 1243-1246.

36. Chambers TJ, Evans M, Gardner TN, Turner-Smith A, and Chow JW (1993) Induction of bone formation in rat tail vertebrae by mechanical loading. *Bone Miner* **20**, 167-178.

37. Chen MM, Yeh JK, Aloia JF, Tierney JM, and Sprintz S (1994) Effect of treadmill exercise on tibial cortical bone in aged female rats: a histomorphometry and dual energy x-ray absorptiometry study. *Bone* **15**, 313-319.

38. Cheng MZ, Zaman G, and Lanyon LE (1994) Estrogen enhances the stimulation of bone collagen synthesis by loading and exogenous prostacyclin, but not prostaglandin E2, in organ cultures of rat ulnae. *J Bone Miner Res* **9**, 805-816.

39. Chilibeck PD, Calder A, Sale DG, and Webber CE (1996) Twenty weeks of weight training increases lean tissue mass but not bone mineral mass or density in healthy, active young women. *Can J Physiol Pharmacol* **74**, 1180-1185.

40. Chiquet M, Matthisson M, Koch M, Tannheimer M, and Chiquet-Ehrismann R (1996) Regulation of extracellular matrix synthesis by mechanical stress. *Biochem Cell Biol* **74**, 737-744.

41. Chow JW, Jagger CJ, and Chambers TJ (1993) Characterization of osteogenic response to mechanical stimulation in cancellous bone of rat caudal vertebrae. *Am J Physiol* **265** , E340-E347

42. Chow JW, Wilson AJ, Chambers TJ, and Fox SW (1998) Mechanical loading stimulates bone formation by reactivation of bone lining cells in 13-week-old rats. *J Bone Miner Res* **13**, 1760-1767.

43. Cochran GV, Dell DG, Palmieri VR, Johnson MW, Otter MW, and Kadaba MP (1989) An improved design of electrodes for measurement of streaming potentials on wet bone in vitro and in vivo. *J Biomech* **22**, 745-750.

44. Cormack DH (1987) *Ham's Histology.* Lippincott, Philadelphia PA.

45. Courteix D, Lespessailles E, Peres SL, Obert P, Germain P, and Benhamou CL (1998) Effect of physical training on bone mineral density in prepubertal girls: a

comparative study between impact-loading and non-impact-loading sports. *Osteoporos Int* **8**, 152-158.

46. Cowin SC (1984) Mechanical modeling of the stress adaptation process in bone. *Calcif Tissue Int* **36**, S98-S103
47. Cowin SC, Weinbaum S, and Zeng Y (1995) A case for bone canaliculi as the anatomical site of strain generated potentials. *J Biomech* **28**, 1281-1297.
48. Cummings SR, Rubin SM, and Black D (1990) The future of hip fractures in the United States. Numbers, costs, and potential effects of postmenopausal estrogen. *Clin Orthop* 163-166.
49. Cunningham J, Segre GV, Slatopolsky E, and Avioli LV (1985) Effect of heavy exercise on mineral metabolism and calcium regulating hormones in humans. *Calcif Tissue Int* **37**, 598-601.
50. Dalen N and Olsson KE (1974) Bone mineral content and physical activity. *Acta Orthop Scan* **45**, 170-174.
51. Dallas SL, Zaman G, Pead MJ, and Lanyon LE (1993) Early strain-related changes in cultured embryonic chick tibiotarsi parallel those associated with adaptive modeling in vivo. *J Bone Miner Res* **8**, 251-259.
52. Davee AM, Rosen CJ, and Adler RA (1990) Exercise patterns and trabecular bone density in college women. *J Bone Miner Res* **5**, 245-250.
53. Davies HM, McCarthy RN, and Jeffcott LB (1993) Surface strain on the dorsal metacarpus of thoroughbreds at different speeds and gaits. *Acta Anat (Basel)* **146**, 148-153.
54. Demes B, Stern JTJ, Hausman MR, Larson SG, McLeod KJ, and Rubin CT (1998) Patterns of strain in the macaque ulna during functional activity. *Am J Phys Anthropol* **106**, 87-100.
55. Dodds RA, Ali N, Pead MJ, and Lanyon LE (1993) Early loading-related changes in the activity of glucose 6-phosphate dehydrogenase and alkaline phosphatase in osteocytes and periosteal osteoblasts in rat fibulae in vivo. *J Bone Miner Res* **8**, 261-267.

56. Donahue HJ (1998) Gap junctional intercellular communication in bone: a cellular basis for the mechanostat set point. *Calcif Tissue Int* **62**, 85-88.

57. Donahue HJ, McLeod KJ, Rubin CT, Andersen J, Grine EA, Hertzberg EL, and Brink PR (1995) Cell-to-cell communication in osteoblastic networks: cell line-dependent hormonal regulation of gap junction function. *J Bone Miner Res* **10**, 881-889.

58. Dook JE, James C, Henderson NK, and Price RI (1997) Exercise and bone mineral density in mature female athletes. *Med Sci Sports Exerc* **29**, 291-296.

59. Dornemann TM, McMurray RG, Renner JB, and Anderson JJ (1997) Effects of high-intensity resistance exercise on bone mineral density and muscle strength of 40-50-year-old women. *J Sports Med Phys Fitness* **37**, 246-251.

60. Doty SB (1981) Morphological evidence of gap junctions between bone cells. *Calcif Tissue Int* **33**, 509-512.

61. Duppe H, Gardsell P, Johnell O, and Ornstein E (1996) Bone mineral density in female junior, senior and former football players. *Osteoporos Int* **6**, 437-441.

62. Ensrud KE, Black DM, Palermo L, Bauer DC, Barrett-Connor E, Quandt SA, Thompson DE, and Karpf DB (1997) Treatment with alendronate prevents fractures in women at highest risk: results from the Fracture Intervention Trial. *Arch Intern Med* **157**, 2617-2624.

63. Fehling PC, Alekel L, Clasey J, Rector A, and Stillman RJ (1995) A comparison of bone mineral densities among female athletes in impact loading and active loading sports. *Bone* **17**, 205-210.

64. Fiorelli G, Orlando C, Benvenuti S, Franceschelli F, Bianchi S, Pioli P, Tanini A, Serio M, Bartucci F, and Brandi ML (1994) Characterization, regulation, and function of specific cell membrane receptors for insulin-like growth factor I on bone endothelial cells. *J Bone Miner Res* **9**, 329-337.

65. Forwood MR, Bennett MB, Blowers AR, and Nadorfi RL (1998) Modification of the in vivo four-point loading model for studying mechanically induced bone adaptation. *Bone* **23** , 307-310.

66. Forwood MR and Burr DB (1993) Physical activity and bone mass: exercises in futility? *Bone Miner* **21**, 89-112.

67. Forwood MR and Parker AW (1986) Effects of exercise on bone morphology. Vascular channels studied in the rat tibia. *Acta Orthop Scan* **57**, 204-207.

68. Forwood MR and Parker AW (1991) Repetitive loading, in vivo, of the tibiae and femora of rats: effects of repeated bouts of treadmill-running. *Bone Miner* **13**, 35-46.

69. Forwood MR and Turner CH (1994) The response of rat tibiae to incremental bouts of mechanical loading: a quantum concept for bone formation. *Bone* **15**, 603-609.

70. Forwood MR and Turner CH (1995) Skeletal adaptations to mechanical usage: results from tibial loading studies in rats. *Bone* **17**, 197S-205S.

71. Fraioli F, Moretti C, Paolucci D, Alicicco E, Crescenzi F, and Fortunio G (1980) Physical exercise stimulates marked concomitant release of beta- endorphin and adrenocorticotropic hormone (ACTH) in peripheral blood in man. *Experientia* **36**, 987-989.

72. Friedlander AL, Genant HK, Sadowsky S, Byl NN, and Gluer CC (1995) A two-year program of aerobics and weight training enhances bone mineral density of young women. *J Bone Miner Res* **10**, 574-585.

73. Fritton JC, Rubin CT, Qin YX, and McLeod KJ (1997) Whole-body vibration in the skeleton: development of a resonance-based testing device. *Ann Biomed Eng* **25**, 831-839.

74. Fritton S, McLeod K, Fritton J, Brand R, and Rubin C (1995) Persistent, low magnitude strains as the dominant source of mechanical information in a bone's 24 hour strain history. *Trans Orthop Res Soc 20*, 547. (Abstract)

75. Frost HM (1963) *Bone remodelling dynamics.* Charles C. Thomas, Springfield IL.

76. Frost HM (1987) Bone "mass" and the "mechanostat": a proposal. *Anat Rec* **219**, 1-9.

77. Fyhrie DP and Carter DR (1986) A unifying principle relating stress to trabecular bone morphology. *J Orthop Res* **4**, 304-317.

78. Fyhrie DP and Schaffler MB (1995) The adaptation of bone apparent density to applied load. *J Biomech* **28**, 135-146.

79. Galileo G (1638) *Discorsi e dimonstrazioni matematiche, intorno a due nuove scienze attentanti alla meccanica ed a muovementi localli.* University of Wisconsin Press, Madison WI.

80. Genant HK, Engelke K, Fuerst T, Gluer CC, Grampp S, Harris ST, Jergas M, Lang T, Lu Y, Majumdar S, Mathur A, and Takada M (1996) Noninvasive assessment of bone mineral and structure: state of the art. *J Bone Miner Res* **11**, 707-730.

81. Gibson LJ (1985) The mechanical behaviour of cancellous bone. *J Biomech* **18**, 317-328.

82. Gleeson PB, Protas EJ, LeBlanc AD, Schneider VS, and Evans HJ (1990) Effects of weight lifting on bone mineral density in premenopausal women. *J Bone Miner Res* **5**, 153-158.

83. Grimston SK, Willows ND, and Hanley DA (1993) Mechanical loading regime and its relationship to bone mineral density in children. *Med Sci Sports Exerc* **25**, 1203-1210.

84. Gross D and Williams WS (1982) Streaming potential and the electromechanical response of physiologically-moist bone. *J Biomech* **15**, 277-295.

85. Gross PM, Heistad DD, and Marcus ML (1979) Neurohumoral regulation of blood flow to bones and marrow. *Am J Physiol* **237**, H440-H448

86. Gross TS, Damji AA, Judex S, Bray RC, and Zernicke RF (1999) Bone hyperemia precedes disuse-induced intracortical bone resorption. *J Appl Physiol* **86**, 230-235.

87. Gross TS, Edwards JL, McLeod KJ, and Rubin CT (1997) Strain gradients correlate with sites of periosteal bone formation. *J Bone Miner Res* **12**, 982-988.

88. Gross TS, McLeod KJ, and Rubin CT (1992) Characterizing bone strain distributions in vivo using three triple rosette strain gages. *J Biomech* **25**, 1081-1087.

89. Gross TS and Rubin CT (1995) Uniformity of resorptive bone loss induced by disuse. *J Orthop Res* **13**, 708-714.

90. Grove KA and Londeree BR (1992) Bone density in postmenopausal women: high impact vs low impact exercise. *Med Sci Sports Exerc* **24**, 1190-1194.

91. Gutin B and Kasper MJ (1992) Can vigorous exercise play a role in osteoporosis prevention? A review. *Osteoporos Int* **2**, 55-69.

92. Haapasalo H, Kannus P, Sievanen H, Heinonen A, Oja P, and Vuori I (1994) Long-term unilateral loading and bone mineral density and content in female squash players. *Calcif Tissue Int* **54**, 249-255.

93. Haapasalo H, Kannus P, Sievanen H, Pasanen M, Uusi-Rasi K, Heinonen A, Oja P, and Vuori I (1998) Effect of long-term unilateral activity on bone mineral density of female junior tennis players. *J Bone Miner Res* **13**, 310-319.

94. Hamdy RC, Anderson JS, Whalen KE, and Harvill LM (1994) Regional differences in bone density of young men involved in different exercises. *Med Sci Sports Exerc* **26**, 884-888.

95. Hartley LH, Mason JW, Hogan RP, Jones LG, Kotchen TA, Mougey EH, Wherry FE, Pennington LL, and Ricketts PT (1972) Multiple hormonal responses to prolonged exercise in relation to physical training. *J Appl Physiol* **33**, 607-610.

96. Harvey S, Scanes CG, Chadwick A, and Bolton NJ (1979) Growth hormone and prolactin secretion in growing domestic fowl: influence of sex and breed. *Br Poult Sci* **20**, 9-17.

97. Hasling C, Charles P, Jensen FT, and Mosekilde L (1994) A comparison of the effects of oestrogen/progestogen, high-dose oral calcium, intermittent cyclic etidronate and an ADFR regime on calcium kinetics and bone mass in postmenopausal women with spinal osteoporosis. *Osteoporos Int* **4**, 191-203.

98. Heaney RP (1991) Lifelong calcium intake and prevention of bone fragility in the aged. *Calcif Tissue Int* **49**, S42-S45

99. Hegedus DH and Cowin SC (1976) Bone remodeling II: small adaptive elasticity. *J Elasticity* **6**, 337-352.

100. Heinonen A, Oja P, Kannus P, Sievanen H, Haapasalo H, Manttari A, and Vuori I (1995) Bone mineral density in female athletes representing sports with different loading characteristics of the skeleton. *Bone* **17**, 197-203.

101. Heinonen A, Oja P, Sievanen H, Pasanen M, and Vuori I (1998) Effect of two training regimens on bone mineral density in healthy perimenopausal women: a randomized controlled trial. *J Bone Miner Res* **13**, 483-490.

102. Heinonen A, Sievanen H, Kannus P, Oja P, and Vuori I (1996) Effects of unilateral strength training and detraining on bone mineral mass and estimated mechanical characteristics of the upper limb bones in young women. *J Bone Miner Res* **11**, 490-501.

103. Heinrich CH, Going SB, Pamenter RW, Perry CD, Boyden TW, and Lohman TG (1990) Bone mineral content of cyclically menstruating female resistance and endurance trained athletes. *Med Sci Sports Exerc* **22**, 558-563.

104. Henderson NK, White CP, and Eisman JA (1998) The roles of exercise and fall risk reduction in the prevention of osteoporosis. *Endocrinol Metab Clin North Am* **27**, 369-387.

105. Hert J, Liskova M, and Landa J (1971) Reaction of bone to mechanical stimuli. 1. Continuous and intermittent loading of tibia in rabbit. *Folia Morphol (Praha)* **19**, 290-300.

106. Hou JC, Salem GJ, Zernicke RF, and Barnard RJ (1990) Structural and mechanical adaptations of immature trabecular bone to strenuous exercise. *J Appl Physiol* **69**, 1309-1314.

107. Ingber DE (1997) Tensegrity: the architectural basis of cellular mechanotransduction. *Annu Rev Physiol* **59**, 575-599.

108. Iwamoto J, Takeda T, and Ichimura S (1998) Effects of exercise on bone mineral density in mature osteopenic rats. *J Bone Miner Res* **13**, 1308-1317.

109. Jarvinen TL, Kannus P, Sievanen H, Jolma P, Heinonen A, and Jarvinen M (1998) Randomized controlled study of effects of sudden impact loading on rat femur. *J Bone Miner Res* **13**, 1475-1482.

110. Jendrucko RJ, Hyman WA, Newell PHJ, and Chakraborty BK (1976) Theoretical evidence for the generation of high pressure in bone cells. *J Biomech* **9**, 87-91.

111. Jones HH, Priest JD, Hayes WC, Tichenor CC, and Nagel DA (1977) Humeral hypertrophy in response to exercise. *J Bone Joint Surg [Am]* **59**, 204-208.

112. Judex S, Gross TS, Bray RC, and Zernicke RF (1997) Adaptation of bone to physiological stimuli. *J Biomech* **30**, 421-429.

113. Judex S, Gross TS, and Zernicke RF (1997) Strain gradients correlate with sites of exercise-induced bone-forming surfaces in the adult skeleton. *J Bone Miner Res* **12**, 1737-1745.

114. Judex S and Zernicke RF (1999) High-impact exercise and growing bone -- changes in bone's mechanical milieu induced by jumping. *Proceedings of the 1999 Bioengineering Conference (ASME)* (Abstract)

115. Kannus P, Haapasalo H, Sankelo M, Sievanen H, Pasanen M, Heinonen A, Oja P, and Vuori I (1995) Effect of starting age of physical activity on bone mass in the dominant arm of tennis and squash players. *Ann Intern Med* **123**, 27-31.

116. Karpf DB, Shapiro DR, Seeman E, Ensrud KE, Johnston CCJ, Adami S, Harris ST, Santora AC, Hirsch LJ, Oppenheimer L, and Thompson D (1997) Prevention of nonvertebral fractures by alendronate. A meta-analysis. Alendronate Osteoporosis Treatment Study Groups. *JAMA* **277**, 1159-1164.

117. Kasten TP, Collin-Osdoby P, Patel N, Osdoby P, Krukowski M, Misko TP, Settle SL, Currie MG, and Nickols GA (1994) Potentiation of osteoclast bone-resorption activity by inhibition of nitric oxide synthase. *Proc Natl Acad Sci U S A* **91**, 3569-3573.

118. Kawata A and Mikuni-Takagaki Y (1998) Mechanotransduction in stretched osteocytes--temporal expression of immediate early and other genes. *Biochem Biophys Res Commun* **246**, 404-408.

119. Keller TS and Spengler DM (1989) Regulation of bone stress and strain in the immature and mature rat femur. *J Biomech* **22**, 1115-1127.

120. Kerr D, Morton A, Dick I, and Prince R (1996) Exercise effects on bone mass in postmenopausal women are site-specific and load-dependent. *J Bone Miner Res* **11**, 218-225.

121. Kiiskinen A (1977) Physical training and connective tissues in young mice--physical properties of Achilles tendons and long bones. *Growth* **41**, 123-137.

122. Kleerekoper M (1998) The role of fluoride in the prevention of osteoporosis. *Endocrinol Metab Clin North Am* **27**, 441-452.

123. Klein-Nulend J, Burger EH, Semeins CM, Raisz LG, and Pilbeam CC (1997) Pulsating fluid flow stimulates prostaglandin release and inducible prostaglandin G/H synthase mRNA expression in primary mouse bone cells. *J Bone Miner Res* **12**, 45-51.

124. Klein-Nulend J, Helfrich MH, Sterck JGH, MacPherson H, Joldersma M, Ralston SH, Semeins CM, and Burger EH (1998) Nitric oxide response to shear stress by human bone cell cultures is endothelial nitric oxide synthase dependent. *Biochem Biophys Res Commun* **250**, 108-114.

125. Klein-Nulend J, Roelofsen J, Semeins CM, Bronckers AL, and Burger EH (1997) Mechanical stimulation of osteopontin mRNA expression and synthesis in bone cell cultures. *J Cell Physiol* **170**, 174-181.

126. Klein-Nulend J, Semeins CM, Ajubi NE, Nijweide PJ, and Burger EH (1995) Pulsating fluid flow increases nitric oxide (NO) synthesis by osteocytes but not periosteal fibroblasts--correlation with prostaglandin upregulation. *Biochem Biophys Res Commun* **217**, 640-648.

127. Klein-Nulend J, van der Plas A, Semeins CM, Ajubi NE, Frangos JA, Nijweide PJ, and Burger EH (1995) Sensitivity of osteocytes to biomechanical stress in vitro. *FASEB J* **9**, 441-445.

128. Kohrt WM, Ehsani AA, and Birge SJJ (1997) Effects of exercise involving predominantly either joint-reaction or ground-reaction forces on bone mineral density in older women. *J Bone Miner Res* **12**, 1253-1261.

129. Konieczynski DD, Truty MJ, and Biewener AA (1998) Evaluation of a bone's in vivo 24-hour loading history for physical exercise compared with background loading. *J Orthop Res* **16**, 29-37.

130. Krall EA and Dawson-Hughes B (1993) Heritable and life-style determinants of bone mineral density. *J Bone Miner Res* **8**, 1-9.

131. Kravitz SR, Fink KL, Huber S, Bohanske L, and Cicilioni S (1985) Osseous changes in the second ray of classical ballet dancers. *J Am Podiatr Med Assoc* **75**, 346-348.

132. Kroger H, Kotaniemi A, Kroger L, and Alhava E (1993) Development of bone mass and bone density of the spine and femoral neck--a prospective study of 65 children and adolescents. *Bone Miner* **23**, 171-182.

133. Krolner B, Toft B, Pors NS, and Tondevold E (1983) Physical exercise as prophylaxis against involutional vertebral bone loss: a controlled trial. *Clin Sci* **64**, 541-546.

134. Kufahl RH and Saha S (1990) A theoretical model for stress-generated fluid flow in the canaliculi-lacunae network in bone tissue. *J Biomech* **23**, 171-180.

135. Lane NE, Bloch DA, Jones HH, Marshall WHJ, Wood PD, and Fries JF (1986) Long-distance running, bone density, and osteoarthritis. *JAMA* **255**, 1147-1151.

136. Lanyon LE (1971) Strain in sheep lumbar vertebrae recorded during life. *Acta Orthop Scan* **42**, 102-112.

137. Lanyon LE (1973) Analysis of surface bone strain in the calcaneus of sheep during normal locomotion. Strain analysis of the calcaneus. *J Biomech* **6**, 41-49.

138. Lanyon LE (1987) Functional strain in bone tissue as an objective, and controlling stimulus for adaptive bone remodelling. *J Biomech* **20**, 1083-1093.

139. Lanyon LE (1996) Using functional loading to influence bone mass and architecture: objectives, mechanisms, and relationship with estrogen of the mechanically adaptive process in bone. *Bone* **18**, 37S-43S.

140. Lanyon LE, Goodship AE, Pye CJ, and MacFie JH (1982) Mechanically adaptive bone remodelling. *J Biomech* **15**, 141-154.

141. Lanyon LE, Hampson WG, Goodship AE, and Shah JS (1975) Bone deformation recorded in vivo from strain gauges attached to the human tibial shaft. *Acta Orthop Scan* **46**, 256-268.

142. Lanyon LE and Rubin CT (1984) Static vs dynamic loads as an influence on bone remodelling. *J Biomech* **17**, 897-905.

143. Latimer HB (1927) Postnatal growth of the chicken skeleton. *Am J Anat* **40**, 1-57.

144. Lau KH and Baylink DJ (1998) Molecular mechanism of action of fluoride on bone cells. *J Bone Miner Res* **13**, 1660-1667.

145. Leichter I, Simkin A, Margulies JY, Bivas A, Steinberg R, Giladi M, and Milgrom C (1989) Gain in mass density of bone following strenuous physical activity. *J Orthop Res* 7, 86-90.

146. Leszczynski KW, Shalev S, and Cosby NS (1992) The enhancement of radiotherapy verification images by an automated edge detection technique. *Med Phys* **19**, 611-621.

147. Li KC, Zernicke RF, Barnard RJ, and Li AF (1991) Differential response of rat limb bones to strenuous exercise. *J Appl Physiol* **70**, 554-560.

148. Lindsay R (1998) The role of estrogen in the prevention of osteoporosis. *Endocrinol Metab Clin North Am* **27**, 399-409.

149. Lips P, Graafmans WC, Ooms ME, Bezemer PD, and Bouter LM (1996) Vitamin D supplementation and fracture incidence in elderly persons. A randomized, placebo-controlled clinical trial. *Ann Intern Med* **124**, 400-406.

150. Lohman T, Going S, Pamenter R, Hall M, Boyden T, Houtkooper L, Ritenbaugh C, Bare L, Hill A, and Aickin M (1995) Effects of resistance training on regional and total bone mineral density in premenopausal women: a randomized prospective study. *J Bone Miner Res* **10**, 1015-1024.

151. Loitz BJ and Zernicke RF (1992) Strenuous exercise-induced remodelling of mature bone: relationships between in vivo strains and bone mechanics. *J Exp Biol* **170**, 1-18.

152. Lorich DG, Brighton CT, Gupta R, Corsetti JR, Levine SE, Gelb ID, Seldes R, and Pollack SR (1998) Biochemical pathway mediating the response of bone cells to capacitive coupling. *Clin Orthop* 246-256.

153. MacDougall JD, Webber CE, Martin J, Ormerod S, Chesley A, Younglai EV, Gordon CL, and Blimkie CJ (1992) Relationship among running mileage, bone density, and serum testosterone in male runners. *J Appl Physiol* **73**, 1165-1170.

154. MacGinitie LA, Stanely GD, Bieber WA, and Wu DD (1997) Bone streaming potentials and currents depend on anatomical structure and loading orientation. *J Biomech* **30**, 1133-1139.

155. MacGinitie LA, Wu DD, and Cochran GV (1993) Streaming potentials in healing, remodeling, and intact cortical bone. *J Bone Miner Res* **8**, 1323-1335.

156. Mak AF, Huang DT, Zhang JD, and Tong P (1997) Deformation-induced hierarchical flows and drag forces in bone canaliculi and matrix microporosity. *J Biomech* **30**, 11-18.

157. Martin RB and Burr DB (1989) *Structure, function, and adaptation of compact bone.* Raven Press, New York NY.

158. Mason DJ, Hillam RA, and Skerry TM (1996) Constitutive in vivo mRNA expression by osteocytes of beta-actin, osteocalcin, connexin-43, IGF-I, c-fos and c-jun, but not TNF-alpha nor tartrate-resistant acid phosphatase. *J Bone Miner Res* **11**, 350-357.

159. Mason DJ, Suva LJ, Genever PG, Patton AJ, Steuckle S, Hillam RA, and Skerry TM (1997) Mechanically regulated expression of a neural glutamate transporter in bone: a role for excitatory amino acids as osteotropic agents? *Bone* **20**, 199-205.

160. Matsuda JJ, Zernicke RF, Vailas AC, Pedrini VA, Pedrini-Mille A, and Maynard JA (1986) Structural and mechanical adaptation of immature bone to strenuous exercise. *J Appl Physiol* **60**, 2028-2034.

161. McLeod KJ and Rubin CT (1992) Sensitivity of the bone remodeling response to the frequency of applied strain. *Trans Orthop Res Soc 17*, 533. (Abstract)

162. McLeod KJ, Rubin CT, Otter MW, and Qin YX (1998) Skeletal cell stresses and bone adaptation. *Am J Med Sci* **316**, 176-183.

163. McNamara BP, Prendergast PJ, and Taylor D (1992) Prediction of bone adaptation in the ulnar-osteotomized sheep's forelimb using an anatomical finite element model. *J Biomed Eng* **14**, 209-216.

164. Meazzini MC, Toma CD, Schaffer JL, Gray ML, and Gerstenfeld LC (1998) Osteoblast cytoskeletal modulation in response to mechanical strain in vitro. *J Orthop Res* **16**, 170-180.

165. Mikic B and Carter DR (1995) Bone strain gage data and theoretical models of functional adaptation. *J Biomech* **28**, 465-469.

166. Mikuni-Takagaki Y, Suzuki Y, Kawase T, and Saito S (1996) Distinct responses of different populations of bone cells to mechanical stress. *Endocrinology* **137**, 2028-2035.

167. Miles RR, Turner CH, Santerre R, Tu Y, McClelland P, Argot J, DeHoff BS, Mundy CW, Rosteck PRJ, Bidwell J, Sluka JP, Hock J, and Onyia JE (1998) Analysis of differential gene expression in rat tibia after an osteogenic stimulus in vivo: mechanical loading regulates osteopontin and myeloperoxidase. *J Cell Biochem* **68**, 355-365.

168. Mori S and Burr DB (1993) Increased intracortical remodeling following fatigue damage. *Bone* **14**, 103-109.

169. Morris FL, Naughton GA, Gibbs JL, Carlson JS, and Wark JD (1997) Prospective ten-month exercise intervention in premenarcheal girls: positive effects on bone and lean mass. *J Bone Miner Res* **12**, 1453-1462.

170. Mosley JR and Lanyon LE (1998) Strain rate as a controlling influence on adaptive modeling in response to dynamic loading of the ulna in growing male rats. *Bone* **23**, 313-318.

171. Mosley JR, March BM, Lynch J, and Lanyon LE (1997) Strain magnitude related changes in whole bone architecture in growing rats. *Bone* **20**, 191-198.

172. National Osteoporosis Foundation (1997) *Osteoporosis prevalence report: 1996 and 2015.* Washington DC.

173. Nelson ME, Fiatarone MA, Morganti CM, Trice I, Greenberg RA, and Evans WJ (1994) Effects of high-intensity strength training on multiple risk factors for osteoporotic fractures. A randomized controlled trial. *JAMA* **272**, 1909-1914.

174. Newhall KM, Rodnick KJ, van der Meulen MC, Carter DR, and Marcus R (1991) Effects of voluntary exercise on bone mineral content in rats. *J Bone Miner Res* **6**, 289-296.

175. Nilsson BE and Westlin NE (1971) Bone density in athletes. *Clin Orthop* **77**, 179-182.

176. Nordin M and Frankel V (1989) Biomechanics of bone. In: *Basic Biomechanics of the Musculoskeletal System*; Nordin M, and Frankel V (Eds) Lea and Febiger, Malvern PA,

177. Nordstrom P, Pettersson U, and Lorentzon R (1998) Type of physical activity, muscle strength, and pubertal stage as determinants of bone mineral density and bone area in adolescent boys. *J Bone Miner Res* **13**, 1141-1148.

178. O'Connor JA, Lanyon LE, and MacFie H (1982) The influence of strain rate on adaptive bone remodelling. *J Biomech* **15**, 767-781.

179. Orwoll ES, Ferar J, Oviatt SK, McClung MR, and Huntington K (1989) The relationship of swimming exercise to bone mass in men and women. *Arch Intern Med* **149**, 2197-2200.

180. Otter MW, Palmieri VR, and Cochran GV (1990) Transcortical streaming potentials are generated by circulatory pressure gradients in living canine tibia. *J Orthop Res* **8**, 119-126.

181. Otter MW, Palmieri VR, Wu DD, Seiz KG, MacGinitie LA, and Cochran GV (1992) A comparative analysis of streaming potentials in vivo and in vitro. *J Orthop Res* **10**, 710-719.

182. Owan I, Burr DB, Turner CH, Qiu J, Tu Y, Onyia JE, and Duncan RL (1997) Mechanotransduction in bone: osteoblasts are more responsive to fluid forces than mechanical strain. *Am J Physiol* **273**, C810-C815

183. Parfitt AM, Drezner MK, Glorieux FH, Kanis JA, Malluche H, Meunier PJ, Ott SM, and Recker RR (1987) Bone histomorphometry: standardization of nomenclature, symbols, and units. Report of the ASBMR Histomorphometry Nomenclature Committee. *J Bone Miner Res* **2**, 595-610.

184. Pead MJ and Lanyon LE (1998) Adaptive remodeling in bone: torsion versus compression. *Trans Orthop Res Soc 15*, 104. (Abstract)

185. Pead MJ, Skerry TM, and Lanyon LE (1988) Direct transformation from quiescence to bone formation in the adult periosteum following a single brief period of bone loading. *J Bone Miner Res* **3**, 647-656.

186. Pienkowski D and Pollack SR (1983) The origin of stress-generated potentials in fluid-saturated bone. *J Orthop Res* **1**, 30-41.

187. Pitsillides AA, Rawlinson SC, Suswillo RF, Bourrin S, Zaman G, and Lanyon LE (1995) Mechanical strain-induced NO production by bone cells: a possible role in adaptive bone (re)modeling? *FASEB J* **9**, 1614-1622.

188. Prendergast PJ and Taylor D (1994) Prediction of bone adaptation using damage accumulation. *J Biomech* **27**, 1067-1076.

189. Pruitt LA, Jackson RD, Bartels RL, and Lehnhard HJ (1992) Weight-training effects on bone mineral density in early postmenopausal women. *J Bone Miner Res* **7**, 179-185.

190. Pruitt LA, Taaffe DR, and Marcus R (1995) Effects of a one-year high-intensity versus low-intensity resistance training program on bone mineral density in older women. *J Bone Miner Res* **10**, 1788-1795.

191. Qin YX, McLeod KJ, Guilak F, Chiang FP, and Rubin CT (1996) Correlation of bony ingrowth to the distribution of stress and strain parameters surrounding a porous-coated implant. *J Orthop Res* **14**, 862-870.

192. Qin YX, Otter MW, Rubin CT, and McLeod KJ (1997) Correlation of dilational strain gradients to fluid flow and streaming potentials in an in vivo animal model. *Trans Orthop Res Soc 22*, 112. (Abstract)

193. Qin YX, Rubin CT, and McLeod KJ (1998) Nonlinear dependence of loading intensity and cycle number in the maintenance of bone mass and morphology. *J Orthop Res* **16**, 482-489.

194. Raab DM, Crenshaw TD, Kimmel DB, and Smith EL (1991) A histomorphometric study of cortical bone activity during increased weight-bearing exercise. *J Bone Miner Res* **6**, 741-749.

195. Raab DM, Smith EL, Crenshaw TD, and Thomas DP (1990) Bone mechanical properties after exercise training in young and old rats. *J Appl Physiol* **68**, 130-134.

196. Rawlinson SC, Mosley JR, Suswillo RF, Pitsillides AA, and Lanyon LE (1995) Calvarial and limb bone cells in organ and monolayer culture do not show the same early responses to dynamic mechanical strain. *J Bone Miner Res* **10**, 1225-1232.

197. Ray NF, Chan JK, Thamer M, and Melton LJ (1997) Medical expenditures for the treatment of osteoporotic fractures in the United States in 1995: report from the National Osteoporosis Foundation. *J Bone Miner Res* **12**, 24-35.

198. Recker R, Rubin C, Cullen D, Belongia D, Ryaby J, and McLeod K (1997) Non-invasive biomechanical intervention for the prevention of post-menopausal osteopenia. *J Bone Miner Res 12*, S242. (Abstract)

199. Reich KM and Frangos JA (1993) Protein kinase C mediates flow-induced prostaglandin E2 production in osteoblasts. *Calcif Tissue Int* **52**, 62-66.

200. Reich KM, Gay CV, and Frangos JA (1990) Fluid shear stress as a mediator of osteoblast cyclic adenosine monophosphate production. *J Cell Physiol* **143**, 100-104.

201. Reid IR (1998) The roles of calcium and vitamin D in the prevention of osteoporosis. *Endocrinol Metab Clin North Am* **27**, 389-398.

202. Reilly GC, Currey JD, and Goodship AE (1997) Exercise of young thoroughbred horses increases impact strength of the third metacarpal bone. *J Orthop Res* **15**, 862-868.

203. Rennie MJ and Johnson RH (1974) Alteration of metabolic and hormonal responses to exercise by physical training. *Eur J Appl Physiol* **33**, 215-226.

204. Rico H, Revilla M, Hernandez ER, Gomez-Castresana F, and Villa LF (1993) Bone mineral content and body composition in postpubertal cyclist boys. *Bone* **14**, 93-95.

205. Riggs BL, Hodgson SF, O'Fallon WM, Chao EY, Wahner HW, Muhs JM, Cedel SL, and Melton LJ (1990) Effect of fluoride treatment on the fracture rate in postmenopausal women with osteoporosis. *N Engl J Med* **322**, 802-809.

206. Robinson TL, Snow-Harter C, Taaffe DR, Gillis D, Shaw J, and Marcus R (1995) Gymnasts exhibit higher bone mass than runners despite similar prevalence of amenorrhea and oligomenorrhea. *J Bone Miner Res* **10**, 26-35.

207. Rockwell JC, Sorensen AM, Baker S, Leahey D, Stock JL, Michaels J, and Baran DT (1990) Weight training decreases vertebral bone density in premenopausal women: a prospective study. *J Clin Endocrinol Metab* **71**, 988-993.

208. Roer RD and Dillaman RM (1990) Bone growth and calcium balance during simulated weightlessness in the rat. *J Appl Physiol* **68**, 13-20.

209. Roux W (1885) Beiträge zur Morphologie der funktionellen Anpassung. 3. Beschreibung und Erläuterung einer knöchernen Kniegelenksankylose. In: *Archiv für Anatomie, Physiologie und wissenschaftliche Medizin*; 120-158.

210. Rubin C, Gross T, Qin YX, Fritton S, Guilak F, and McLeod K (1996) Differentiation of the bone-tissue remodeling response to axial and torsional loading in the turkey ulna. *J Bone Joint Surg [Am]* **78**, 1523-1533.

211. Rubin C, Recker R, Cullen D, Ryaby J, and McLeod K (1998) Prevention of bone loss in a post-menopausal population by low-level biomechanical intervention. *Bone 23*, S174. (Abstract)

212. Rubin C, Turner S, Jerome C, Strachan M, Gladwell T, Bain S, and McLeod K (1998) Low magnitude, high-frequency mechanical stimulation increases trabecular density of the proximal femur. *Bone 23*, S179. (Abstract)

213. Rubin C, Turner S, Mallinckrodt C, Fritton J, and McLeod K (1997) Site-specific increase in bone density stimulated non-invasively by extremely low magnitude thirty hertz mechanical stimulation. *Trans Orthop Res Soc 22*, 110. (Abstract)

214. Rubin CT (1984) Skeletal strain and the functional significance of bone architecture. *Calcif Tissue Int* **36**, S11-S18

215. Rubin CT and Lanyon LE (1982) Limb mechanics as a function of speed and gait: a study of functional strains in the radius and tibia of horse and dog. *J Exp Biol* **101**, 187-211.

216. Rubin CT and Lanyon LE (1984) Dynamic strain similarity in vertebrates; an alternative to allometric limb bone scaling. *J Theor Biol* **107**, 321-327.

217. Rubin CT and Lanyon LE (1984) Regulation of bone formation by applied dynamic loads. *J Bone Joint Surg [Am]* **66**, 397-402.

218. Rubin CT and Lanyon LE (1985) Regulation of bone mass by mechanical strain magnitude. *Calcif Tissue Int* **37**, 411-417.

219. Rubin CT and Lanyon LE (1987) Kappa Delta Award paper. Osteoregulatory nature of mechanical stimuli: function as a determinant for adaptive remodeling in bone. *J Orthop Res* **5**, 300-310.

220. Rubin CT, McLeod KJ, and Bain SD (1990) Functional strains and cortical bone adaptation: epigenetic assurance of skeletal integrity. *J Biomech* **23**, 43-54.

221. Rybicki EF, Simonen FA, Mills EJ, Hassler CR, Scoles P, Milne D, and Weis EB (1974) Mathematical and experimental studies on the mechanics of plated transverse fractures. *J Biomech* **7**, 377-384.

222. Salzstein RA and Pollack SR (1987) Electromechanical potentials in cortical bone--II. Experimental analysis. *J Biomech* **20**, 271-280.

223. Salzstein RA, Pollack SR, Mak AF, and Petrov N (1987) Electromechanical potentials in cortical bone--I. A continuum approach. *J Biomech* **20**, 261-270.

224. Saville PD and Whyte MP (1969) Muscle and bone hypertrophy. Positive effect of running exercise in the rat. *Clin Orthop* **65**, 81-88.

225. Scheiber LB and Torregrosa L (1998) Evaluation and treatment of postmenopausal osteoporosis. *Semin Arthritis Rheum* **27**, 245-261.

226. Simkin A, Leichter I, Swissa A, and Samueloff S (1989) The effect of swimming activity on bone architecture in growing rats. *J Biomech* **22**, 845-851.

227. Simkin PA, Huang A, and Benedict RS (1990) Effects of exercise on blood flow to canine articular tissues. *J Orthop Res* **8**, 297-303.

228. Singh S and Saha S (1984) Electrical properties of bone. A review. *Clin Orthop* 249-271.

229. Skedros JG, Mason MW, Nelson MC, and Bloebaum RD (1996) Evidence of structural and material adaptation to specific strain features in cortical bone. *Anat Rec* **246**, 47-63.

230. Skerry TM (1997) Mechanical loading and bone: what sort of exercise is beneficial to the skeleton? *Bone* **20**, 179-181.

231. Skerry TM, Bitensky L, Chayen J, and Lanyon LE (1989) Early strain-related changes in enzyme activity in osteocytes following bone loading in vivo. *J Bone Miner Res* **4**, 783-788.

232. Slemenda CW and Johnston CC (1993) High intensity activities in young women: site specific bone mass effects among female figure skaters. *Bone Miner* **20**, 125-132.

233. Smith EL and Gilligan C (1991) Physical activity effects on bone metabolism. *Calcif Tissue Int* **49**, S50-S54

234. Smith EL and Gilligan C (1996) Dose-response relationship between physical loading and mechanical competence of bone. *Bone* **18**, 455-505.

235. Smith EL, Gilligan C, McAdam M, Ensign CP, and Smith PE (1989) Deterring bone loss by exercise intervention in premenopausal and postmenopausal women. *Calcif Tissue Int* **44**, 312-321.

236. Smith JA, Gray AB, Pyne DB, Baker MS, Telford RD, and Weidemann MJ (1996) Moderate exercise triggers both priming and activation of neutrophil subpopulations. *Am J Physiol* **270**, R838-R845

237. Smith R and Rutherford OM (1993) Spine and total body bone mineral density and serum testosterone levels in male athletes. *Eur J Appl Physiol* **67**, 330-334.

238. Snow-Harter C, Bouxsein ML, Lewis BT, Carter DR, and Marcus R (1992) Effects of resistance and endurance exercise on bone mineral status of young women: a randomized exercise intervention trial. *J Bone Miner Res* **7**, 761-769.

239. Snow-Harter C and Marcus R (1991) Exercise, bone mineral density, and osteoporosis. *Exerc Sport Sci Rev* **19**, 351-388.

240. Snow-Harter C, Whalen R, Myburgh K, Arnaud S, and Marcus R (1992) Bone mineral density, muscle strength, and recreational exercise in men. *J Bone Miner Res* **7**, 1291-1296.

241. Snow CM (1996) Exercise and bone mass in young and premenopausal women. *Bone* **18**, 51S-55S.

242. Srinivasan S and Gross TS (1998) Distinct fluid flow profiles engendered by temporal and spatial stimuli. *Trans Orthop Res Soc 23*, 575. (Abstract)

243. Stanford CM, Morcuende JA, and Brand RA (1995) Proliferative and phenotypic responses of bone-like cells to mechanical deformation. *J Orthop Res* **13**, 664-670.

244. Stanford CM, Stevens JW, and Brand RA (1995) Cellular deformation reversibly depresses RT-PCR detectable levels of bone-related mRNA. *J Biomech* **28**, 1419-1427.

245. Starkebaum W, Pollack SR, and Korostoff E (1979) Microelectrode studies of stress-generated potentials in four-point bending of bone. *J Biomed Mater Res* **13**, 729-751.

246. Steinberg ME and Trueta J (1981) Effects of activity on bone growth and development in the rat. *Clin Orthop* 52-60.

247. Stillman RJ, Lohman TG, Slaughter MH, and Massey BH (1986) Physical activity and bone mineral content in women aged 30 to 85 years. *Med Sci Sports Exerc* **18**, 576-580.

248. Sun YQ, McLeod KJ, and Rubin CT (1995) Mechanically induced periosteal bone formation is paralleled by the upregulation of collagen type one mRNA in osteocytes as measured by in situ reverse transcript-polymerase chain reaction. *Calcif Tissue Int* **57**, 456-462.

249. Swartz SM, Bertram JE, and Biewener AA (1989) Telemetered in vivo strain analysis of locomotor mechanics of brachiating gibbons. *Nature* **342**, 270-272.

250. Swissa-Sivan A, Azoury R, Statter M, Leichter I, Nyska A, Nyska M, Menczel J, and Samueloff S (1990) The effect of swimming on bone modeling and composition in young adult rats. *Calcif Tissue Int* **47**, 173-177.

251. Szivek JA, Anderson PL, and DeYoung DW (1997) In vivo strain measurements collected using calcium phosphate ceramic- bonded strain gauges. *J Invest Surg* **10**, 263-273.

252. Szivek JA, Johnson EM, Magee FP, Emmanual J, Poser R, and Koeneman JB (1994) Bone remodeling and in vivo strain analysis of intact and implanted greyhound proximal femora. *J Invest Surg* **7**, 213-233.

253. Taaffe DR, Robinson TL, Snow CM, and Marcus R (1997) High-impact exercise promotes bone gain in well-trained female athletes. *J Bone Miner Res* **12**, 255-260.

254. Taaffe DR, Snow-Harter C, Connolly DA, Robinson TL, Brown MD, and Marcus R (1995) Differential effects of swimming versus weight-bearing activity on bone mineral status of eumenorrheic athletes. *J Bone Miner Res* **10**, 586-593.

255. Tate ML, Niederer P, and Knothe U (1998) In vivo tracer transport through the lacunocanalicular system of rat bone in an environment devoid of mechanical loading. *Bone* **22**, 107-117.

256. Tommerup LJ, Raab DM, Crenshaw TD, and Smith EL (1993) Does weight-bearing exercise affect non-weight-bearing bone? *J Bone Miner Res* **8**, 1053-1058.

257. Tondevold EW and Eliasen P (1982) Regional vascular volumes and dynamic haematocrit compared to regional perfusion in canine cancellous and cortical bone. *Acta Orthop Scand* **53**, 197-203.

258. Torrance AG, Mosley JR, Suswillo RF, and Lanyon LE (1994) Noninvasive loading of the rat ulna in vivo induces a strain-related modeling response uncomplicated by trauma or periostal pressure. *Calcif Tissue Int* **54**, 241-247.

259. Turner CH, Akhter MP, Raab DM, Kimmel DB, and Recker RR (1991) A noninvasive, in vivo model for studying strain adaptive bone modeling. *Bone* **12**, 73-79.

260. Turner CH, Anne V, and Pidaparti RM (1997) A uniform strain criterion for trabecular bone adaptation: do continuum-level strain gradients drive adaptation? *J Biomech* **30** , 555-563.

261. Turner CH and Burr DB (1993) Basic biomechanical measurements of bone: a tutorial. *Bone* **14**, 595-608.

262. Turner CH and Forwood MR (1994) On animal models for studying bone adaptation. *Calcif Tissue Int* **55**, 316-317.

263. Turner CH and Forwood MR (1995) What role does the osteocyte network play in bone adaptation? *Bone* **16**, 283-285.

264. Turner CH, Forwood MR, and Otter MW (1994) Mechanotransduction in bone: do bone cells act as sensors of fluid flow? *FASEB J* **8**, 875-878.

265. Turner CH, Owan I, Brizendine EJ, Zhang W, Wilson ME, and Dunipace AJ (1996) High fluoride intakes cause osteomalacia and diminished bone strength in rats with renal deficiency. *Bone* **19**, 595-601.

266. Turner CH, Owan I, and Takano Y (1995) Mechanotransduction in bone: role of strain rate. *Am J Physiol* **269**, E438-E442

267. Turner CH, Takano Y, and Hirano T (1996) Reductions in bone strength after fluoride treatment are not reflected in tissue-level acoustic measurements. *Bone* **19**, 603-607.

268. Turner CH, Yoshikawa T, Forwood MR, Sun TC, and Burr DB (1995) High frequency components of bone strain in dogs measured during various activities. *J Biomech* **28**, 39-44.

269. Umemura Y, Ishiko T, Yamauchi T, Kurono M, and Mashiko S (1997) Five jumps per day increase bone mass and breaking force in rats. *J Bone Miner Res* **12**, 1480-1485.

270. Uusi-Rasi K, Sievanen H, Vuori I, Pasanen M, Heinonen A, and Oja P (1998) Associations of physical activity and calcium intake with bone mass and size in healthy women at different ages. *J Bone Miner Res* **13**, 133-142.

271. Vander MM, Rubin CT, McLeod KJ, McCauley LK, and Donahue HJ (1996) Gap junctional intercellular communication contributes to hormonal responsiveness in osteoblastic networks. *J Biol Chem* **271**, 12165-12171.

272. Vuori I, Heinonen A, Sievanen H, Kannus P, Pasanen M, and Oja P (1994) Effects of unilateral strength training and detraining on bone mineral density and content in young women: a study of mechanical loading and deloading on human bones. *Calcif Tissue Int* **55**, 59-67.

273. Wang N, Butler JP, and Ingber DE (1993) Mechanotransduction across the cell surface and through the cytoskeleton. *Science* **260**, 1124-1127.

274. Watson PA (1991) Function follows form: generation of intracellular signals by cell deformation. *FASEB J* **5**, 2013-2019.

275. Webb CM, Zaman G, Mosley JR, Tucker RP, Lanyon LE, and Mackie EJ (1997) Expression of tenascin-C in bones responding to mechanical load. *J Bone Miner Res* **12**, 52-58.

276. Weinans H and Prendergast PJ (1996) Tissue adaptation as a dynamical process far from equilibrium. *Bone* **19**, 143-149.

277. Weinbaum S, Cowin SC, and Zeng Y (1994) A model for the excitation of osteocytes by mechanical loading-induced bone fluid shear stresses. *J Biomech* **27**, 339-360.

278. Wheeler DL, Graves JE, Miller GJ, Vander GR, Wronski TJ, Powers SK, and Park HM (1995) Effects of running on the torsional strength, morphometry, and bone mass of the rat skeleton. *Med Sci Sports Exerc* **27**, 520-529.

279. Williams JA, Wagner J, Wasnich R, and Heilbrun L (1984) The effect of long-distance running upon appendicular bone mineral content. *Med Sci Sports Exerc* **16**, 223-227.

280. Wittich A, Mautalen CA, Oliveri MB, Bagur A, Somoza F, and Rotemberg E (1998) Professional football (soccer) players have a markedly greater skeletal mineral content, density and size than age- and BMI-matched controls. *Calcif Tissue Int* **63**, 112-117.

281. Wolff J (1892) *Das Gesetz der Transformation der Knochen (The Law of Bone Remodeling)*. Verlag von August Hirschwald, Berlin.

282. Woo SL, Kuei SC, Amiel D, Gomez MA, Hayes WC, White FC, and Akeson WH (1981) The effect of prolonged physical training on the properties of long bone: a study of Wolff's Law. *J Bone Joint Surg [Am]* **63**, 780-787.

283. Wyman J (1857) On the cancellated structure of some of the bones of the human body. *Memoirs Boston Soc Nat Hist* **4**, 125-140.

284. Xia SL and Ferrier J (1995) Calcium signal induced by mechanical perturbation of osteoclasts. *J Cell Physiol* **163**, 493-501.

285. Yoshikawa T, Mori S, Santiesteban AJ, Sun TC, Hafstad E, Chen J, and Burr DB (1994) The effects of muscle fatigue on bone strain. *J Exp Biol* **188**, 217-233.

286. Zeng Y, Cowin SC, and Weinbaum S (1994) A fiber matrix model for fluid flow and streaming potentials in the canaliculi of an osteon. *Ann Biomed Eng* **22**, 280-292.